https://theses.gla.ac.uk/

Theses Digitisation:

https://www.gla.ac.uk/myglasgow/research/enlighten/theses/digitisation/

This is a digitised version of the original print thesis.

Copyright and moral rights for this work are retained by the author

A copy can be downloaded for personal non-commercial research or study, without prior permission or charge

This work cannot be reproduced or quoted extensively from without first obtaining permission in writing from the author

The content must not be changed in any way or sold commercially in any format or medium without the formal permission of the author

When referring to this work, full bibliographic details including the author, title, awarding institution and date of the thesis must be given

Enlighten: Theses
https://theses.gla.ac.uk/
research-enlighten@glasgow.ac.uk

The Optical Properties of Evaporated Metal Films

by Gordon Henderson

Summary of a Thesis presented for the Degree of
Doctor of Philosophy in the Faculty of
Science of the University of Glasgow

1963

This work is concerned with the investigation of the optical constants of metal films formed by evaporation under vacuum.

Two methods of optical investigation were employed. In the first method the equations of Drude were applied to polarimetric measurements of the relative phase change and relative amplitude reduction of a light beam reflected from the surface of an opaque metal film at varying angles of incidence. Since most metals rapidly form an oxide film on exposure to the atmosphere a more complicated form of the Drude theory was applied to determine the optical constants of the clean metal film. A vacuum polarizing spectrometer was constructed which measured films without breaking the vacuum of formation. Results obtained from the vacuum polarizing spectrometer were used as a guide in performing the calculation of optical constants. These calculations were performed with the aid of a digital computer.

Continued ...

ProQuest Number: 10647429

All rights reserved

INFORMATION TO ALL USERS
The quality of this reproduction is dependent upon the quality of the copy submitted.

In the unlikely event that the author did not send a complete manuscript
and there are missing pages, these will be noted. Also, if material had to be removed,
a note will indicate the deletion.

ProQuest 10647429

Published by ProQuest LLC (2017). Copyright of the Dissertation is held by the Author.

All rights reserved.
This work is protected against unauthorized copying under Title 17, United States Code
Microform Edition © ProQuest LLC.

ProQuest LLC.
789 East Eisenhower Parkway
P.O. Box 1346
Ann Arbor, MI 48106 – 1346

The second method of optical investigation was based on that of Malé and involved the measurement of the transmittance and reflectances of films using light at normal incidence. Results obtained from these investigations determined the variation of the refractive index of chromium and copper films with changing thickness. The existence of a relationship, the Wolter Relationship, between the transmittance and reflectances for various metal films was verified.

Electron microscopy and electron diffraction were employed to determine the evolution of the structure of films of several metals as the film thickness varied.

A model based on that due to David which regards a thin metal film as being composed of small ellipsoidal particles was successfully applied to the results obtained for chromium and copper films.

A comparison of the results obtained for the optical constants of chromium and copper films by the two methods, viz. (a) polarimetry involving oblique incidence of light and (b) reflectance and transmittance measurements involving only normal incidence of light, showed a wide discrepancy. A possible explanation is suggested which regards with caution results obtained by methods involving oblique incidence as it appears that metal films are not homogeneous isotropic uniform layers.

THE OPTICAL PROPERTIES OF EVAPORATED METAL FILMS

by

Gordon Henderson

A Thesis submitted for the Degree of
Doctor of Philosophy in the Faculty of
Science of the University of Glasgow

1963

ACKNOWLEDGMENTS.

The author wishes to express his appreciation to Professor John Irving and the late Professor J.S. Rankin for departmental facilities during the execution of this work. He also wishes to thank the technical staff of the Department of Natural Philosophy at the Royal College of Science and Technology for assistance rendered.

In the process of performing the calculations on the computers at Glasgow University and at the Royal College of Science and Technology, valuable help was given by Mr. G. Frazer of the Department of Mathematics, the Royal College of Science and Technology.

Throughout the five years during which this work was carried out, Doctor Charles Weaver of the Department of Natural Philosophy at the Royal College of Science and Technology has acted as supervisor to the author. Doctor Weaver's constant assistance to the author will always be remembered by him with a deep feeling of gratitude.

Finally, the author wishes to express his grateful appreciation to his wife Margaret, who has patiently performed the typing work.

PREFACE

This work is concerned with the investigation of the optical constants of metal films formed by evaporation under vacuum and was conducted in the Department of Natural Philosophy, the Royal College of Science and Technology, Glasgow, while the author was employed as an Assistant Lecturer in that Department.

The production of the films (Chapter 3.2.) was performed solely by the author on a vacuum deposition unit built in the Department. An additional vacuum deposition unit (Chapter 3.20.) was designed by the author and constructed by departmental technical staff under his supervision. This second unit, called a Vacuum Polarizing Spectrometer, enabled the author to manufacture films and investigate them by polarimetry without breaking the vacuum. A polarizing spectroscope (Chapter 3.17.) was built by the author based on a design due to Tronstad(3.11.) with the modification that a photo-electric detection system was employed enabling accurate measurements to be made at high angles of incidence without the use of half-shade devices. The use of the photo-electric detector avoided the strain on the observer which accompanies prolonged visual measurements.

The method adopted to determine the optical constants of metal films by polarimetry follows that published by Hill and Weaver(4.1.). An improvement on the accuracy of the method was /

was provided by performing the laborious calculations involved on the "Sirius" computer in the Colville Computing Laboratory of the Mathematics Department of the Royal College of Science and Technology. The scope of the method was extended and the accuracy of the calculations improved by the use of the computer. The production of the computer programmes and the operation of the computer were all carried out by the author.

In a second series of investigations on the optical properties of metal films a method of determining simultaneously the optical constants and thickness of metal films by transmittance and reflectance measurements was used (Chapter 3.11.). The method was a modification of one devised by Malé(3.2.) who used a nomogram method to construct the comprehensive sets of curves required for investigations over a range of specimens. Here again a computer was employed by the author in place of the nomogram to calculate the required values for the construction of the curves. A reflectometer was constructed by the author to make the measurements of transmittance and reflectance of metal films.

The determination of the absolute phase change on reflection of light by a metal film was measured over a range of film thicknesses for chromium films(Chapter 3.8.). These measurements were made by two different methods. The first method /

method was a modification of one devised by Rouard(3.13.). The modification of the method improved the accuracy of the measurements and removed the necessity of employing photography for the observations. The second method of determining phase change on reflection was one devised by Weaver, Hill and MacLeod(3.15.). This latter method required verification in its applicability and this was obtained by comparing results with those of the well-tried Rouard method. The experimental results of phase change measurements were compared with calculated values obtained using the optical constants of the films derived by the Malé method. A good agreement was found to exist.

To examine the structure of the metal films electron microscope specimens were prepared and examined in a high resolution microscope which also provided electron diffraction patterns of the same specimens(Chapter 8). This work was performed entirely by the author.

A structural model based on one developed by David(9.4.) was found to give a satisfactory account of the optical constants of chromium and copper films (Chapter 9).

INDEX

CHAPTER 1 : INTRODUCTION.

Page

1.1. Film Formation.

1.3. Optical Properties of Metal Films.

1.4. Spectrophotometry.

1.6. Interferometry.

1.7. Polarimetry.

1.9. Aim and Scope of Present Work.

CHAPTER 2 : THEORY.

Page

2.1. Maxwell's Equations and Metallic Reflection.

2.4. Oblique Incidence.

2.6. Normal Incidence.

2.7. Reflectance and Transmittance of a Thin Metal Film.

2.11. Malé Method of Determination of Optical Constants of Metal Films.

2.14. Polarimetry.

2.18. The Poincaré Sphere.

CHAPTER 3 : EXPERIMENTAL.

Page

3.1. The Vacuum System.

3.2. Film Production.

3.4. Film Substrate Preparation.

3.6. Film Thickness Determination.

3.11. Reflectance and Transmittance Measurements.

3.17. Polarization Measurements.

3.20. The Vacuum Polarization Spectrometer.

3.22. Phase Change Measurements by the Rouard Method.

3.28. Phase Change Measurements by the Thickness Discrepancy Method.

Continued ...

INDEX (Continued)

CHAPTER 4 : RESULTS OF POLARIMETRY MEASUREMENTS.

Page

4.1. Description of Tables of Results.

4.3. Chromium.

4.4. Copper.

4.6. Tin.

Manganese.

4.7. Nickel.

CHAPTER 5 : RESULTS OF REFLECTANCE AND TRANSMITTANCE MEASUREMENTS.

Page

5.1. Necessity for Precautions in cases of Chromium and Copper.

5.4. The Wolter Relationship.

5.6. Malé investigations into the Wolter Relationship.

CHAPTER 6 : THE OPTICAL CONSTANTS OF CHROMIUM AND COPPER FILMS.

Page

6.1. Chromium Films.

6.3. Copper Films.

CHAPTER 7 : RESULTS OF PHASE CHANGE MEASUREMENTS.

Page

7.1. Theoretical Determination of Absolute Phase Change.

7.2. Comparison between Theory and Experiment.

Continued ...

INDEX (Continued)

CHAPTER 8 : RESULTS OF ELECTRON MICROSCOPY.

Page

8.1. Correspondence between Films on Formvar and Films on Glass.

8.2. Results for Chromium Films.

Results for Copper Films.

8.3. Results for Antimony Films.

Results for Manganese Films.

Results for Nickel Films.

8.4. Summary of Electron Microscopy Investigations.

CHAPTER 9 : DISCUSSION.

Page

9.1. Maxwell-Garnett Model of Thin Metal Films.

9.2. David Model.

9.11. Schopper's Distribution Function.

9.13. Comparison between Experimental Results and Theoretical Model for Chromium and Copper Films.

9.14. Comparison of Normal Incidence and Oblique Incidence Methods.

CHAPTER 10 : SUMMARY.

Page

10.1. Polarimetry Investigations.

10.3. Malé Method Investigations.

10.4. Electron Microscopy.

10.7. Suggestions for Further Work.

CHAPTER 1 : INTRODUCTION.

a) Film Formation.

The physical properties of thin films of metals are in general different from those of the same metals in bulk form. The reason for such differences has been attributed to the fact that such thin films generally possess a structure quite distinct from that of metals in bulk. Various workers, notably Levinstein(1.1.), Sennett and Scott(1.2.) and Picard and Duffendack(1.3.), have shown by means of electron microscopy that metal films have an aggregated structure. The existence of aggregation was postulated by earlier workers; thin metal films exhibit an anomalously high specific resistivity and a high scattering coefficient to incident light. These effects could conveniently be explained by a model which involved the gathering of the metal atoms in a growing film into small agglomerates, relatively isolated from each other and becoming more and more interconnected as the film thickness increased, until a thickness was attained where the film became continuous. This model also helped in the interpretation of the evolution of the mechanical adhesive and cohesive strength and the electrical, magnetic and optical properties of metal films.

The existence of aggregates in metal films is in accordance with our knowledge of the kinetics of film formation, Lennard-Jones(1.4.) and Appleyard(1.5.). Considering the case where /

where films are formed on a substrate such as glass either by cathodic sputtering or thermal evaporation under vacuum, the metal atoms arrive at the condensing surface with a certain amount of kinetic energy. If the substrate is kept at a very low temperature, viz. of the order of $-200^{\circ}C$, then an incident metal atom will immediately lose its kinetic energy and become "frozen" to the substrate at the point of impact. Films formed in this way have been investigated by various workers and have been found to be amorphous and show no aggregation whatsoever. Allowing the temperature of the substrate to increase, a temperature is reached where impinging atoms can move over the surface of the substrate and form groups which act as nucleation centres for further growth. The very high surface tension forces present in small metal particles also serve to promote the growth of aggregates. Additional heating of a substrate will allow impinging atoms to retain, or gain, sufficient kinetic energy to leave the condensing surface and hence inhibit film formation.

This work is concerned with metal films formed by thermal evaporation at pressures of the order of 10^{-5} m.m. Hg. onto glass substrates whose temperatures are generally within a few degrees of $25^{\circ}C$. The range of film types is thus restricted to those showing some degree of aggregation.

b) Optical Properties of Metal Films.

The electromagnetic theory was first applied by Drude(1.6.) to the study of the optical properties of thin metal films. A fundamental assumption made by Drude in his treatment was that the films were homogeneous, isotropic and bounded by plane parallel faces. Later investigations clearly showed that in the case of very thin films the assumption of a plane homogeneous film was incorrect. However the conception of a plane parallel-sided, homogeneous, isotropic film, whether or not such a film actually exists in any investigation, enables one to define the two parameters which would govern the optical behaviour of such a film. These are namely $\underline{n} = n - ik$, the complex refractive index, and d, the thickness of the film.

There are in existence today many methods of determining the refractive index and the thickness of metal films. In every case, although not explicitly stated, what are actually determined are the parameters of an equivalent uniform, isotropic, homogeneous film whose optical behaviour is similar to that of the actual film being investigated. This actual film may well bear little other physical resemblance to our hypothetical equivalent film.

If the parameters $\underline{n}$ and d of a film are given it is possible using Maxwell's equations to calculate the optical properties of the film, i.e. the factors of reflection and transmission, and the phase change on reflection and transmission. The reverse problem, viz. /

viz. that of determining n and d given some or all of the other quantities is considerably more complex. Since the original investigations of Drude at the end of the last century many workers have been concerned with the evaluation and interpretation of the optical constants of films. The result has been that there now exists a wide variety of methods for determining the optical constants and thickness of metal films. These may generally be classified according to the method of measurement, viz.
(i) Spectrophotometry, (ii) Interferometry and (iii) Polarimetry.

(i) Spectrophotometry : In this method the transmittance of a film is measured together with the reflectance at one or both boundaries. These measurements are made either at normal or oblique incidence, depending on the method of evaluation being employed. If oblique incidence is used then it is necessary to use light polarized in the plane of incidence, or perpendicular to this plane. An example of the latter type of measurement is that of Abelès and Creignou(1.7.) wherein the reflectance of an opaque metal film is measured for light polarized parallel and perpendicular to the plane of incidence for various angles of incidence. Assuming a simple metal/air interface, theory gives a value for the refractive index of the opaque metal film for each angle of incidence. By the use of opaque films contributions to the reflectance by multiple reflections within the film are eliminated, however this condition precludes the use of the method for thinner films. An important example of the /

the photometric method using normal incidence is that of Murmann(1.8.). In this method an independent determination of the thickness of the film is required. The films are formed on transparent substrates and the reflectance at each side of the film is measured together with the transmittance. From the determined value of the film thickness, and using the wavelength employed in the measurements, two reflectances, R and R', are calculated for a range of pairs of values n, k. The calculations are performed using standard formulae developed by Murmann. Curves of R and R' vs. k for various selected n values are then constructed (see fig. 1.1.). After allowing for any necessary corrections due to multiple reflections within the support the observed R and R' are drawn to intersect their respective sets of curves. The intersections of the observed R with the various n curves give values of n and k which satisfy R and hence a curve of k vs. n can be drawn, all points on which give the observed R. A similar process is adopted using R' and where the two final curves meet we get an n, k pair which simultaneously satisfy the observed R and R'. In practice the final curves often intersect in two points. By using the observed transmittance T and constructing a curve of T vs. n for various k a third final curve can help to select the correct n, k pair. Murmann and others who applied his method used a thickness value for their films obtained by finding the weight of film per unit area and dividing this quantity by the bulk density /

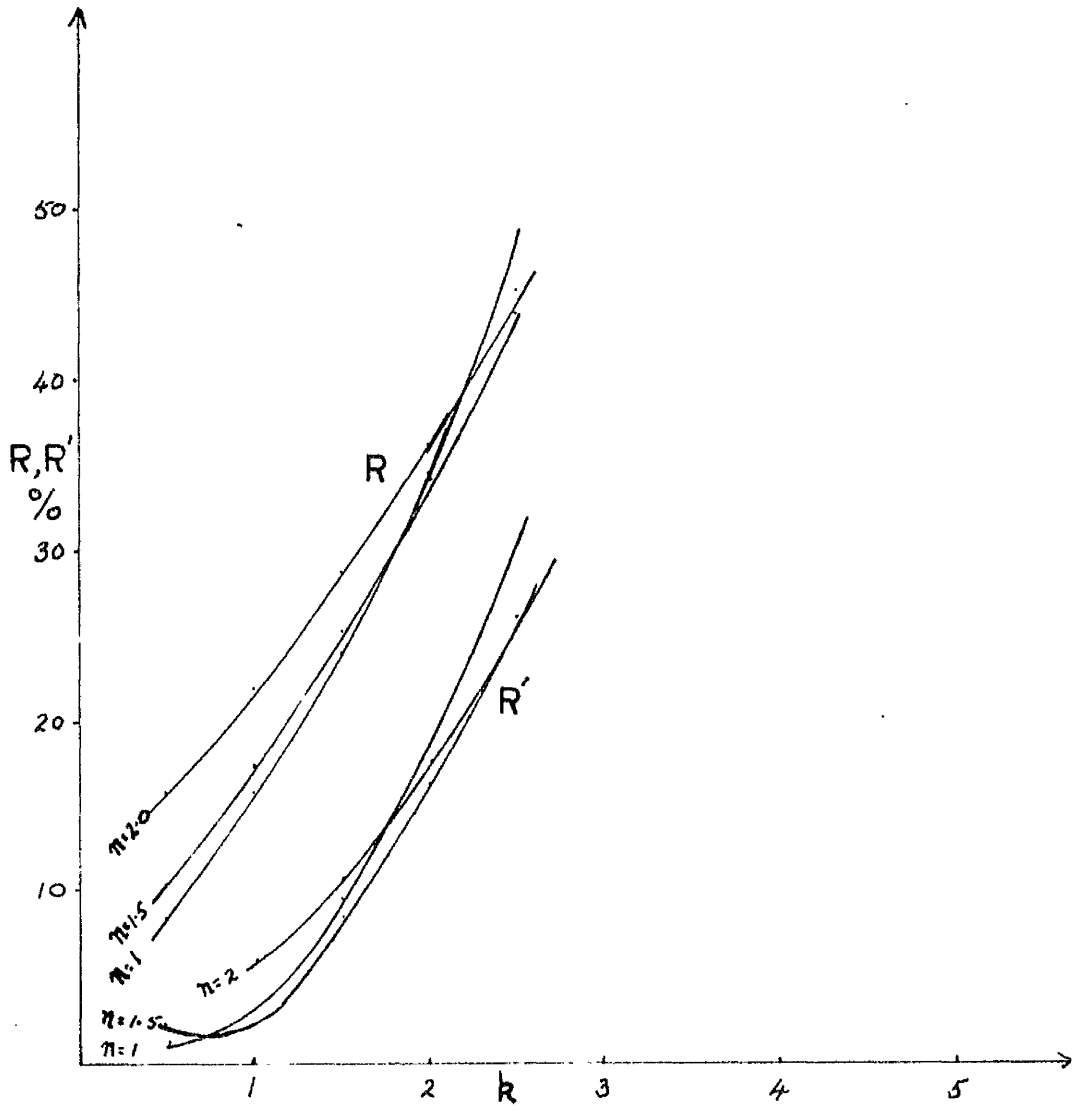

Fig. 1.1. R and R' for various n values expressed as a Function of k, for d = 300 A.

density of the material. This so-called "weight thickness" ignored the existence of a structure within a metal film and hence led to erroneous results in the case of very thin films, i.e. d < 200 - 300 A. However in the case of thicker films in which the structure effects are negligible the method gives good results.

Considerable space has been given to the method of Murmann as it was in fact the forerunner of a very important method of determination of film constants, viz. the method of Malé(1.9.). This method is fully described in Chapter 2 of this work and so further discussion of it will be left until then. It may be noted however that the fundamental difference between the methods of Murmann and that of Malé is that the Murmann method requires an independent measurement of thickness to be made whereas in the Malé method a thickness is obtained from the optical measurements along with a value for n and k.

(ii) Interferometry : The methods of interferometry as applied to the case of metal films cannot alone give the optical constants of films. The principal determinations made using the various techniques of interferometry are those of absolute phase changes on reflection by, and transmission through, a metal film, and the determination of a thickness value for a metal film. These techniques when used with other measurements provide powerful methods of determining film constants.

The accurate determination of absolute phase change on reflection or transmission by a film is the most difficult of all optical observations on thin films. Various workers, notably Rouard(1.10.), Faust(1.11.) and Schopper(1.12.), have described methods of performing these measurements. An accurate knowledge of absolute phase change on reflection is essential in the use of devices such as the Fabry-Perot Interferometer. More recently, (1.13.), work on optical masers has promoted interest in phase changes due to strict phase relationships which govern the operation of such devices. A description of the Rouard method is given in Chapter 3.

The other application of interferometry listed above, viz. the determination of film thickness, has been extensively developed in the last fifteen years, mainly by Tolansky(1.14.). A detailed discussion of the method of Tolansky is given in Chapter 3.

(iii) Polarimetry : This method of investigating the optical properties of surfaces and films was first developed, both theoretically and practically, by Drude(1.15.). Considering first the case of a clean metal surface, the method consists essentially of projecting a beam of linearly polarized light, usually in azimuth 45°, onto the metal surface and measuring the relative amplitude reduction and relative phase change of the components parallel and perpendicular to the plane of incidence. This is done by analyzing the elliptically polarized light reflected from the /

the metal surface. In the case of thin films on metal surfaces the equations relating the various parameters to the observed effects become so complicated that no method of obtaining an explicit solution exists for the general case. However, for a non-absorbing film on metal whose thickness is small compared to the wavelength of the light, such as occurs for several metals covered with a thin layer of transparent metal oxide, it is possible to obtain a solution to the equations. Vasicek(1.16.) who has studied the application of polarimetry to the study of thin films in great detail, has developed a graphical interpolation method of determining optical constants and has published tables suitable for use with the method.

The literature contains many examples of discrepancies between various authors in results of work done on similar metals. It is well known that one cause of the disagreements has been that of differing conditions of formation of the films by different workers. However, even in cases where conditions of formation are essentially similar, different results can be obtained if different methods of evaluation are employed. As an example, Malé(1.17.) has recalculated the optical constants of sputtered gold films from measurements made by Goos(1.18.). The values of n and k expressed as a function of thickness differ radically between the two authors despite the fact that they used the same data.

Workers in this field in the last fifteen years have generally adopted methods of evaluation which yield simultaneously the refractive index n and the thickness d of metal films. In addition methods of measurement involving normally incident light only have been favoured in order to avoid any possible effects due to anisotropy should this exist in the specimens.

Bousquet and Rouard(1.19.) have drawn attention to methods of measurement involving oblique incidence. They remark that should metal films not conform to the model of being plane parallel-sided, homogeneous and isotropic then the researches of many workers in the field would be suspect, due to the fact that they have used methods involving oblique incidence. Hence the polarimetric methods of measurement employed by Försterling(1.20.), Essers-Rheindorf(1.21.), Sommer(1.22.), Odenbach(1.23.), Vasicek(1.16.), etc., the methods of intensity measurement of polarized light at oblique incidence employed by Abelès(1.24.) and the method of Schulz(1.25.) involving the differential phase change of polarized components at oblique incidence, would all be involved.

Aim and Scope of Present Work.

Broadly the work consists of two parts.

(a) The method of Malé using normal incidence was used to determine concurrently the optical constants and the thickness of films throughout a range of thickness values. An attempt has been /

been made to interpret the results obtained using a model due to David(1.26.) which regards the thin metal film as composed of an assembly of ellipsoidal particles whose dimensions are small compared to the wavelength of the light used and whose unique axes lie perpendicular to the film substrate. The existence of a structure was confirmed using electron microscopy.

The conditions under which the Malé method may be used when only reflectance and transmittance measurements are available have been investigated. It was found that the Wolter relationship(1.26.) successfully indicated within the experimental error the limitations of the method.

A check was performed on the experimental results in the case of chromium. This was done by calculating the absolute phase change on reflection at the chromium films from the experimental values of the optical constants and thickness. The absolute phase change was also measured experimentally over a thickness range and good agreement was obtained with calculated values.

(b) Measurements were made at oblique incidence on thick metal films using polarimetry and results obtained were compared with those obtained by the Malé method. The same specimens were used for this work and for measurements by the Malé method. The effects of possible variations in the conditions of formation of the films were thereby eliminated.

The results of the two different methods were compared to give an indication of whether both methods are valid or whether the existence of a structure in the films precluded agreement.

CHAPTER 1 : REFERENCES.

1.1.) Levinstein, H., J. App. Phys. Vol. 20, 1949, p.306.
1.2.) Sennett, R.S. and Scott, A.D., J. Opt. Soc. Am., Vol. 40, 1950, p.203.
1.3.) Picard, R.G. and Duffendack, O.S., J. App. Phys., Vol. 14, 1943, p.291.
1.4.) Lennard-Jones, J.E., Trans. Far. Soc., Vol. 28, 1932, p.333.
1.5.) Appleyard, E.T.S., Proc. Phys. Soc. (London), Vol. 49, 1937, p.118.
1.6.) Drude, P., Wied. Ann., Vol. 35, 1888, p.508, and ibid., Vol. 50, 1893, p.595.
1.7.) Abeles, F., and Creignou, M., J. de Phys. (L); April 1954.
1.8.) Murmann, H., Zeit. Physik., Vol. 105, 1937, p.269.
1.9.) Male, D., Thesis, University of Paris; Masson et Cie., Paris, 1953.
1.10.) Rouard, P., Ann. Phys., Paris, Vol. 7, 1937, p.290.
1.11.) Faust, R.G., Phil. Mag., Vol. 41, 1950, p.1238.
1.12.) Schopper, H., Zeit. Physik., Vol. 135, 1953, p.p. 516 - 522.
1.13.) Bruesehke, E.E., Vacuum (GB), Vol. 11, No. 5 - 6, 255 - 9, 1961.
1.14.) Tolansky, S., Multiple Beam Interferometry, Oxford, 1948.
1.15.) Drude, P., Wied. Ann., Vol. 36, 1889, p.865.
1.16.) Vasicek, A., Czechols. J. Phys., Vol. 4, 1954, p.204.
J. Opt. Soc. Am., Vol. 37, 1947, p.p. 145, 623.
ibid., Vol. 39, 1949, p.409.
J. de Phys., Vol. 11, 1950, p.p. 342, 346.
ibid., Vol. 12, 1951, p.590.
1.17.) Male, D., Thesis, University of Paris; Masson et Cie., Paris, 1953.
1.18.) Geos, F., Z. Physik., Vol. 106, 1937, p.606.
1.19.) Bousquet, P. and Rouard, P., J. de Phys., Vol. 21, Dec. 1960, p.873.
1.20.) Forsterling, K., Ann. Physik., Vol. 30, 1937, p.745.
1.21.) Essers-Rheindorf, G., Ann. Physik., Vol. 28, 1937, p.297.
1.22.) Sommer, A., Thesis, Hamburg, 1940.
1.23.) Odenbach, F., Ann. Physik., Vol. 38, 1940, p.469.
1.24.) Abeles, F., Comptes Rendus. Acad. Sci., Vol. 238, 1954, p.881.
ibid., Vol. 32, 1953, p.257.
ibid., Vol. 231, 1950, p.958.
1.25.) Schulz, L.G., J. Opt. Soc. Am., Vol. 44, 1954, p.357.
1.26.) David, E., Z. Physik, Vol. 114, 1939, p.389.
1.27.) Wolter, H., Z. Physik., Vol. 105, 1937, p.269.

CHAPTER 2 : THEORY.

2.1.) Maxwell's Equations and Metallic Reflection.

Maxwell's equations for the propagation of an electromagnetic wave in a conducting isotropic non-magnetic medium may be summarized thus :-

$$\text{div } \underline{D} = \varepsilon \text{ div } \underline{E} = 4\pi\rho \qquad \ldots \quad (2.1.)$$

$$\text{div } \underline{B} = \mu \text{ div } \underline{H} = 0 \qquad \ldots \quad (2.2.)$$

$$\text{curl } \underline{E} = -\frac{\mu}{v}\frac{\underline{H}}{t} \qquad \ldots \quad (2.3.)$$

$$\text{curl } \underline{H} = \frac{4\pi}{v}\underline{j} + \frac{1}{v}\frac{\partial \underline{D}}{\partial t} \qquad \ldots \quad (2.4.)$$

$$= \frac{4\pi\sigma}{v}\underline{E} + \frac{\varepsilon}{v}\frac{\partial \underline{E}}{\partial t} \qquad \ldots \quad (2.5.)$$

where the various factors have their usual meaning.

In the above equations electrical quantities are measured in electrostatic units in the c.g.s. system and magnetic quantities in the electromagnetic c.g.s. system.

We can eliminate $\underline{E}$ and $\underline{H}$ in turn from the two equations (2.3.) and (2.5.), using the vector identity,

$\text{curl } (\text{curl } \underline{A}) = \text{grad } (\text{div } \underline{A}) - \nabla^2 \underline{A}$;

where $\underline{A}$ is any vector.

This gives the equations,

$$\frac{\varepsilon\mu}{v^2}\frac{\partial^2 \underline{E}}{\partial t^2} + \frac{4\pi\mu\sigma}{v^2}\frac{\partial \underline{E}}{\partial t} = \nabla^2 \underline{E} \qquad \ldots \quad (2.6.)$$

$$\frac{\varepsilon\mu}{v^2}\frac{\partial^2 \underline{H}}{\partial t^2} + \frac{4\pi\mu\sigma}{v^2}\frac{\partial \underline{H}}{\partial t} = \nabla^2 \underline{H} \qquad \ldots \quad (2.7.)$$

which represent the propagation of the electro-magnetic disturbance in the medium. By putting the conductivity equal to zero the equations (2.6.) and (2.7.) represent the propagation of an electro-magnetic wave through a non-conducting medium. We then have

$$\frac{\varepsilon\mu}{v^2}\frac{\partial^2 \underline{E}}{\partial t^2} = \nabla^2 \underline{E} \qquad \ldots \quad (2.8.)$$

$$\frac{\varepsilon\mu}{v^2}\frac{\partial^2 \underline{H}}{\partial t^2} = \nabla^2 \underline{H} \qquad \ldots \quad (2.9.)$$

This form of the wave equations shows that the disturbance is propagated with velocity $\frac{v}{\sqrt{\varepsilon\mu}}$. By definition the refractive index n, of any non-absorbing medium is the ratio of the velocity of light in vacuum to the velocity of light in the medium. We therefore have that $n = \sqrt{\varepsilon\mu}$. At optical frequencies μ is very nearly unit for all materials so that we may write $n = \sqrt{\varepsilon}$. We consider only sinusoidal solutions. Such a solution for the equation of the vector wave of the electric field strength $\underline{E}$ in general form is

$$\underline{E} = E_0 \exp i\omega\left\{t - \frac{n(ax + by + cz)}{v}\right\} \qquad \ldots \quad (2.10.)$$

To consider the case of electromagnetic propagation in conducting media ($\sigma \neq 0$) we return to equations (2.1.) - (2.9.) /

$$\frac{\partial \underline{E}}{\partial t} = i\omega \underline{E}$$

from which $\sigma \underline{E} = -\frac{i\sigma}{\omega}\frac{\underline{E}}{t}$

Equation (2.5.) can also be written as

$$\text{curl } \underline{H} = \frac{4\pi}{v}\left(-\frac{i\sigma}{\omega}\right)\frac{\partial \underline{E}}{\partial t} + \frac{\varepsilon}{v}\frac{\partial \underline{E}}{\partial t}$$

$$= \frac{1}{v}\left(\varepsilon - \frac{i4\pi\sigma}{v}\right)\frac{\partial \underline{E}}{\partial t} = \frac{\underline{\varepsilon}}{v}\frac{\partial \underline{E}}{\partial t}$$

where $\underline{\varepsilon}$ is the Complex Permittivity,

$$\underline{\varepsilon} = \varepsilon - \frac{i4\pi\sigma}{\omega}$$

Equation (2.5.) may therefore be written

$$\text{curl } \underline{H} = \frac{\underline{\varepsilon}}{v}\frac{\partial \underline{E}}{\partial t}$$

This substitution allows Maxwell's equation for isotropic conducting media to be expressed in the same way as for isotropic dielectrics except that for a dielectric the permittivity is real while for metals it is a complex number. We may write for a solution the expression :-

$$\underline{E} = \underline{E}_0 \exp i\omega\left[t - \frac{\alpha(ax + by + cz)}{v} + \frac{i\beta(a'x + b'y + c'z)}{v}\right] \quad \ldots \quad (2.11.)$$

a, b, c represent the direction-cosines of planes of equal phase; a', b', c' represent the direction-cosines of planes of equal amplitude.

2.2.) Oblique Incidence.

The solution for the wave equation may now be written in an analogous form to that for non-conducting media. If the metal surface is represented by the plane z = 0 and the incidence plane of the light is that defined by the x and z directions, the solution for the vector wave of the electric field strength may be written

$$\underline{E} = \underline{E}_0 \exp i\omega\left(t - \frac{\underline{a}x + \underline{b}z}{c}\right)$$

Substituting into the generalized wave equation we obtain

$$\frac{1}{c^2}\left(\varepsilon\mu - \frac{i4\pi\sigma\mu}{\omega}\right) = \frac{\mu\underline{\varepsilon}}{c^2} = \frac{\underline{a}^2 + \underline{b}^2}{c^2} \qquad \text{i.e. } \mu\underline{\varepsilon} = \underline{a}^2 + \underline{b}^2$$

If it is assumed that the conductivity is not zero the cosines $\underline{a}$ and $\underline{b}$ cannot be generally real numbers. We may thus express $\underline{a}$ and $\underline{b}$ in the general form

$\underline{a} = \text{Sin}\,\phi - ik'x$

$\underline{b} = \text{Cos}\,\phi - ik'z$

So that the wave equation for the electric field strength is

$$\underline{E} = \underline{E}_0 \exp - \frac{\omega}{c}\left(k'_x x + k'_z z\right) \exp i\omega\left(t - \frac{x\,\text{Sin}\,\phi + z\,\text{Cos}\,\phi}{c}\right) \qquad \ldots \qquad (2.12.)$$

Equation (2.12.) shows that planes of constant phase are given by

$$x\,\text{Sin}\,\phi + z\,\text{Cos}\,\phi = P \qquad \ldots \qquad (2.13.)$$

and planes of equal amplitude by

$$k'_x x + k'_z z = Q \qquad \ldots \quad (2.14.)$$

Writing $k'_x = k' \operatorname{Sin} \alpha \qquad k'_z = k' \operatorname{Cos} \alpha$ ... (2.15.)

we can write (2.14.) in the form

$$k' (x \operatorname{Sin}\alpha + z \operatorname{Cos}\alpha) = Q \qquad \ldots \quad (2.16.)$$

where k is termed the Index of Absorption. ϕ is the angle between the z-axis and the normal to the plane of equal phase. Similarly α is the angle between the z-axis and the normal to the plane of equal amplitude. P and Q are constants. In materials having a high absorption like metals, the plane of equal amplitude may be taken as the plane parallel to that of z = 0. Hence α may be put equal to zero. The equation for the wave vector then simplifies to

$$\underline{E} = \underline{E}_0 \exp -\left(\frac{\omega}{v} k' z\right) \exp i\omega \left(t - \frac{x \operatorname{Sin} \phi + z \operatorname{Cos} \phi}{v} \right) \qquad \ldots \quad (2.17.)$$

If we put the path of the ray $z = \lambda' = \frac{v}{\omega}$, the amplitude is attenuated in the ratio $1 : \exp - (2\pi n k')$.

The factor k', which is a measure of the amplitude, is therefore called the Index of Absorption. The factor $nk' = k$ is termed the Absorption Coefficient.

There are in existence two methods of indicating complex refractive index. These are

$\underline{n} = n(1 - ik')$, and

$\underline{n} = n - ik$.

Throughout this work the second form, viz. $\underline{n} = n - ik$ will be employed.

2.3.) Normal Incidence.

For a plane wave incident normally on a metal the direction of maximum damping given by (a', b', c') coincides with the direction of phase propagation given by (a, b, c). We may thus write in place of equation (2.11.) the expression

$$\underline{E} = \underline{E}_0 \exp i\omega \left[t - \frac{(n - ik)(ax + by + cz)}{c}\right] \qquad \ldots \quad (2.18.)$$

As before n represents the ratio of the velocity of light in the medium to the velocity in vacuum, k' is termed the Absorption Coefficient and represents the amplitude reduction. It can be seen that the amplitude of the electric vector decreases by the factor $\exp\left(-\frac{\omega k}{c}\right)$ - i.e. $\exp(-2\pi k)$, for a path length of one vacuum wavelength in the medium. We write $\underline{n} = n - ik$, where $\underline{n}$ is termed the complex refractive index of the medium for the wavelength used. It can be seen from the equation of propagation that

$\underline{n}^2 = (n - ik)^2 = \underline{\varepsilon} = \varepsilon - i\,\frac{2\sigma}{f}$. Hence

$n^2 - k^2 - 2ink = \varepsilon - i\,\frac{2\sigma}{f}$.

Equating real and imaginary parts gives

$$n^2 - k^2 = \varepsilon$$

$$nk = \frac{\sigma}{f}.$$

2.4.) Reflectance and Transmittance of a Thin Metal Film on a Non-absorbing Substrate at Normal Incidence.

The derivation of the expressions for the reflected and transmitted intensities of a beam of monochromatic light at a metal film bounded by two semi-infinite non-absorbing media has been dealt with by various authors. Abelès(2.1.) devised a matrix method involving Fresnel Coefficients which was suitable for any number of layers on a substrate. The method was suitable for use when any number of the layers was absorbing and also if the substrate was absorbing too. However in such cases the resulting expressions for reflectance and transmittance become extremely cumbersome. In the present investigation the relevant situation is that of a single metal film on a non-absorbing substrate, viz. glass, receiving a normally incident light beam. It will be seen that in this case the resulting expressions are fairly amenable to computation.

Consider a plane monochromatic infinite wave train of unit intensity travelling in air or vacuo to fall normally on a semi-infinite glass slab on which lies a metal film. We define R to be the intensity reflected back into the air and T to be the intensity transmitted through to the glass. Reversing the direction of the incident beam and allowing it to fall normally on the metal film from the glass side we define R' to be the intensity reflected back into the glass and T' to be the intensity transmitted to the air. The equations obtained are ultimately expressed in terms of,

n_o the refractive index of the air,

n_1 and k_1 the real and imaginary parts respectively of the complex refractive index of the metal film,

n_2 the refractive index of the glass substrate,

d_1 the thickness of the metal film, and

λ the vacuum wavelength of the light beam.

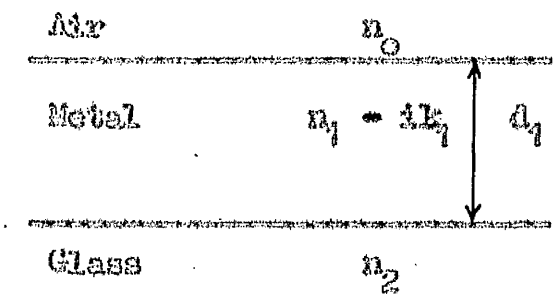

Heavens (Optical Properties of Thin Solid Films, Butterworths, London, 1955.) gives equations for R, R' and T which for convenience are expressed in terms of the following functions :-

$$g_1 = \frac{n_o^2 - n_1^2 - k_1^2}{(n_o + n_1)^2 + k_1^2}, \quad h_1 = \frac{2n_o k_1}{(n_o + n_1)^2 + k_1^2},$$

$$g_2 = \frac{n_1^2 - n_2^2 + k_1^2}{(n_1 + n_2)^2 + k_1^2}, \quad h_2 = \frac{-2n_2 k_1}{(n_1 + n_2)^2 + k_1^2},$$

$$p_2 = \mathrm{Exp}\left(\frac{+2\pi k_1 d_1}{\lambda}\right)\mathrm{Cos}\,\frac{2\pi n_1 d_1}{\lambda}, \quad q_2 = \mathrm{Exp}\left(\frac{+2\pi k_1 d_1}{\lambda}\right)\mathrm{Sin}\,\frac{2\pi n_1 d_1}{\lambda},$$

$$t_2 = \mathrm{Exp}\,\frac{-2\pi k_1 d_1}{\lambda}\left(g_2\,\mathrm{Cos}\,\frac{2\pi n_1 d_1}{\lambda} + h_2\,\mathrm{Sin}\,\frac{2\pi n_1 d_1}{\lambda}\right),$$

$$u_2 = \mathrm{Exp}\,\frac{-2\pi k_1 d_1}{\lambda}\left(h_2\,\mathrm{Cos}\,\frac{2\pi n_1 d_1}{\lambda} - g_2\,\mathrm{Sin}\,\frac{2\pi n_1 d_1}{\lambda}\right),$$

$$p_{12} = p_2 + g_1 t_2 - h_1 u_2 .$$

$$q_{12} = q_2 + h_1 t_2 + g_1 u_2 \quad ,$$

$$t_{12} = t_2 + g_1 p_2 - h_1 q_2 \quad ,$$

$$u_{12} = u_2 + h_1 p_2 + g_1 q_2 \quad ,$$

$$R_1 = \frac{t_{12}^2 + u_{12}^2}{p_{12}^2 + q_{12}^2}$$

$$\text{Hence } R = \frac{(g_1^2 + h_1^2)e^{2\alpha_1} + (g_2^2 + h_2^2)e^{-2\alpha_1} + A \cos 2\gamma_1 + B \sin 2\gamma_1}{e^{2\alpha_1} + (g_1^2 + h_1^2)(g_2^2 + h_2^2)e^{-2\alpha_1} + C \cos 2\gamma_1 + D \sin 2\gamma_1} \quad \ldots \quad (2.19.)$$

where

$$A = 2(g_1 g_2 + h_1 h_2) \quad , \qquad B = 2(g_1 h_2 - g_2 h_1) \quad ,$$

$$C = 2(g_1 g_2 - h_1 h_2) \quad , \qquad D = 2(g_1 h_2 + g_2 h_1) \quad ,$$

$$\alpha_1 = \frac{2\pi k_1 d_1}{\lambda} \quad , \qquad \gamma_1 = \frac{2\pi n_1 d_1}{\lambda}$$

Also

$$R' = \frac{(g_2^2 + h_2^2)e^{2\alpha_1} + (g_1^2 + h_1^2)e^{2\alpha_1} + A \cos 2\gamma_1 - B \sin 2\gamma_1}{e^{2\alpha_1} + (g_1^2 + h_1^2)(g_2^2 + h_2^2)e^{-2\alpha_1} + C \cos 2\gamma_1 + D \sin 2\gamma_1} \quad \ldots \quad (2.20.)$$

and

$$T = \frac{n_2}{n_0} \frac{\left[(1 + g_1)^2 + h_1^2\right]\left[(1 + g_2)^2 + h_2^2\right]}{e^{2\alpha_1} + (g_1^2 + h_1^2)(g_2^2 + h_2^2)e^{2\alpha_1} + C \cos 2\gamma_1 + D \sin 2\gamma_1} \quad \ldots \quad (2.21.)$$

For a check the identity $R + T < 1$ may be employed.

An approximate value for T may be obtained from the equation,

$$T \doteq \frac{n_2}{n_0} \exp \frac{(-4\pi k_1 d_1)}{\lambda} ,$$

if the film is heavily absorbing and of such a thickness that multiple reflections within the film may be neglected.

It may be noted here that the equation (2·20) differs from that given by Heavens in that the sign before the last term in the numerator is negative.

In general R and R' are different when the refractive indices of the two bounding media of the film are different. T_1 is the same however irrespective of the direction of travel of the incident light beam, i.e. T = T'.

The expressions (2.19.) - (2.21.) obtained above allow the evaluation of the two reflectances and transmittance when the optical constants pertaining are known. The converse problem, viz. to obtain the optical constants of a given metal film knowing R, R', T and the optical constants of the bounding media, cannot be directly solved by analytical methods. To circumvent this difficulty several authors have devized graphical methods to obtain n and k for a metal film. These usually involve knowledge of at least three of the following quantities :-

R, R', T, as previously defined,

ϕ_R the phase change of the light on reflection at the metal/air interface,

$\phi_{R'}$ the phase change of the light on reflection at the metal/glass interface,

ϕ_T the phase change of the light on transmission through the film, the incident light being from the air side,

$\phi_{T'}$ the phase change of the light on transmission through the film, the incident light being from the glass side,

d the thickness of the film.

In this work the method employed is one due to Malé(2.2.). This method uses R, R' and T to give a simultaneous determination of n, k and d. An outline of the method is as follows :-

Using equations (2.19.), (2.20.) and (2.21.), R, R' and T are obtained for varying values of n_1, k_1 and d_1, each of which is allowed to vary independently. The value assigned to δ is that employed in the experimental determination of R, etc. Graphs of R vs. δ where $\delta = \frac{4\pi n_1 d_1}{\lambda}$ for the various n_1, k_1, d_1 values are constructed. Similarly graphs of R' and T vs. δ are constructed. These curves are represented diagramatically in figure 21(a), (b) and (c).

Along the value of T derived from experiment a horizontal line is drawn on the curve of T vs. δ, fig. 21(c). At the intersection of this line with the various curves the values of δ are /

are noted, viz. δ_1, δ_2, etc. In the curve of R' vs. perpendiculars are drawn through the δ_1, δ_2, etc. to intersect their corresponding curves of $n_1 k_1$, etc. The points obtained are used to construct curves of R vs. n for various k as shown in figure22.a. Points on this set of curves satisfy R and T simultaneously. A similar process is adopted for δ_1, δ_2, etc. and R', giving curves of R' vs. n for various k, (fig.22.b.).

The experimental values of R and R' are now drawn as horizontal lines on their appropriate curves, viz. figs.22.a. and 22.b. The intersections with the curves give points which enable two curves of n vs. k to be drawn, one derived from R vs. n, and one from R' vs. n, viz. fig. 2.3. The point of intersection of the two curves gives a value of n and k which satisfied simultaneously R, R' and T.

To obtain the film thickness a horizontal line is drawn corresponding to the experimental value of R on the curve of R vs. δ fig.21.a. This enables a curve of n vs. δ for various k to be constructed, viz. fig. 2.4. When the final values of n and k have been determined the point corresponding to these values on the n vs. δ curve of fig. 2.4. will give δ and hence d.

It is apparent that the compilation of a set of curves of R, R' and T for a range of n, k and d is a tedious process. Malé(2.2.) avoided this task by use of a nomogram to calculate the Fresnel Coefficients for a given n and k pair. Using the derived /

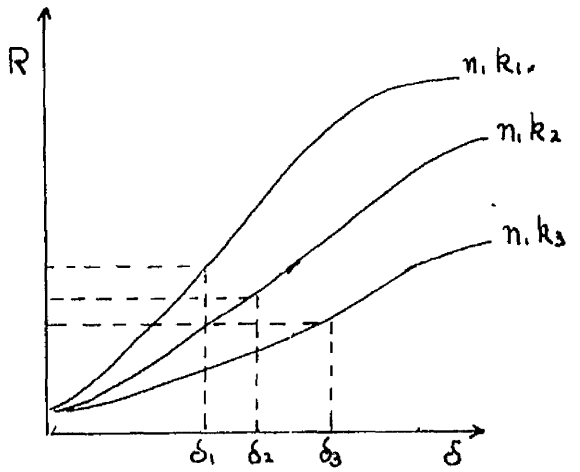

Fig. 2.1.a.

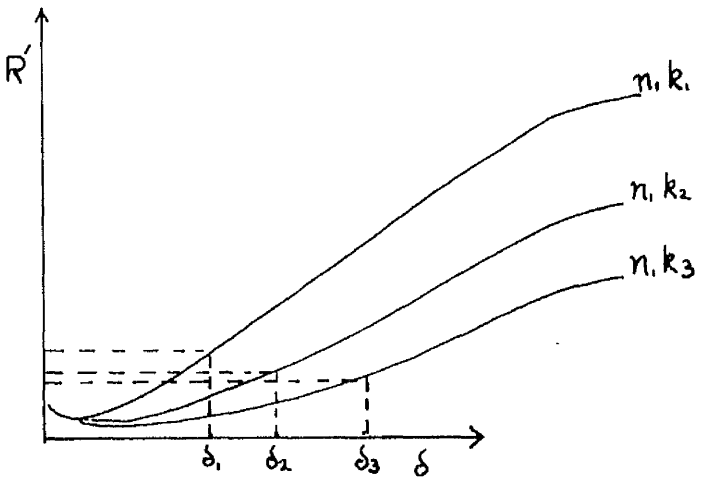

Fig. 2.1.b.

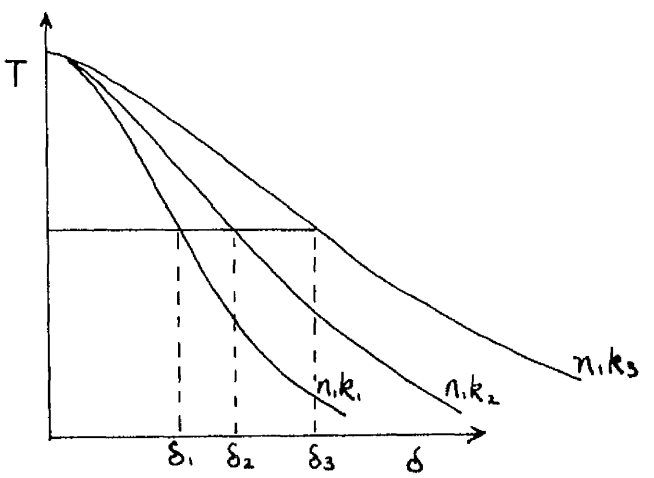

Fig. 2.1.c.

Figs. 2.1.a, b, c. Curves for Use with the Malé Method of Determining Refractive Index and Thickness of Thin Films.

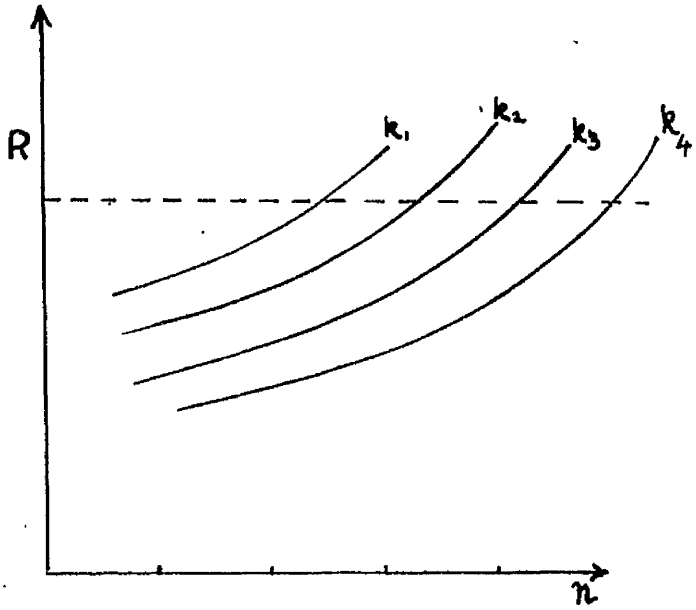

Fig. 2.2.a. R vs. n for various k's.

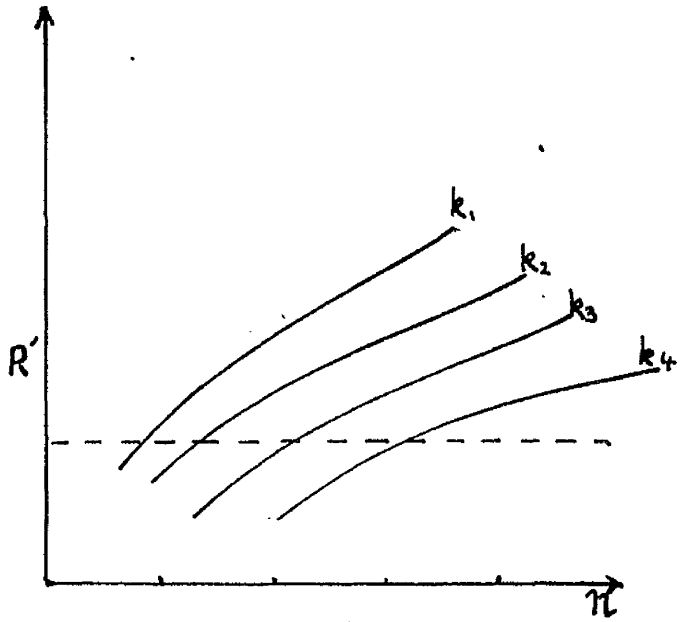

Fig. 2.2.b. R' vs. n for various k's.

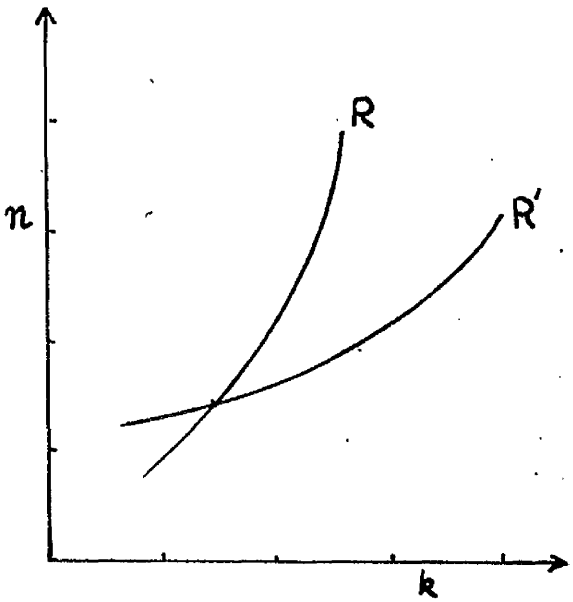

Fig. 2.3. n vs. k curves for R and R'.

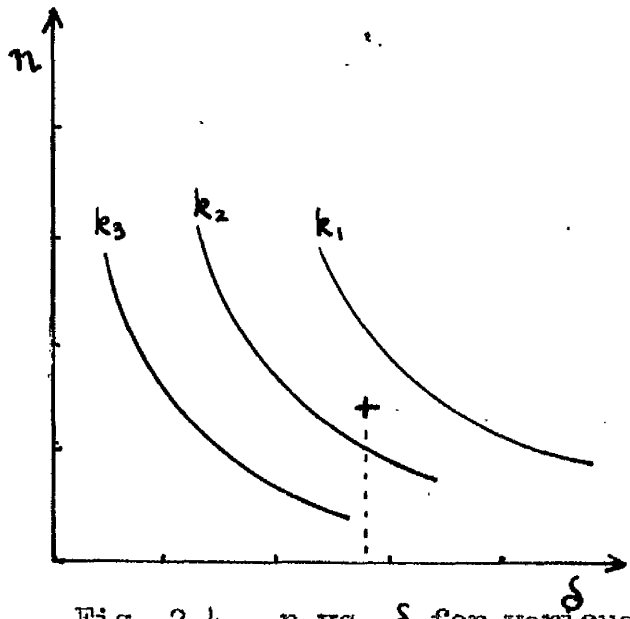

Fig. 2.4. n vs. δ for various k's. Derived from Fig. 1.a.

derived Coefficients and a specific δ value he then constructed a simple vector diagram to obtain R, R' and T. In the present work a programme was constructed for the "Deuce" computer at Glasgow University. From the existing values of n and k for bulk metals a range of n, k and δ was selected which would be suitable for all metals investigated. The range and intervals of the parameters is given in table (1).

To obtain an accuracy consistent with that of the computer the reflectances and transmittances were graphed on large squared sheets with a scale of 1 centimetre equal to an interval of 1% in reflectance and transmittance, and 5 centimetres equal to an interval of 0.1 in δ.

In the case of thick films, i.e. those for which T is zero, we may employ the approximate relationships derived by Rouard(2.3.) :-

$$n = \frac{n_2^2 - n_o^2}{2(n_2 B_2 - n_o B_o)} \qquad \ldots \quad (2.22.)$$

$$\left.\begin{aligned} k^2 &= 2n_o B_o n_1 - (n_1^2 + n_o^2) \\ &= 2n_2 B_2 n_1 - (n_1^2 + n_2^2) \end{aligned}\right\} \qquad \ldots \quad (2.23.)$$

where, $B_o = \frac{1 - R}{1 + R}$, $B_2 = \frac{1 - R'}{1 + R'}$.

These expressions permit the direct calculation of n and k for thick films providing R and R' are not too high.

TABLE 1.

Range of n, k, δ Values for Computation of T, R and R'.

n	k	δ
0	0	0
0.5	0.5	0.025
1.0	1.0	0.05
1.5	1.5	0.1
2.0	2.0	0.25
2.5	2.5	0.5
3.0	3.0	0.75
3.5	3.5	1.0
4.0	4.0	2.0
4.5	4.5	3.0
5.0	5.0	5.0
		8.0

2.5.) Determination of Optical Constants Using Polarimetry.

Drude(2.4.) showed that when a beam of light, plane polarized at an angle of $\pi/4$ to the plane of incidence, is reflected from a metal surface, the reflected beam is in general elliptically polarized and the optical constants of the metal can be deduced from measurements of the ellipticity.

The Fresnel equations for reflection of a beam of light incident at an angle ϕ at the interface between two media are

$$r_p = \frac{\mathrm{Tan}\,(\phi - \theta)}{\mathrm{Tan}\,(\phi + \theta)} \qquad \ldots \quad (2.24.)$$

$$r_s = \frac{\mathrm{Sin}\,(\phi - \theta)}{\mathrm{Sin}\,(\phi + \theta)} \qquad \ldots \quad (2.25.)$$

$$t_p = \frac{2\,\mathrm{Sin}\,\theta\,\mathrm{Cos}\,\phi}{\mathrm{Sin}\,(\phi + \theta)\,\mathrm{Cos}\,(\phi - \theta)} \qquad \ldots \quad (2.26.)$$

$$t_s = \frac{2\,\mathrm{Sin}\,\theta\,\mathrm{Cos}\,\phi}{\mathrm{Sin}\,(\phi + \theta)} \qquad \ldots \quad (2.27.)$$

r_p and t_p are the reflection and transmission coefficients of the component parallel to the plane of incidence,

r_s and t_s are the reflection and transmission coefficients of the component perpendicular to the plane of incidence,

ϕ is angle of refraction of the light beam in the second medium.

In the case where both media are non-absorbing θ and ϕ are real. In the case of a light beam in air striking a metal surface, ϕ is real but θ is complex; we may therefore write :-

$$\underline{r}_p = r_p \exp i\,\delta_p$$

$$\underline{r}_s = r_s \exp i\,\delta_s \,.$$

$$\frac{\underline{r}_s}{\underline{r}_p} = \frac{r_s}{r_p} \exp i\,(\delta_s - \delta_p) = \operatorname{Tan}\psi \exp i\Delta = -\frac{\operatorname{Cos}(\phi - \theta)}{\operatorname{Cos}(\phi + \theta)} \qquad \ldots \qquad (2.28.)$$

where $\frac{r_s}{r_p} = \operatorname{Tan}\psi$. $\qquad (\delta_s - \delta_p) = \Delta$.

From Snell's Law,

$$\operatorname{Sin}\theta = \frac{\operatorname{Sin}\phi}{\underline{n}} = \frac{\operatorname{Sin}\phi}{n - ik}$$

Re-arranging equation (2.22.) we get

$$\frac{1 + \operatorname{Tan}\psi \exp i\Delta}{1 - \operatorname{Tan}\psi \exp i\Delta} = \frac{\operatorname{Sin}\phi \operatorname{Sin}\theta}{\operatorname{Cos}\phi \operatorname{Cos}\theta} = \frac{\operatorname{Sin}\phi \operatorname{Tan}\phi}{\sqrt{\underline{n} - \operatorname{Sin}^2\phi}}$$

and

$$\frac{1 - \operatorname{Tan}\psi \exp i\Delta}{1 + \operatorname{Tan}\psi \exp i\Delta} \cdot \frac{1 + \operatorname{Tan}\psi \exp - i\Delta}{1 + \operatorname{Tan}\psi \exp - i\Delta} = \frac{1 - 2\,i \operatorname{Tan}\psi \operatorname{Sin}\Delta - \operatorname{Tan}^2\psi}{1 + 2 \operatorname{Tan}\psi \operatorname{Cos}\Delta + \operatorname{Tan}^2\psi} \,.$$

$$= \frac{\operatorname{Cos} 2\psi - i \operatorname{Sin} 2\psi \operatorname{Sin}\Delta}{1 + \operatorname{Sin} 2\psi \operatorname{Cos}\Delta}$$

For $|\underline{n}| > 1$ and since $\operatorname{Sin}\phi < 1$, we therefore can neglect $\operatorname{Sin}^2\phi$ compared with $\underline{n}^2$. We can therefore write

$$\frac{\operatorname{Cos} 2\psi}{1 + \operatorname{Sin} 2\psi \operatorname{Cos}\Delta} - i\,\frac{\operatorname{Sin} 2\psi \operatorname{Sin}\Delta}{1 + \operatorname{Sin} 2\psi \operatorname{Cos}\Delta} = \frac{n}{\operatorname{Sin}\phi \operatorname{Tan}\phi} - i\,\frac{k}{\operatorname{Sin}\phi \operatorname{Tan}\phi}$$

and equating real and imaginary parts we get

$$n = \frac{\operatorname{Sin}\phi \operatorname{Tan}\phi \operatorname{Cos} 2\psi}{1 + \operatorname{Sin} 2\psi \operatorname{Cos}\Delta} \qquad \ldots \qquad (2.29.)$$

$$k = \frac{\operatorname{Sin}\Delta \operatorname{Tan} 2\psi}{n} \qquad \ldots \qquad (2.30.)$$

Many metals, however, are covered with a non-absorbing film or skin, usually an oxide; and the equations (2.29.) and (2.30.) were derived without regard to the existence of such a film. Drude extended his theory to take into account the existence of such a film of refractive index n_1 and thickness L_1 where the metal constants are still (n, k). The equations he derived are -

$$\Delta - \bar{\Delta} = - \frac{4\pi L}{\lambda} \frac{\cos\phi \sin^2\phi}{(\cos^2\phi - a)^2 + a'^2} \left(1 - \frac{1}{n_1^2}\right) (\cos^2\phi - a) \quad \ldots \quad (2.31.)$$

$$2(\psi - \bar{\psi}) = \frac{4\pi L}{\lambda} \frac{\sin 2\bar{\psi} \cos\phi \sin^2\phi \, a'}{(\cos^2\phi - a)^2 + a'^2} (1 - n_1^2 \cos^2\phi) \left(1 - \frac{1}{n_1^2}\right) \quad \ldots \quad (2.32.)$$

where $a = \dfrac{n^2 - k^2}{(n^2 + k^2)^2}$

$a' = \dfrac{2nk}{(n^2 + k^2)^2}$

Δ and $\bar{\Delta}$ represent the relative phase shifts on reflection with the film and without the film respectively,

Tan ψ and Tan $\bar{\psi}$ represent the amplitude reflection ratios with and without the film,

λ is the wavelength of the light,

the measurements being made in air or vacuo.

Tronstad(2.5.) re-arranged the above equations to give n_1 and L directly as functions of the other variables, i.e.

$$n_1^2 = \left(1 + \frac{2(\psi - \bar{\psi})}{(\Delta - \bar{\Delta})} \frac{\cos^2\phi - a}{a' \sin 2\bar{\psi} \cos^2\phi}\right) \frac{1}{\quad} \qquad \ldots \quad (2.33.)$$

$$L = - \frac{\pi (\Delta - \bar{\Delta})}{180 A \left(1 - \frac{1}{n_1^2}\right)} \qquad \ldots \quad (2.34.)$$

where $(\Delta - \bar{\Delta})$ is measured in degrees and, likewise $(\psi - \bar{\psi})$.

$$A = \frac{4\pi}{\lambda} \frac{\cos\phi \sin^2\phi (\cos^2\phi - a)}{(\cos^2\phi - a)^2 + a'^2}$$

Re-arranging equations (2.29.) and (2.30.) it can be seen that,

$$\cos 2\bar{\psi} = \frac{2n \sin\phi \tan\phi}{(n^2 + k^2 + \sin^2\phi \tan^2\phi)} \qquad \ldots \quad (2.35.)$$

$$\sin \bar{\Delta} = k/(n \tan 2\bar{\psi}) \qquad \ldots \quad (2.36.)$$

Since it is generally impossible to obtain a perfectly clean surface of the metal to give measurements of $\bar{\psi}$, $\bar{\Delta}$ and hence n and k, the method used to obtain n_1 and L is to substitute trial values of n and k for a particular ϕ in equations (2.35.) and (2.36.) to obtain values of $\bar{\psi}$ and $\bar{\Delta}$. An outline of the procedure is as follows :-

(1) Set ϕ

(2) Measure ψ, Δ

(3) Select spaced pairs of n and k in the neighbourhood of an expected value (n_1k_1, n_1k_2, n_1k_3 ..., n_2k_1, n_2k_2, n_2k_3, ..., etc.)

(4) Obtain n_1 and L for each pair of n,k.

(5) Reset ϕ

(6) Measure new ψ, Δ

(7) Using same n,k pairs as in (3) obtain n_1 and L for each n,k pair.

Repeat this process (5) to (7) for five or six values of ϕ and search for n,k pairs giving constancy in the calculated values of n_1 and L for the various ϕ. When a pair of values of n and k have been found which give a degree of constancy in n_1 and L for various ϕ then the process is repeated for a short range of n and k in the neighbourhood of the selected values, the interval between successive values being greatly reduced. There should occur a new pair of n,k for which a higher degree of constancy in n_1 and L is obtained. Successive approximation gives n and k to any required degree of accuracy.

2.6.) <u>The Poincaré Sphere.</u>

A convenient method of describing polarized light and the action of different optical components on such a beam of light is the use of the Poincaré Sphere(2.6.), so called after its originator. Various authors (2.7.)-(2.11.) have used the method to eliminate the more elaborate analytical methods of treating the transmission and reflection of light by media exhibiting optical rotation, berefringence, etc. By its use the relations of spherical trigonometry which enable calculations to be made connecting optical changes with observable quantities can be easily visualized and the required equations obtained.

The three possible forms of polarized light are (a) elliptic, (b) circular, (c) linear. By consideration of the /

the general equation for an ellipse we see that the circle and straight line may be regarded as particular cases of it. To derive the Poincaré representation therefore we need only consider the case of the ellipse and the other two types of polarization should follow from it. In the geometry of conic sections each type of conic may be regarded as having asymptotes in the plane of the section. In the cases of the hyperbola and parabola these asymptotes are real and can be drawn. If one carries the analogy to the case of the ellipse it is found that the solutions for the equation of the asymptotes are complex numbers. We may therefore characterise an ellipse by plotting a point on the complex plane whose co-ordinates give the parameters of the equation of one of the complex asymptotes of the ellipse.

Consider a Cartesian co-ordinate system OX, OY, OZ and let the OZ direction be that in which a beam of monochromatic elliptically polarized light is travelling. The light vector describing the beam rotates about the Z-axis as it travels along while at the same time its magnitude varies sinusoidally. This vector can be resolved into two mutually perpendicular components which in general differ in magnitude and have a constant phase difference. Let the leading or fast component lie along the OX axis, then the lagging or slow component will lie along the OY axis. We may then represent the disturbance by its component equations -

$$X = A \exp i(\omega t - \Delta) \qquad \ldots \quad (2.37.)$$

$$Y = B \exp i\omega t \qquad \ldots \quad (2.38.)$$

where $\omega = \frac{2\pi}{T}$ represents the angular velocity of the vector, T the vibration period, and t the time which has elapsed. Δ represents the phase lag of Y behind X.

We have therefore,

$$\frac{Y}{X} = \frac{B}{A} \exp i\Delta = \frac{B}{A} \operatorname{Cos}\Delta + i\frac{B}{A} \operatorname{Sin}\Delta = u + iv \qquad \ldots \quad (2.39.)$$

Considering only the real parts of equations (2.37.) and (2.38.) we can eliminate t and get :-

$$\frac{X^2}{A^2} + \frac{Y^2}{B^2} - \frac{2XY}{AB} \operatorname{Cos}\Delta = \operatorname{Sin}^2\Delta \qquad \ldots \quad (2.40.)$$

We see that equation (2.40.) represents an ellipse lying in the XY plane inscribed in a rectangle of sides 2A and 2B as shown in fig. 2.5. The shape of the ellipse is given by the ellipticity e which is the ratio of the major to the minor axis, i.e. $e = \frac{b}{a}$. The orientation of the ellipse is given by the angle θ which is termed the Azimuthal Angle measured from some reference plane $(0 \leq \theta \leq \pi)$. From fig. 2.5. the following relations are apparent,

$$\operatorname{Tan} \epsilon = \frac{b}{a} \qquad (0 \leq \epsilon \leq \tfrac{\pi}{2}) \qquad \ldots \quad (2.41.)$$

$$\operatorname{Tan} \gamma = \frac{B}{A} \qquad (0 \leq \epsilon \leq \tfrac{\pi}{2}) \qquad \ldots \quad (2.42.)$$

The direction of rotation of the light vector is termed positive when the rotation of the vector is anti-clockwise as seen /

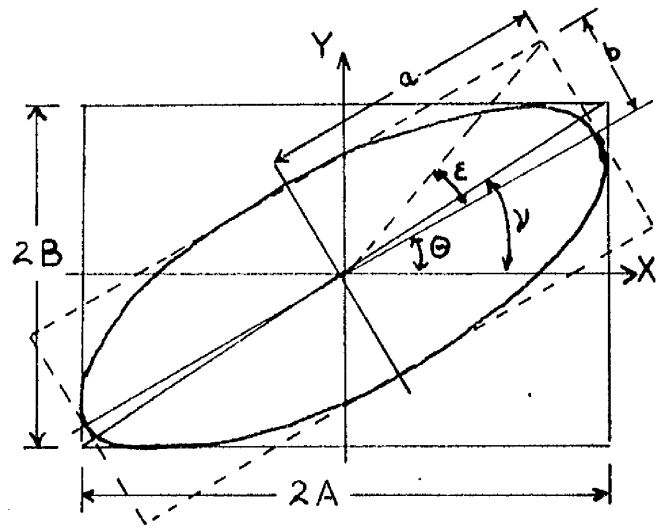

Fig. 2.5. Parameters of an elliptical vibration having components of amplitude A and B along the ox and oy axes, respectively. Tan ε = b/a. The major and minor axes of the ellipse are 2a and 2b; the ellipticity e = b/a = Tan ε ; the azimuth is θ with respect to the axis ox.

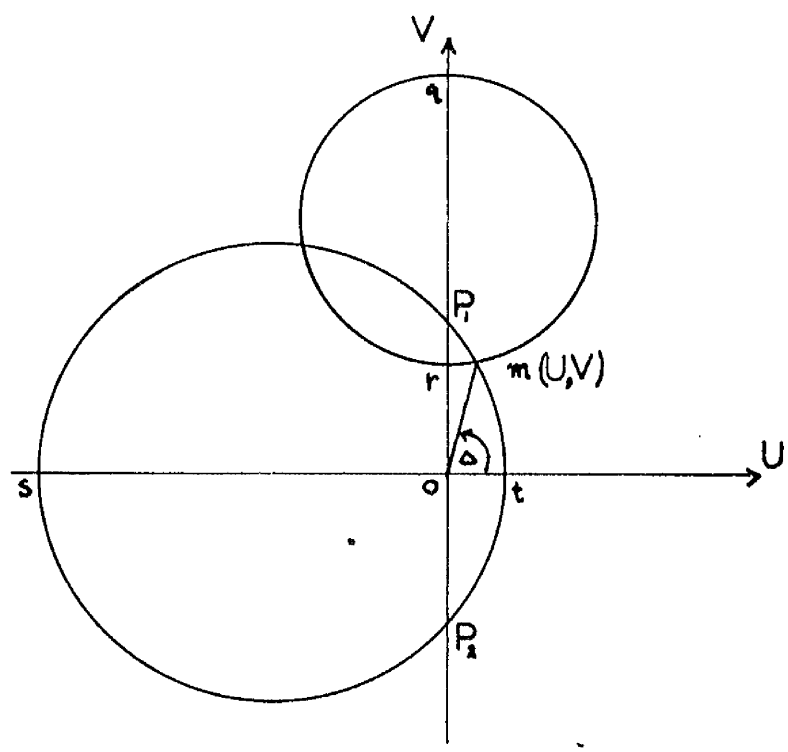

Fig. 2.6. Representation of elliptically polarized light by a point m on a plane. Δ is the phase difference between the components of the ellipse.

seen by an observer looking along the beam towards the source, and negative when rotation is in the opposite sense. Born(2.12.) has suggested that this convention might be replaced by that of the well-known Right-Hand Screw Rule applied to the light vector. This would result in an interchange of the terms positive and negative as used in this work.

The following relationships also exist(2.7.),

$$A^2 + B^2 = a^2 + b^2 \quad \ldots \quad (2.43.)$$

$$A^2 - B^2 = (a^2 - b^2) \operatorname{Cos} 2\theta \quad \ldots \quad (2.44.)$$

$$AB \operatorname{Sin} \Delta = \pm ab \quad \ldots \quad (2.45.)$$

$$2AB \operatorname{Cos} \Delta = (a^2 - b^2) \operatorname{Sin} 2\theta \quad \ldots \quad (2.46.)$$

Substitution from (2.41.) and (2.42.) into equations (2.43.) - (2.46.) gives the following relationships

$$\operatorname{Cos} 2\epsilon = \operatorname{Cos} 2\nu \operatorname{Cos} 2\theta + \operatorname{Sin} 2\nu \operatorname{Sin} 2\theta \operatorname{Cos} \Delta \quad \ldots \quad (2.47.)$$

$$\pm \operatorname{Sin} 2\epsilon = \operatorname{Sin} 2\nu \operatorname{Sin} \Delta \quad \ldots \quad (2.48.)$$

$$\operatorname{Tan} 2\theta = \operatorname{Tan} 2\nu \operatorname{Cos} \Delta \quad \ldots \quad (2.49.)$$

From equations (2.47.) to (2.49.),

$$\operatorname{Cos} 2\nu = \operatorname{Cos} 2\epsilon \operatorname{Cos} 2\theta \quad \ldots \quad (2.50.)$$

$$\pm \operatorname{Tan} 2\epsilon = \operatorname{Sin} 2\theta \operatorname{Tan} \Delta \quad \ldots \quad (2.51.)$$

In equations (2.48.) and (2.51.) the upper or lower sign holds according as the direction of rotation of the vector is to the left or right respectively.

The equation for the asymptotes is derived from equation (2.40.) and may be written,

$$\frac{X^2}{A^2} - \frac{2\cos\Delta}{AB}XY + \frac{Y^2}{B^2} = 0$$

i.e. $$\frac{X^2}{A^2} - \frac{\exp i\Delta + \exp - i\Delta}{AB}XY + \frac{Y^2}{B^2} = 0$$

i.e. $$\left(\frac{X}{A} - \frac{Y}{B}\exp i\Delta\right)\left(\frac{X}{A} - \frac{Y}{B}\exp - i\Delta\right) = 0$$

i.e. $\frac{X}{A} - \frac{Y}{B}\exp \pm i\Delta = 0$ represents the asymptotes.

Hence $Y = \frac{B}{A}\exp(\pm i\Delta) \cdot X$ ... (2.52.)

which is similar to equation (2.39.). Therefore given A, B and Δ we define uniquely the ellipse which represents the wave vector and this ellipse may be represented by a point m on a plane for which the abscissa and ordinate are u and v respectively. The Argand diagram is shown in fig. 2.6. where the vector Om represents the ratio $^B/_A$ and angle mOu represents Δ, the phase difference.

From equations (2.39.), (2.48.), (2.49.),

$$u^2 + v^2 + 2\cot 2\theta \cdot u - 1 = 0 \qquad \ldots \quad (2.53.)$$

$$u^2 + v^2 - 2\operatorname{cosec}\epsilon \cdot v + 1 = 0 \qquad \ldots \quad (2.54.)$$

From equation (2.53.) different values of θ give a set of circles which form a family with centres at the point $(-\cot 2\theta, 0)$ and of radius $\operatorname{cosec} 2\theta$. Similarly equation (2.54.) gives another family of circles for different values of ϵ, each of radius $\cot 2\epsilon$ and with centre at the point $(0, \operatorname{cosec} 2\epsilon)$. It may be shown that /

that the two systems of circles are orthogonal. Figure 2.6. shows two such circles. They intersect at m. By equation (2.53.), if $v = 0$, then $u = -\cot\theta$ or $\tan\theta$ giving the points s and t corresponding to linearly polarised light in azimuth $\cot^{-1}(-u)$ and $\tan^{-1}u$ respectively; if $u = 0$, then $v = \pm 1$, giving the points p_1 and p_2 corresponding to left or right circularly polarised light.

By a suitable stereographic projection(2.13.), the point m in the plane may be projected as a point M on a sphere. Thus if a sphere of diameter unity be described at O tangential to the plane uv and the points in the plane projected onto the surface of the sphere by joining them to O', where OO' is a diameter as shown in fig. 2.7., then the points p_1 and p_2 project into the poles P_1 and P_2 of the sphere, and by the principles of stereographic projection the families of circles given by equations (2.53.) and (2.54.) project into meridians of longitude (constant azimuth) and parallels of latitude (constant ellipticity), respectively. The vector Om on the uv plane projects into the arc OM on the sphere whose length is 2ν and the spherical angle MOT is Δ. Thus the point M on the sphere represents as does m on the plane, the state of polarization of the light.

To find the relationships between the co-ordinates of M and the parameters of the light, i.e. the ellipticity, azimuth, sense and phase difference, it is necessary to determine the co-ordinates in /

in terms of Θ and ϵ. If the centre of the sphere (fig. 2.7.) be taken as the origin of a co-ordinate system OX, OY, OZ, then the co-ordinates of m and O' referred to this origin are $(-\frac{1}{2}\text{Cos } 2\nu, -\frac{1}{2}\text{Sin } 2\nu \text{ Cos}\Delta, +\frac{1}{2}\text{Sin } 2\nu \text{ Sin}\Delta)$ and $(\frac{1}{2}, 0, 0)$, respectively. The co-ordinates of m as shown here do not agree with those given by Jerrard(2.10.).

We may now write the equation of the straight line O'm :-

$$\frac{x - \frac{1}{2}}{-\frac{1}{2}\text{Cos } 2\nu - \frac{1}{2}} = \frac{y}{-\frac{1}{2}\text{Sin } 2\nu \text{ Cos}\Delta} = \frac{z}{\frac{1}{2}\text{Sin } 2\nu \text{ Sin}\Delta} \quad \ldots \quad (2.55.)$$

The equation of the sphere is

$$x^2 + y^2 + z^2 = \frac{1}{4} \quad \ldots \quad (2.56.)$$

By solving (2.55.) and (2.56.) for x, y and z we obtain the co-ordinates of M the point of intersection of the line O'm with the sphere. Solving we obtain,

$$2x = \text{Cos } 2\epsilon \,.\, \text{Cos } 2\Theta \quad \ldots \quad (2.57.)$$

$$2y = \text{Cos } 2\epsilon \,.\, \text{Sin } 2\Theta \quad \ldots \quad (2.58.)$$

$$2z = \text{Sin } 2\epsilon \quad \ldots \quad (2.59.)$$

Thus if l $(-90^\circ \leq l \leq +90^\circ)$, and k $(0 \leq k \leq 360^\circ)$, represent the latitude and longitude, respectively, of the point M on the sphere, then,

$$\text{Sin } l = 2z = \text{Sin } 2\epsilon, \quad \ldots \quad (2.60.)$$

$$\text{and Tan } k = y/x = \text{Tan } 2\Theta \quad \ldots \quad (2.61.)$$

Hence by equation (2.60.), $l = 2\epsilon$, i.e. the tangent of half the latitude corresponds to the ellipticity, the sign of ϵ indicating the sence of rotation of the light vector, and by equation (2.61.) the longitude corresponds to twice the azimuth. The sphere for which points on its surface satisfy the equations (2.57.) to (2.61.) is called the Poincaré Sphere. In fig. 2.7. application of the cosine rule to the spherical triangle OMT gives equations (2.47.) and (2.50.), and application of the sine rule gives equation (2.48.). Equations (2.49.) and (2.51.) are derived from equations (2.47.), (2.48.) and (2.50.). Thus it can be seen that once M has been fixed the values of θ and ϵ can be found by relationships of equations (2.47.) to (2.51.). The spherical representation presents the advantage over the plane of being independent of the axis of reference.

The location of M is governed by the preceding theory in the following way: Any one vertical great circle may be taken as zero longitude. In fig. 2.8. zero longitude is taken as the great circle P_1OP_2 which may conveniently represent the direction of the OX axis of fig. 2.5. Azimuths are measured from this great circle, the direction OTO' being taken as positive. Points along the same longitude (e.g. P_1TP_2) represent light of the same azimuth but varying ellipticity. Points on the same parallel of latitude (e.g. RMQ) represent light of the same ellipticity but varying azimuth.

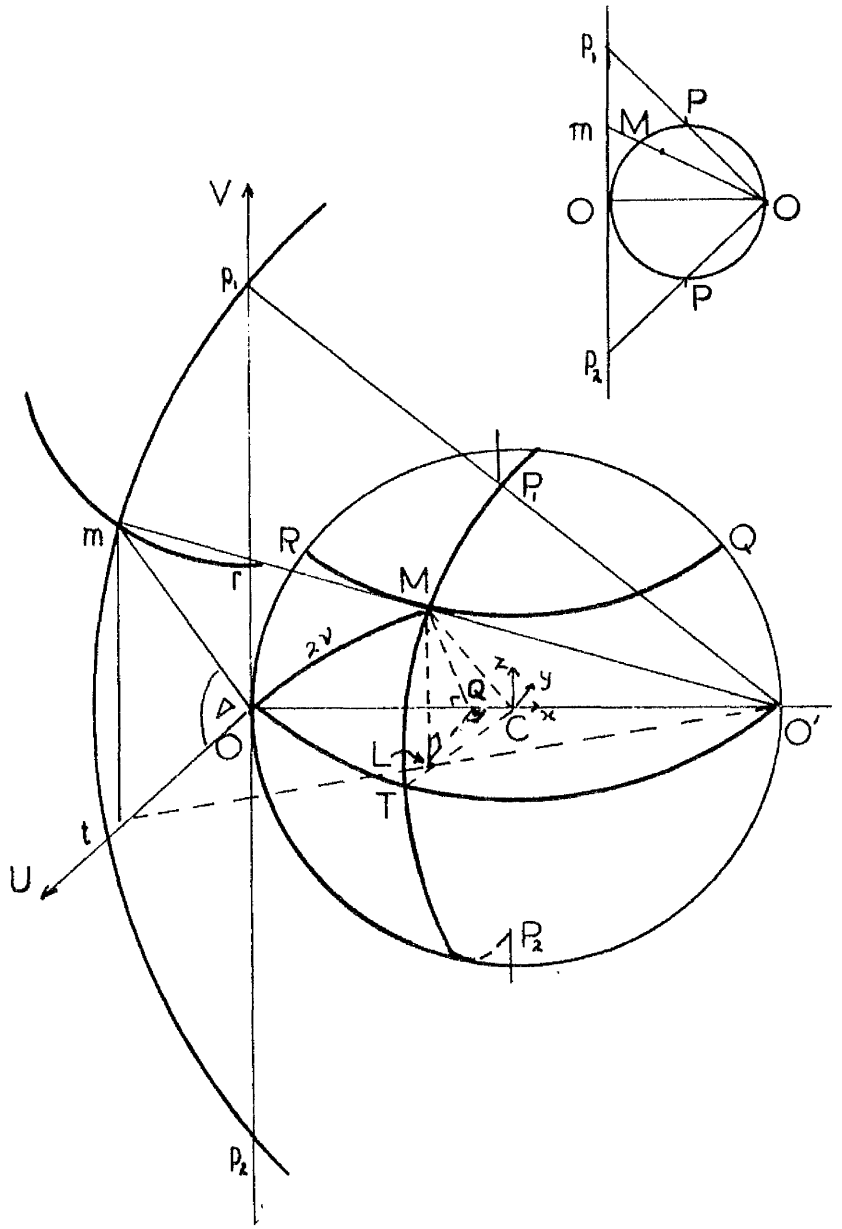

Fig. 2.7. Stereographic projection of a plane on a sphere. Elliptically polarized light is represented by the points m and M on the plane and sphere respectively. The vector Om projects into the arc OM of length 2ν; the angle projects into the spherical angle MOT. The latitude and longitude of M are l and k respectively,

For the upper and lower hemispheres ϵ is regarded as positive and negative respectively, corresponding to left and right elliptically polarized light. Points on the equator represent linearly polarized light; points at the poles P_1 and P_2 represent left and right circularly polarized light respectively. The effect of different components on a light beam may be traced by rotation of the sphere about the appropriate axes. If the ellipticity is maintained constant and the ellipse referred to different co-ordinate axes the values of the phase difference Δ, the azimuth θ, and the angle ν change. On the sphere this transformation is represented by a rotation about the vertical axis P_1P_2 while O is held fixed in direction in space, so that M moves along the parallel of latitude MQ. Rotation about the axis P_1P_2 is also equivalent to passage of polarized light through a plate with rotary power. In this case the azimuth of the elliptical vibration changes. The phase difference between the components does not change. One may imagine that the triangle OMF of fig. 2.8. has rotated bodily around P_1P_2 to a new position governed by the rotary power of the plate. Rotation of the sphere about the OO' axis with O fixed in space would move M along the small circle ns. In this case ν remains constant but Δ, ϵ and θ change, i.e. the phase difference, ellipticity and azimuth change. Such a transformation could be achieved by passage of the light beam represented by point M through a doubly refracting plate in azimuth zero, i.e. CO in fig. 2.8. and OX in fig. 2.5., or by reflection of /

of the light beam represented by M from a metal surface oriented in such a way that the azimuth of the vibration M is zero with respect to the metal surface, i.e. the normal to the metal surface and the azimuth of M are coplanar.

Calculation of Relative Phase Retardation Δ, and of Relative Amplitude Reduction, Tan ψ, from Polarization Spectrometer Readings.

The compensation process in the case of the polarizing spectrometer may now be illustrated and the relationship between the observed quantities and the constants of the elliptic vibration obtained. In fig. 2.9. the compensator plate of retardation δ with fast and slow axes at points K_F and K_S acting on the linear polarization represented by P produces the elliptical polarization Z by a rotation of δ about $K_F K_S$ in a clockwise direction. The arc PZ is a small circle with centre K_F. The reflection of this elliptical polarization at the mirror then produces a linear polarization by an anti-clockwise rotation of Δ, the relative phase retardation, about an axis through $I^P I^S$. The point L represents the resultant linear vibration whose azimuth is determined by the analyzer in azimuth A. The amplitude reduction ratio, Tan ψ, is given by the ratio of the straight lines LI^P / LI^S which is seen from the figure to be equal to Tan l where 2l is the longitude of L. Since the crossed analyzer is at right angles to the direction of the linear polarization L then A is 180° from L and hence,

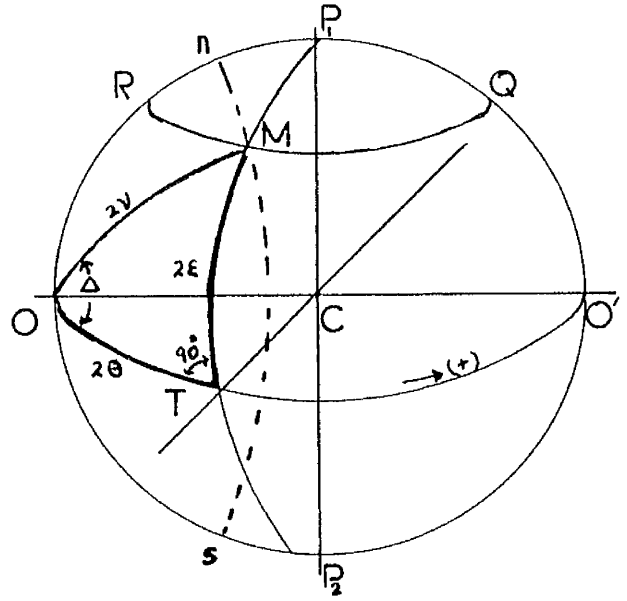

Fig. 2.8. The Poincaré sphere showing the representation of an elliptically polarized vibration by a point M. From the spherical triangle OMT, the parameters of the vibration can be found. Points on the equator OO' represent linearly polarized light. The sense of rotation of the ellipse is left and right in the upper and lower hemispheres respectively. The poles P_1 and P_2 represent left and right circularly polarized light respectively.

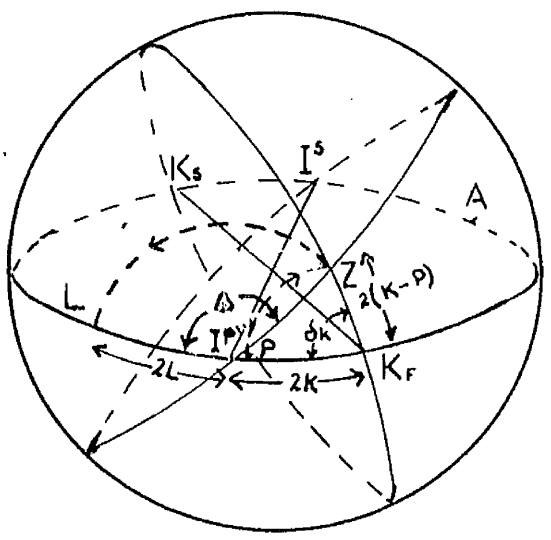

Fig. 2.9. Poincaré representation of the compensation process, where linear polarization P is converted into elliptical polarization Z by doubly refracting plate with fast axis in azimuth K_F. Z is converted into linear polarization L by the reflection at the metal mirror (plane of incidence azimuth I^P). The azimuth of L is detected by the analyzer in azimuth A.

$$l = (180^{\circ} - a) \qquad \ldots \qquad (2.61.)$$

where a is longitude of A.

The solution of the spherical triangle $ZT^{P}K_{P}$ gives the relations between the instrument readings and the relative phase retardation, Δ and the azimuth of the restored linear polarization L. Standard forms for this case are :-

$$\left.\begin{aligned} \operatorname{Cot}(\pi - \Delta) \,.\, \operatorname{Sin}\delta &= \operatorname{Sin} 2(k - p) - \operatorname{Cos} 2k \,.\, \operatorname{Cos}\delta \\ \operatorname{Cos} 2l &= \operatorname{Cos} 2k \,.\, \operatorname{Cos} 2(k - p) + \operatorname{Sin} 2k \,.\, \operatorname{Sin} 2(k - p) \,.\, \operatorname{Cos}\delta \end{aligned}\right\} \qquad (2.63.)$$

If the compensator azimuth, k, is $\frac{\pi}{4}$, these become :-

$$\left.\begin{aligned} \operatorname{Tan}\left(\Delta - \frac{\pi}{2}\right) &= \frac{\operatorname{Tan} 2p}{\operatorname{Sin}\delta} \\ \operatorname{Cos} 2l &= \operatorname{Cos} 2p \,.\, \operatorname{Cos}\delta \end{aligned}\right\} \qquad (2.64.)$$

For $\delta = \frac{\pi}{2}$ i.e. a quarter wave compensator, these reduce to :-

$$\left.\begin{aligned} \operatorname{Tan}\left(\Delta - \frac{\pi}{2}\right) &= \operatorname{Tan} 2p \text{ or } \Delta = \frac{\pi}{2} + 2p \\ 2l &= \frac{\pi}{2} \\ \Psi &= a. \end{aligned}\right\} \qquad (2.65.)$$

CHAPTER 2 : REFERENCES.

2.1.) Abelès, F., Ann. de Physique, Vol. 3, 1948, p.504.
2.2.) Malo, D., Thesis, University of Paris, Masson et Cie, 1953.
2.3.) Rouard, M.P., Proprietes Optiques des Lames Minces Solides, Mem. des Sci. Phys., 54, 1952.
2.4.) Drude, P., Wied. Ann. Vol. 43, 1891, p.126.
2.5.) Tronstad, L., Trans. Far. Soc., Vol. 31, 1935, 1151.
2.6.) Poincare, H., Theorie Mathematique de la Lumiere, Vol. 2, 1892, 275.
2.7.) Skinner, C.A., J. Opt. Soc. Amer., Vol. 10, 1925, 491.
2.8.) Turner, A.F., Benford, J.R., and McLean, W.J., A Polarized Light Compensator for Opaque Minerals. Econ. Geol., Vol. 40, 1945, 18.
2.9.) Winterbottom, A.B., Optical Properties of Metal Surfaces. Kgl. Norske Videnskabers Selskabs Skrifter, 1955, No. 1.
2.10.) Jerrard, H.G., Transmission of Light through Optically Active Media. The Poincare Sphere. J. Opt. Soc. Amer., Vol. 44, 8, 1954, p.634.
2.11.) Ramachandran, G.N., and Ramaseshan, S., Magneto-Optic Rotation in Birefringent Media-Application of the Poincare Sphere. J. Opt. Soc. Amer., Vol. 42, 1, 1952, p.49.
2.12.) Born, M., and Wolff. Principles of Optics, Pergamon Press, 1959.
2.13.) Johannsen, A., Manual of Petrographic Methods. McGraw-Hill, New York, 1918, 2nd Edn., Chap. 2.

CHAPTER 3 : EXPERIMENTAL.

3.1.) The Vacuum System.

The manufacture of the film specimens is effected by the evaporation of the film material at a pressure of the order of 10^{-5} m.m. Hg. In fig. 3.1. is shown a sketch outlining the main features of the vacuum deposition unit. A photograph of the unit appears on plate 3.1.

The vacuum is produced by a Metrovac 03B oil diffusion pump backed by a rotary pump. A pressure of 2×10^{-5} m.m. Hg. is readily obtainable after outgassing by means of a high tension glow discharge in the vacuum chamber. The efficacy of a glow discharge as a method of outgassing surfaces under vacuum is debatable, especially when compared to the use of an oven. However, with a large demountable system employing rubber O-rings, L-rings and vacuum greases it is not possible to use an oven. The arrangement of the terminals in the vacuum chamber ensured that the intense region of discharge was produced near the condensing surfaces. This operation assisted in the removal of adsorbed layers on the substrates.

The evaporation of the material was effected by Joule heating. The evaporant was contained in a heater through which the heating current passed. The heating current was obtained from a single phase mains supply through a heavy current transformer regulated to provide up to 60 amperes at 15 volts. Control/

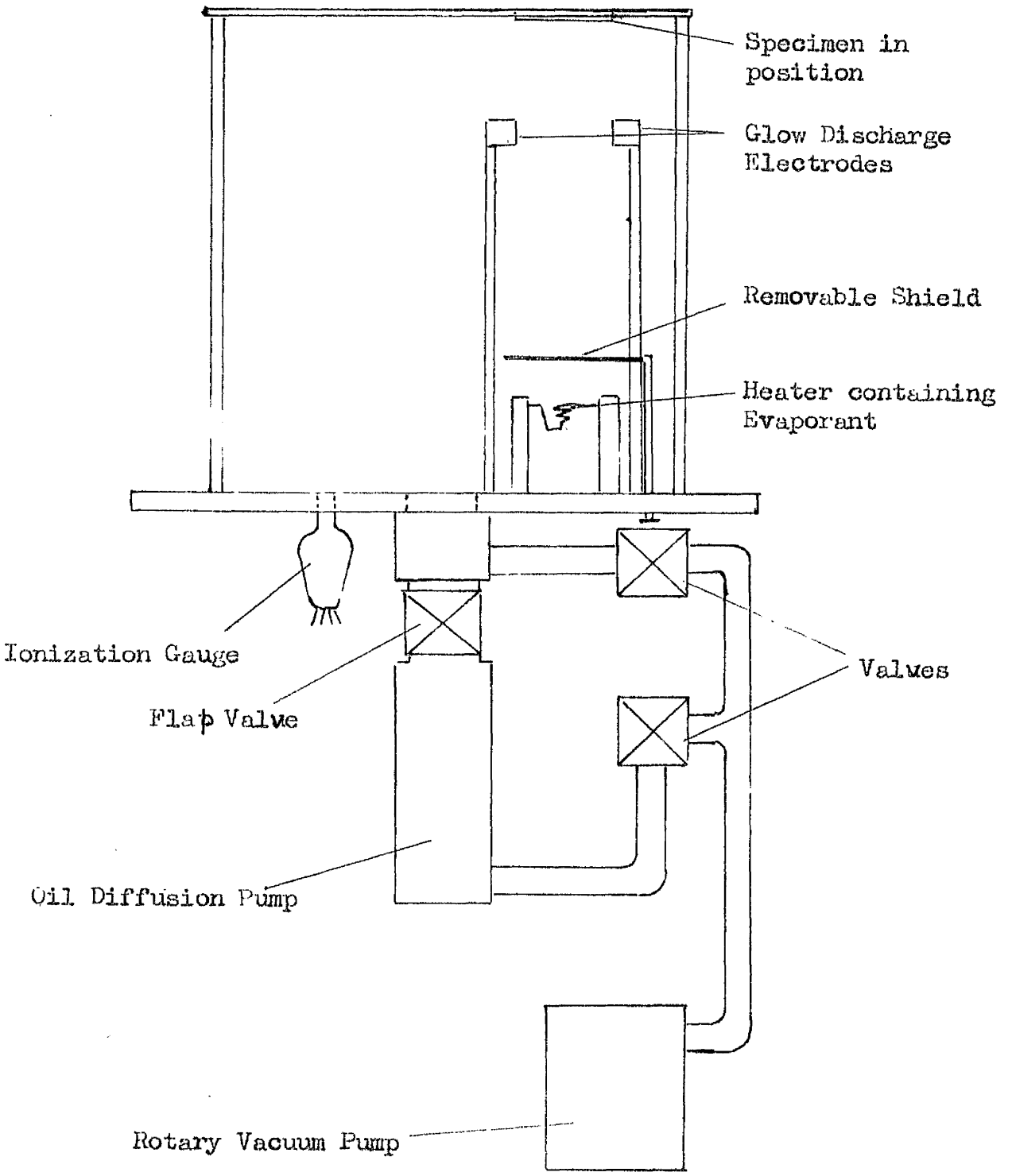

Fig. 34. Layout of Vacuum Deposition Unit.

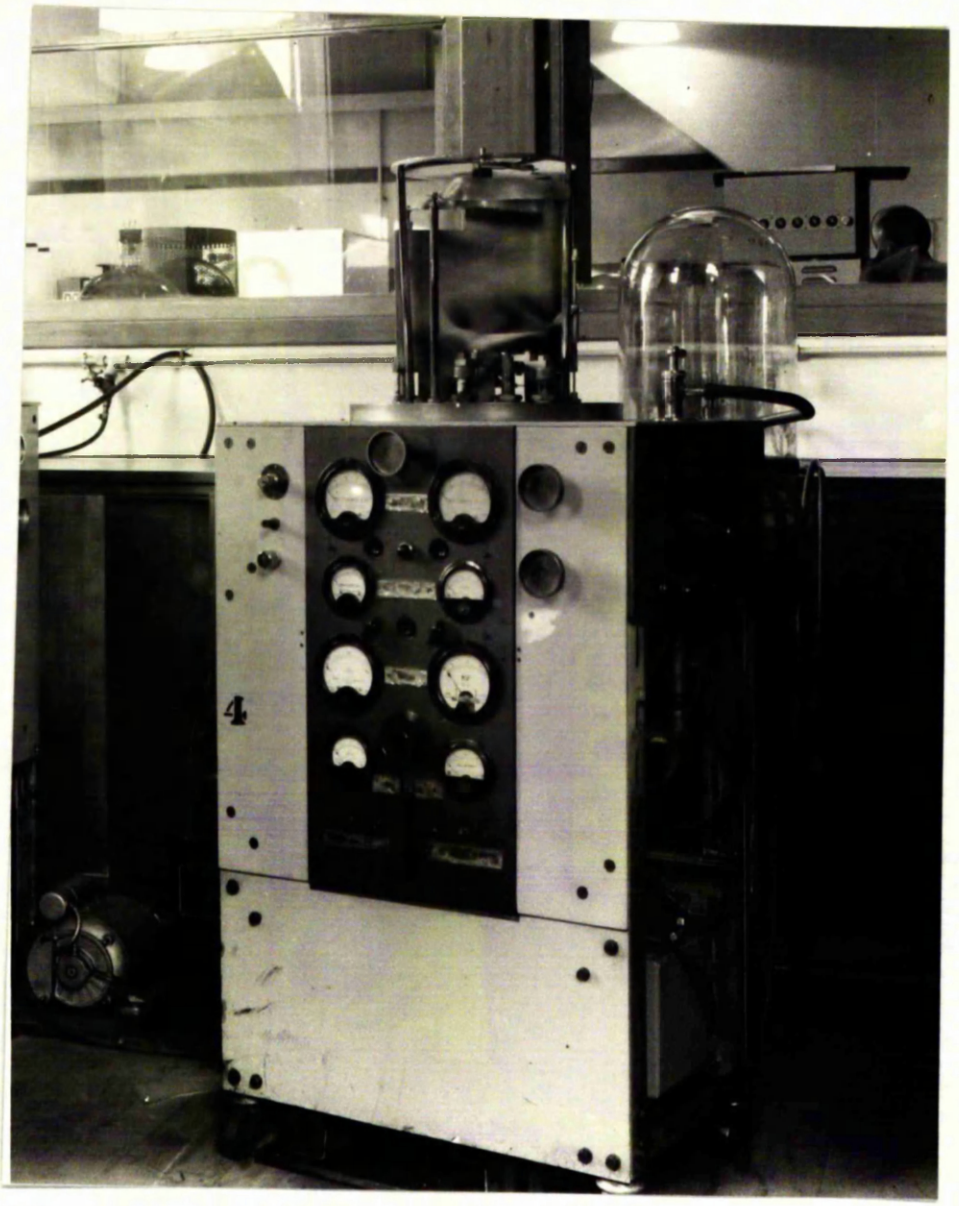

Plate 3.1. Normal Deposition Unit.

Control of the heating current was effected by a Variac in series with the primary winding of the transformer.

The technique of vacuum deposition has been the subject of study by many workers in the last two decades. Holland(3.1.) has outlined techniques for the deposition of a wide range of materials from dielectrics to metals. In the present work the methods recommended by Holland have been adopted where applicable.

The type of heater used varied with type of metal to be evaporated. Generally a molybdenum or tantalum boat or a tungsten spiral was the form employed.

3.2.) Film Production.

In the earlier investigations on Ni, Cr, Mn, Cu, the optical measurements showed a spread in results which necessitated a very large number of films to be produced in order to obtain statistical accuracy. In this earlier method each film specimen was produced singly. Since it is well known that film characteristics are highly sensitive to the conditions pertaining during the formation of the film (e.g. residual gas pressure, nature of residual gas, rate of evaporation, disposition of condensing surface with respect to source, purity of source material, etc.), a later series of experiments used a modified version of the evaporation unit. This version is shown in fig. 3.2. and plate 3.2. With the Talbot Disc(3.2.) a film of six different thicknesses is formed on the substrate where before a single film/

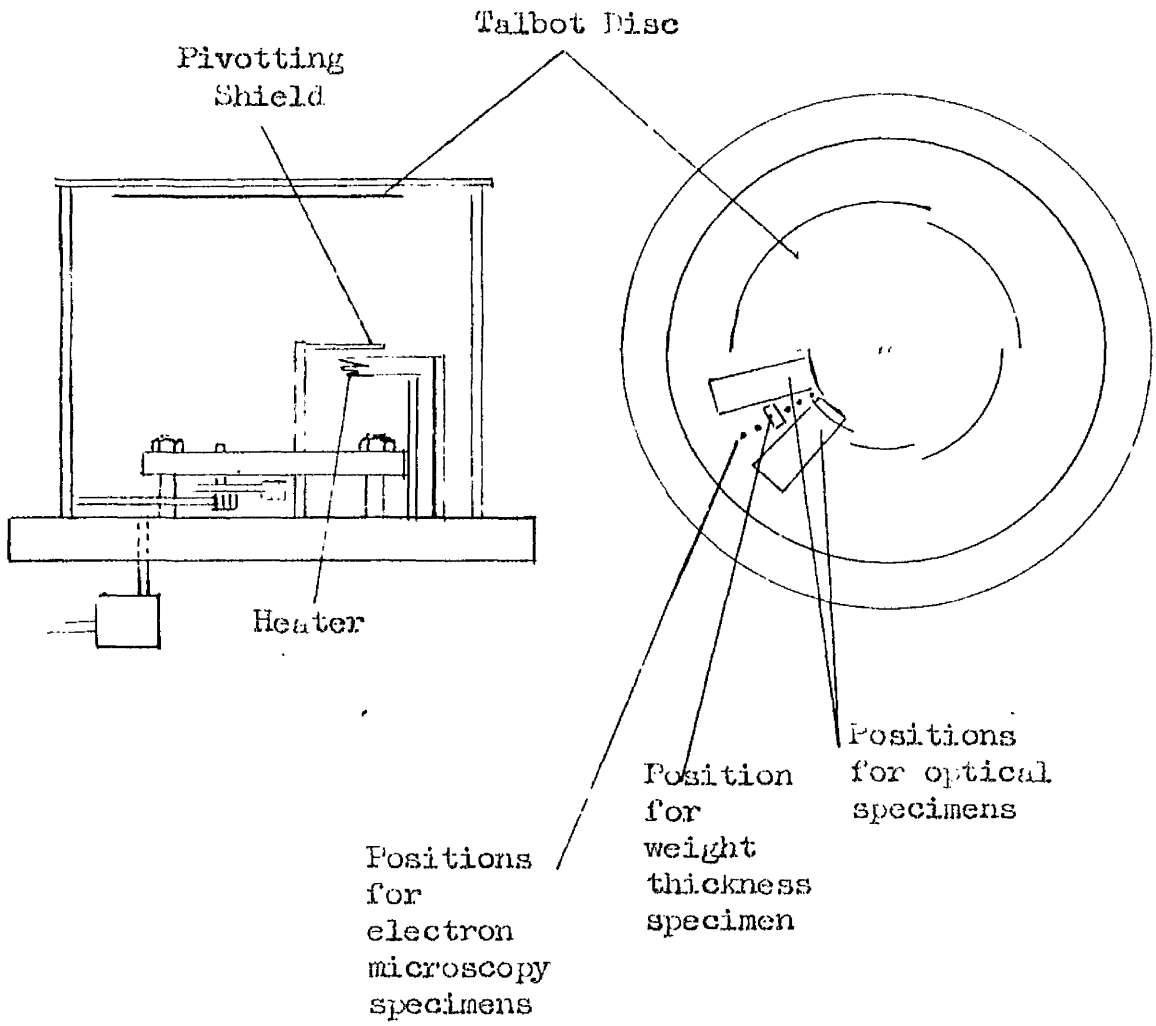

Fig. 3.2. Deposition Unit with Talbot Disc.

film thickness was obtained. A sketch of the Talbot Disc is shown in fig. 3.3. At a pressure of 10^{-5} m.m. Hg. the mean free path of air molecules is of the order of 400 cms. There are therefore relatively few collisions between evaporating metal atoms and residual gas molecules. A radial distribution of the metal atoms takes place. The disc is positioned as close to the substrate as shielding considerations will permit. The disc shaft is directly geared to an electric motor fitted underneath the bell jar and outside the vacuum. The drive from the motor passes into the chamber through a standard Edwards rotating seal. The motor drive gives a rotation of 60 r.p.m., and the gearing gives a final disc speed of 120 r.p.m. Since most evaporations are greater than 30 seconds in duration the selected disc speed allows a large number of revolutions to occur during an evaporation which ensures uniformity of thickness across a sector. Higher disc speeds of rotation would not be practicable as gearing problems then arise and the leak rate through the vacuum seal also becomes significant at higher motor speeds (3.3.).

In the present investigation the disc fashioned was such as to give six sectors whose thicknesses were in the ratio :-

100 : 70 : 50 : 30 : 20 : 10

The jig for use with the Talbot Disc is shown in fig. 3.4. This arrangement permits the simultaneous production of corresponding film thicknesses for each of the following purposes,

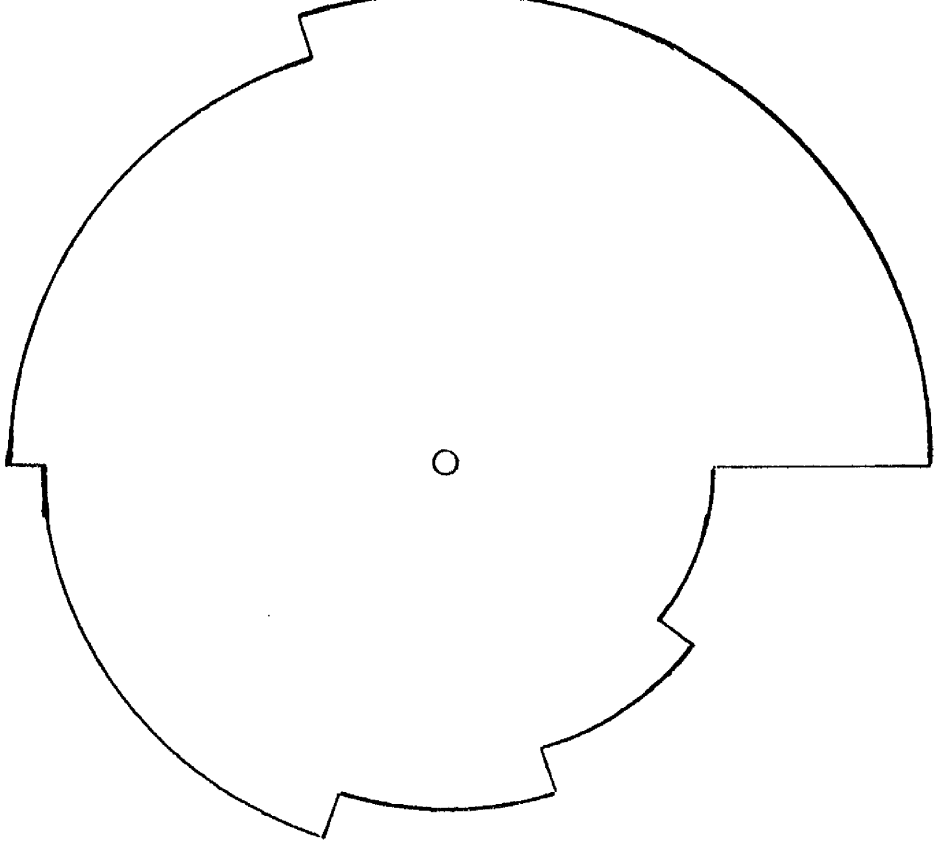

Fig. 3.3. Talbot Disc Arrangement.

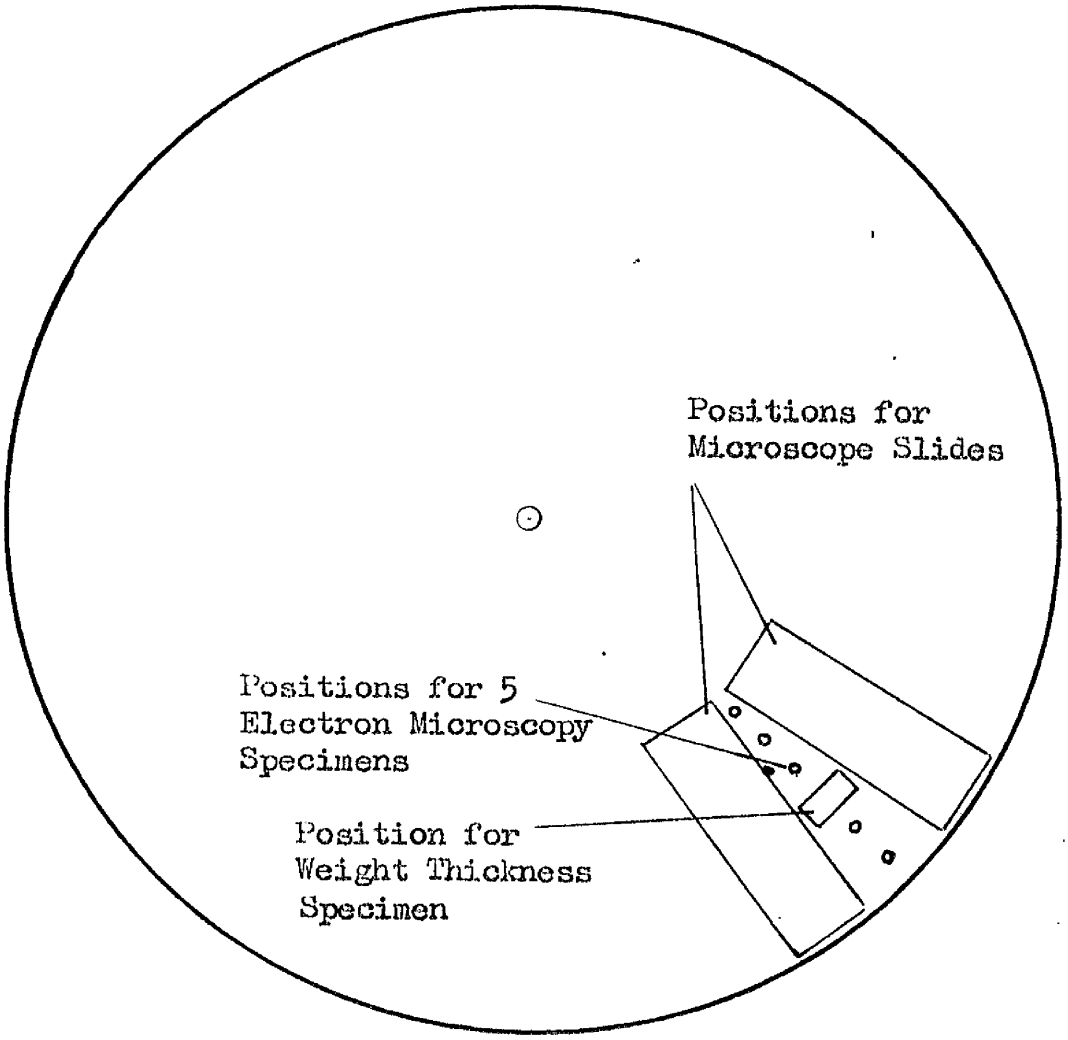

Fig. 3.4. Jig for Use with Talbot Disc.

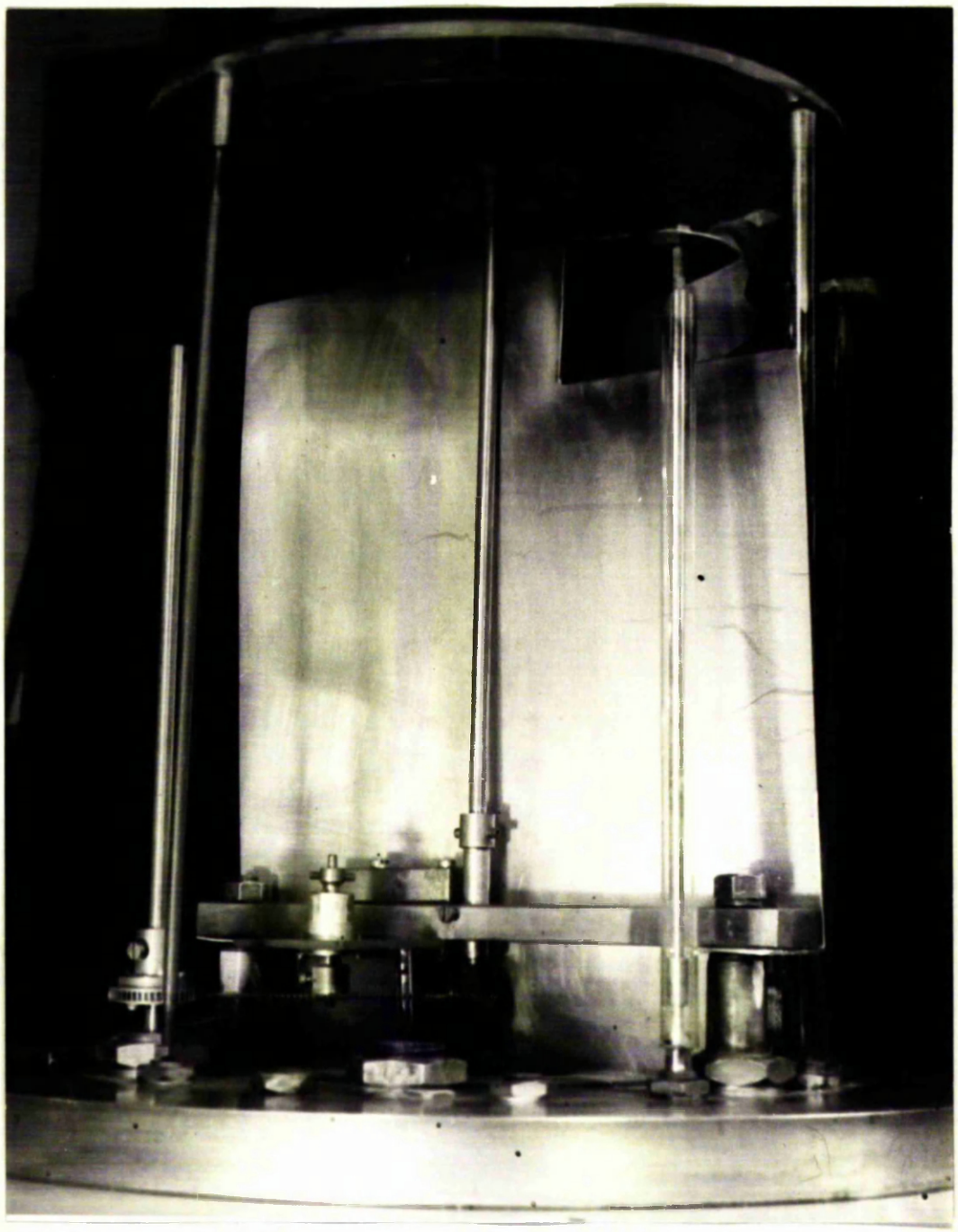

Plate 3.2. Deposition Unit with Talbot Disc.

a) R, R' and T measurements

b) Measurement of Phase Change

c) Thickness determination by multiple-beam interferometry

d) Electron microscope examination and electron diffraction

e) Weight thickness determination (one thickness only)

3.3.) Film Substrate Preparation.

The films used in sections (a) to (c) above were deposited onto glass microscope slides measuring three inches long, one inch wide and one twentieth of an inch thick. As mentioned earlier the cleanliness of the substrate is of prime importance in vacuum deposition work. There is little doubt that discrepancies between many workers' results may be traced to the cleanliness and method of preparation of substrates.

In the present work the cleaning of substrate was as follows: the glass slide was washed with cotton wool in near-boiling running water, using a soap detergent called Teepol; it was then thoroughly rinsed and then dried with a clean linen cloth. Clean lens tissue was then rubbed over the surfaces. To ensure that all greases had been removed the slide was held up to the light so as to give a bright reflection and was lightly breathed on. If any greasy areas remain on the slide they are outlined in the reflected light by this so-called breath test. A final polish with clean lens tissue was then applied. At all times during the handling of the slide only the shorter edges of the/

the slide were touched in order to prevent smearing by the fingers. In the final stages of cleaning and in positioning the slide in the vacuum chamber it was held at the edges using lens tissue. Inside the chamber the slide was placed in the intense positive column region of the gas discharge and thus a final cleaning was obtained by ionic bombardment.

The substrate employed in the preparation of electron microscope specimens referred to in section (d) above was a Formvar film about 150 A thick on a standard electron microscope grid. The preparation of the grids was as follows: a glass microscope slide was cleaned with Teepol and very hot water as above and thoroughly dried. A solution of 5% Formvar in dry Dioxan was applied from a dropper to the top edge of the slide which was held at its edges at about 45° to the horizontal with a flat face up. A sufficient flow from the dropper was applied to let the solution flow evenly down the whole width of the slide before evaporation of the Dioxan. It was necessary however to avoid a prolonged application from the dropper as this tended to give films too thick for use. The absolute dryness of the slide was important as the presence of water tends to turn the Formvar cloudy. After the evaporation of the Dioxan the slide was left with a thin film of Formvar. A scalpel was next drawn round the perimeter of the slide and one end slowly immersed into distilled water keeping the filmed face uppermost. The formvar film released itself progressively as more of the glass was immersed and floated on the surface. Electron/

Electron microscope grids were dropped gently onto the film as it floated on the water until all clear areas were occupied. To remove the grids plus film from the water a piece of newspaper was applied to the film in such a manner that contact was obtained all over the film at the same instant. The application of the newspaper was very brief and it was removed vertically avoiding any movement across the surface of the water. When successfully performed this left the newspaper with the grids sticking to it and a Formvar film covering the grids. After allowing the water to evaporate, each grid was removed with forceps after breaking the Formvar film around the periphery with a needle.

The substrate employed for weight thickness determination listed in section (e) above was a glass microscope cover slip measuring 1 x $\frac{7}{8}$ square inches. The area coated was $\frac{1}{5}$ x $\frac{3}{4}$ square inches.

The preparation of this substrate was similar to that for the substrate in sections (a) to (e) with the added precaution of more gentle handling due to the thinness of the cover slip.

3.4.) <u>Film Thickness Determination.</u>

The thickness of thin metal films formed by evaporation depends upon the method used for obtaining it. In the present work three separate and in general different thickness values could be obtained for a given film. These are :-

a) The weight thickness referred to in section 3.2.

b) The thickness obtained by Multiple Beam Interferometry.

c) The Optical Thickness, so called by virtue of its derivation from optical reflectance and transmittance measurements.

Any theoretical treatment of the optical properties of thin metal films usually requires a knowledge of the thickness of the film as determined by weighing the amount of film deposited over a known area and using the bulk metal density to determine the required thickness.

Film weights were obtained by microbalance and colorimetry. The accuracy of the microbalance method of obtaining the weight of a specimen is of the same order as that obtainable by colorimetry, viz. ± 1 microgram. This section of the work was performed with the aid of the services of the Department of Chemical Technology.

Due to limitations of space and geometry in the evaporation chamber, one specimen only for weight thickness determination was prepared. The weight thickness for each section was obtained by applying the knowledge of the ratios which the sections bore to each other by virtue of the use of the Talbot Disc. The area of the measured specimen was found by travelling microscope to an accuracy of 1% in length and breadth giving an accuracy of 2% in area.

The weight thickness of a film is given by

$$d_w = \frac{M}{\rho A}$$

where M is mass in gms. of deposited films,

ρ is the bulk density of the film material,

A is the area of the film.

To determine the percentage accuracy at the lower limit of thickness (100 A) where the accuracy is at its lowest we take differentials,

$$\frac{\Delta d_w}{d_w} = \frac{\Delta M}{M} + \frac{\Delta \rho}{\rho} + \frac{\Delta A}{A}$$

For a typical film of about 100 A thickness we have,

$$\frac{\Delta M}{M} = \frac{10^{-6}}{10^{-5}}$$

$$\frac{\Delta \rho}{\rho} = \frac{.1}{8}$$

$$\frac{\Delta A}{A} = 2 \times 10^{-2}$$

Summing gives a percentage error in weight thickness of around 15%. The accuracy increases with the mass deposited. This accuracy is of the same order as was obtained by optical methods for the same thickness region.

The method of multiple beam interferometry for film thickness determination was first used by Wiener(3.4.) in 1887. Tolansky(3.5.) has developed to a high degree of accuracy the two methods of interferometry employed in the present work. These two/

two methods are named after the type of fringes they employ, viz. Fizeau Fringes and Fringes of Equal Chromatic Order. The apparatus and mode of operation of the Fizeau system have already been well described, viz. Tolansky(3.5.), Hill(3.6.), Benjamin(3.7.). It was found that for thinner films, i.e. 200 A the Fizeau method tended to have less accuracy and so an arrangement to produce Equal Chromatic Order (E.C.O.) fringes was set up. This apparatus is shown in fig. 3.5. and plate 3.3. The theory dealing with the formation of the fringes and with the measurement of step heights using them, has been dealt with by Tolansky(3.5.), Heavens(3.8.) and Holland(3.1.). It might be noted here that Holland's description includes a sketch which depicts light converging to form an image of the light source in the interferometer, whereas in this work collimated white light was used. In fig. 3.5. is shown an attachment to the spectroscope called a "Locating Lamp". This device was employed to locate the actual area of the film selected by the spectroscope slit. This is achieved by allowing a 6 volt lamp to be focussed to illuminate the inside of the spectroscope slit by reflection at 45° from a piece of perspex at the lower end of the tube. An image of the slit was obtained on the film surface when the instrument was correctly focussed. The film was arranged so that the step to be measured lay under the slit image. The use of the Locating Lamp eliminated searching for the step in the observed fringe system. The lamp was retractable/

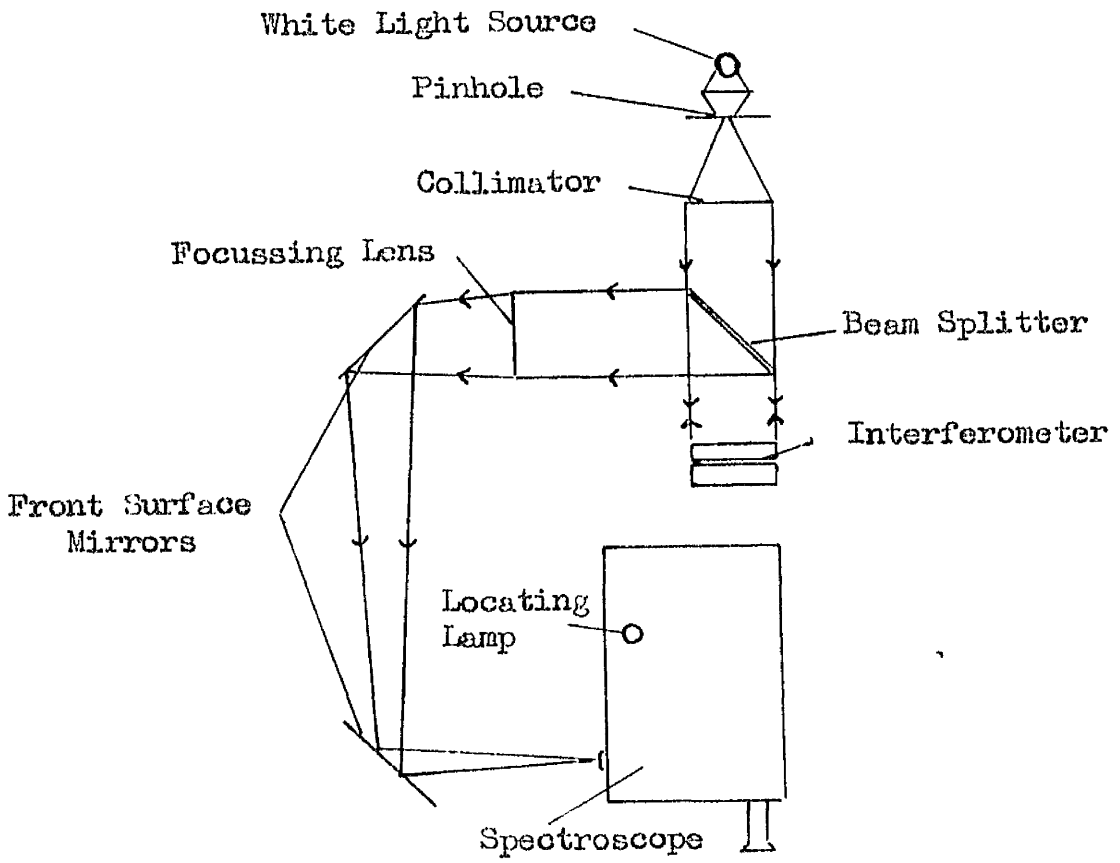

Fig. 3.5. E.C.O. Apparatus.

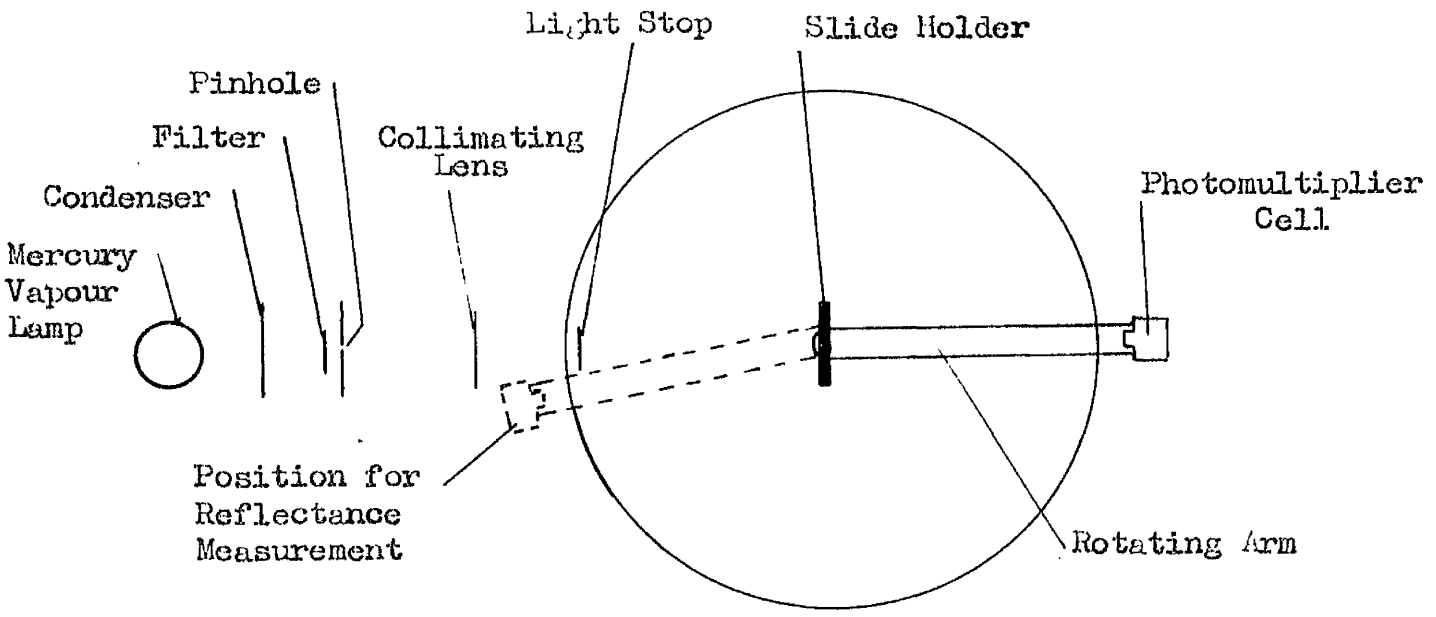

Fig. 3.6. Reflectometer.

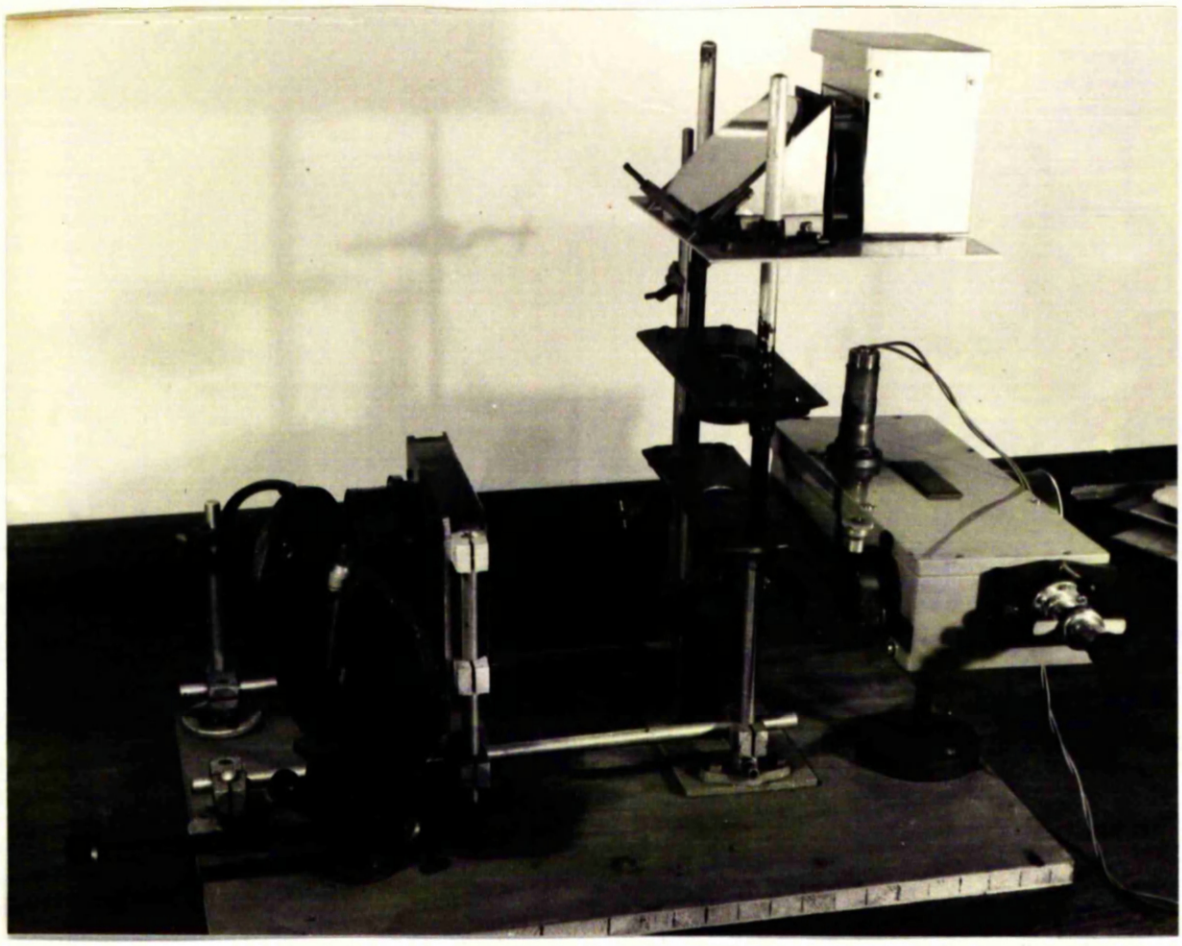

Plate 3.3. E.C.O. Apparatus.

retractable in its tube so that when the apparatus was in use the perspex reflector did not interfere with the fringe system.

The accuracy of film thickness measurement by interferometry was limited by the fact that ordinary microscope slides were used as substrates. Tolansky(3.5.) has shown that an accuracy of ±10 A can be obtained by using high quality optical flats, however the presence of local irregularities in the microscope slides puts a practical limit to the accuracy of the order of 30-40 A on the measurements made in this work.

The third thickness value obtained in this work was that termed the Malé thickness. The definition of this thickness and the method by which it was determined is explained in Chapter 2, Section 4.

As already stated these three thicknesses generally tended to be different from each other especially for thinner films. The weight thickness was always the smallest of the three. This observation is attributed to the fact that films adopt an aggregated structure during the process of formation unless the substrate temperature is maintained at a very low value throughout the deposition or the evaporation rate is very high, i.e. 100 A/sec. Sennett and Scott(3.9.) showed clearly using electron microscopy that for silver films whose rate of deposition was of the order of 100 A/sec. the aggregation was finer for any particular thickness than was the case for slower evaporation/

evaporation rates. Also for the faster deposition rate aggregation was not observable at thicknesses of the order of 150 A while in the slower cases aggregation was still visible up to 500 A thick. The aggregation causes voids or fissures in the film which gives an effective density less than the density of the bulk material. The determination of a weight thickness is however of importance when it comes to devising a theoretical model which would account for the observed optical properties of films.

It has been found that over a wide range of thicknesses for various metals the weight thickness, d_w, and the interferometric thickness, d_δ, do not differ greatly from each other. The Mali thickness on the other hand can be up to five or six times greater than the weight thickness. A reason for this is very likely that the observed transmittance of a film is influenced by the scattering ability of the film which is in turn affected by the degree of aggregation.

3.5.) Reflectance and Transmittance Measurements.

The reflectance and transmittance of films were measured on the simple reflectometer shown in fig. 3.6. A mercury gas discharge lamp filtered to give only the mercury green line of 5461 A was used as a light source. Although strictly speaking the theory requires collimated light falling on the film it was found in practice that a slightly convergent beam gave greater consistency./

Accordingly the optical arrangement was such as to render an image of a pinhole 1 m.m. in diameter on a diffusing screen in front of a photomultiplier cell at a distance of one metre. The diameter of the image was 2 m.m. In simple reflectometers of this type it is important that the light should always strike the exact same region of the photocell and also that intensity variations across the section of the light beam should be eliminated. The first requirement was met by arranging that a supplementary image was formed by another pinhole to give an image approximately one centimetre above the original image. This image was formed on a marked area on the photomultiplier case. The second requirement was fulfilled by the use of a ground glass diffusing screen immediately before the envelope of the photomultiplier tube. The photomultiplier tube was a 27M1.

This is a nine stage device giving a maximum gain of one million. The power pack was a standard Ediswan R184 giving an operating stabilized voltage of 1,100 volts. The output was displayed on a D.C. microammeter with a full scale deflection of 10 μ A. When in use the lamp and photomultiplier were switched on and the light allowed to fall on the photocell for about half an hour before measurements were made. The table which acted as base for the reflectometer was circular of radius 50 cm.ϕ and thickness 2 cm.ϕ. The material used was steel. This provided a massive base for a rigid assembly thus eliminating the possibility/

possibility of misalignments due to vibrations and constant handling. The design was such as to allow a near-normal reflectance at 3° angle of incidence.

The method of measuring reflectance and transmittance was to note the reading given by the direct unhindered beam, then insert the film in its holder on the centre of the table and note the new direct reading for transmittance or the reflected reading if reflectance was being measured. Finally the direct unhindered beam was measured again and the mean of this and the first value taken as denominator of a ratio whose numerator was given by the transmitted or reflected reading. This ratio expressed as a percentage was termed the Observed Reflectance or Observed Transmittance.

The quantities T, R, R' as required by the Malé theory are the reflectance and transmittance for a thin film of the material bounded on either side by semi-infinite non-absorbing media, viz. air and glass, as shown in fig. 3.7. Experimentally, however, the glass backing has a finite thickness and we must eliminate the contribution to the required quantities from multiple reflections within the glass substrate. Let R_o be the reflectance on the air side of the film, R'_o that for the glass side and T_o the observed transmittance which can be shown by theory to be the same for both directions. Multiple reflections/

reflections occur between three different pairs of boundaries as shown in fig. 3.8.

The expression representing the sum of the contributions to the reflectance as shown in fig. 3.8., neglecting absorbtion, may be written :-

$$R_o = R_1 + T_1^2 R_2 (1 + R_1' R_2 + \ldots\ldots) + T_1^2 T_2^2 R_3 (1 + R_2' R_3 + \ldots\ldots)$$

$$+ T_1^2 T_2^4 R_1' R_3 (1 + T_2^2 R_1' R_3 + \ldots\ldots)$$

$$= R_1 + \frac{T_1^2 R_2}{1 - R_1' R_2} + \frac{T_1^2 T_2^2 R_3}{1 - R_2' R_3} + \frac{T_1^2 T_2^4 R_1' R_3}{1 - T_2^2 R_1' R_3} \qquad \ldots \quad (3.1.)$$

R_1', R_2', T_1', T_2', etc., are the coefficients applying when the direction of the light is opposite to that where R_1, R_2, T_1, T_2, etc., apply. Theory shows that $R_1' = R_1$, $R_2' = R_2$, $T_1' = T_1$, $T_2' = T_2$, etc. R_o is the observed reflectance. Equation (3.1.) is the result of the addition of intensity and not amplitude. The random variations in the thickness of the glass backing inherent in its manufacture and the great thickness of the backing compared to that of the film are presumed to justify the use of intensity addition (3.10.). The expression required is that which gives the reflection at the film surface together with the multiple reflections occurring within the film itself. By re-arrangement of equation (3.1.) we get,

$$R = R_1 + \frac{T_1^2 R_2}{1 - R_1' R_2} = R_o - \frac{T_1^2 T_2^2 R_3}{1 - R_2' R_3} - \frac{T_1^2 T_2^4 R_1' R_3}{1 - T_2^2 R_1' R_3}$$

where R represents the required expression. The last term on the right-hand side may be neglected for practical purposes, leaving

$$R \doteq R_o - \frac{T_1^2 T_2^2 R_3}{1 - R_2' R_3} \qquad \ldots \quad (3.2.)$$

Referring again to fig. 3.8. the observed transmittance T_o can be seen as composed of several terms involving reflectances between various pairs of surfaces :-

$$T_o = T_1 T_2 T_3 \left(1 + R_1' R_2 + R_1'^2 R_2^2 + \ldots\right) + T_1 T_2 T_3 R_2' R_3 \left(1 + R_2' R_3 + R_2'^2 R_3^2 + \ldots\right)$$

$$+ T_1 T_2^3 T_3 R_1' R_3 \left(1 + R_1' R_3 T_2^2 + R_1'^2 R_3 T_2^4 + \ldots\right)$$

$$\doteq \frac{T_1 T_2 T_3}{1 - R_1' R_2}$$

The required expression is that involving only reflections occurring in the metal film, viz. :-

$$T = \frac{T_1 T_2}{1 - R_1' R_2} \doteq \frac{T_o}{T_3} \qquad \ldots \quad (3.3.)$$

Rewriting equation (3.2.) we get,

$$R = R_o - R_3 \left(\frac{T_o}{T_3}\right)^2 \frac{(1 - R_1' R_2)^2}{(1 - R_2' R_3)}$$

$$\doteq R_o - R_3 \left(\frac{T_o}{T_3}\right)^2 \qquad \ldots \quad (3.4.)$$

Finally the observed reflectance from the glass side is

$$R'_o = R'_3 + T'^2_3 T'^2_2 R'_1 (1 + R'_1 R'_2 + \ldots) + T'^2_2 R'_2 (1 + R'_2 R_3 + \ldots)$$

$$+ T'^2_3 T'^4_2 R'^2_1 R'_3 (1 + T'^2_2 R'_1 R_3 + \ldots)$$

$$\doteq R'_3 \quad \frac{T'^2_3 T'^2_2 R'_1}{(1 - R'_1 R_2)} + \frac{T'^2_3 R'_2}{(1 - R'_2 R_3)}$$

$$\doteq R'_3 + R_2 T'^3_3 + \frac{T'^2_3 T'^2_2 R'_1}{(1 - R'_2 R_2)} \qquad \ldots(3.5.)$$

The required expression can be seen from fig. 3.7. to be

$$R' = R'_2 + R'_1 T_2^{\ 2} + R'^2_1 T_2^{\ 2} R_2 + R'^2_1 T_2^{\ 2} + R'^3_1 T_2^{\ 2} R_2^{\ 2} + \ldots)$$

$$= R'_2 + R'_1 T_2^{\ 2} (1 + R'_1 R_2 + \ldots)$$

$$= R'_2 + \frac{R'_1 T_2^{\ 2}}{(1 - R'_1 R_2)} \qquad \ldots(3.6.)$$

From equation (3.5.) therefore we get

$$R' \doteq \frac{R'_o - R_3}{T_3^{\ 2}} \qquad \ldots(3.7.)$$

Equations (3.3.), (3.4.) and (3.7.) were used to convert the observed quantities into the parameters from which the optical constants were obtained. The value of R_3 was calculated to be .04 using the measured refractive index of the glass slides which was 1.52.

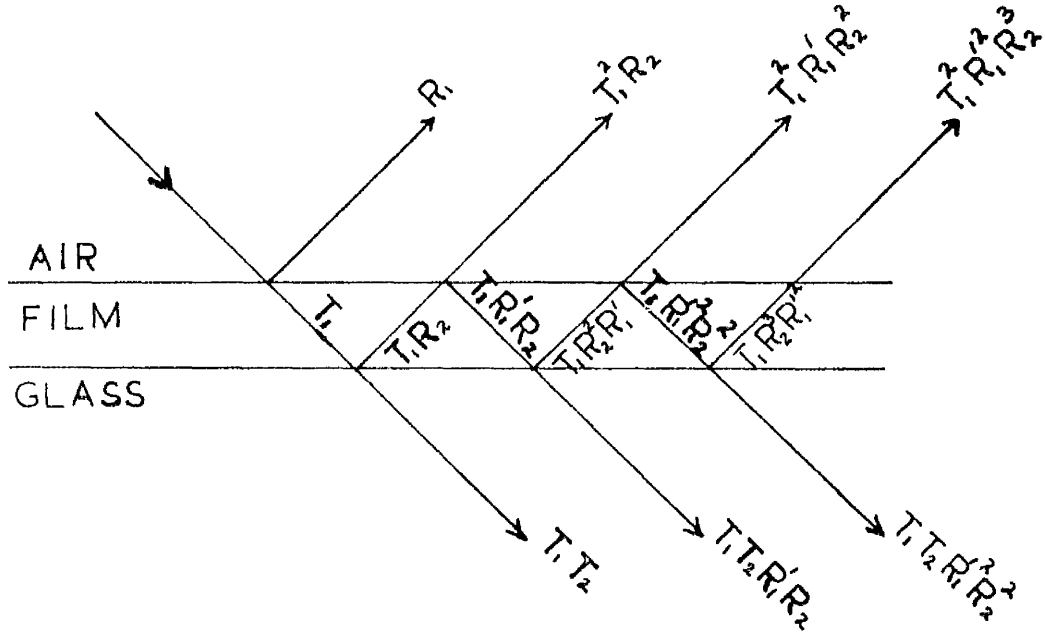

Fig. 3.7. Reflections Occurring in a Thin Film Bounded by Two Semi-Infinite Media.

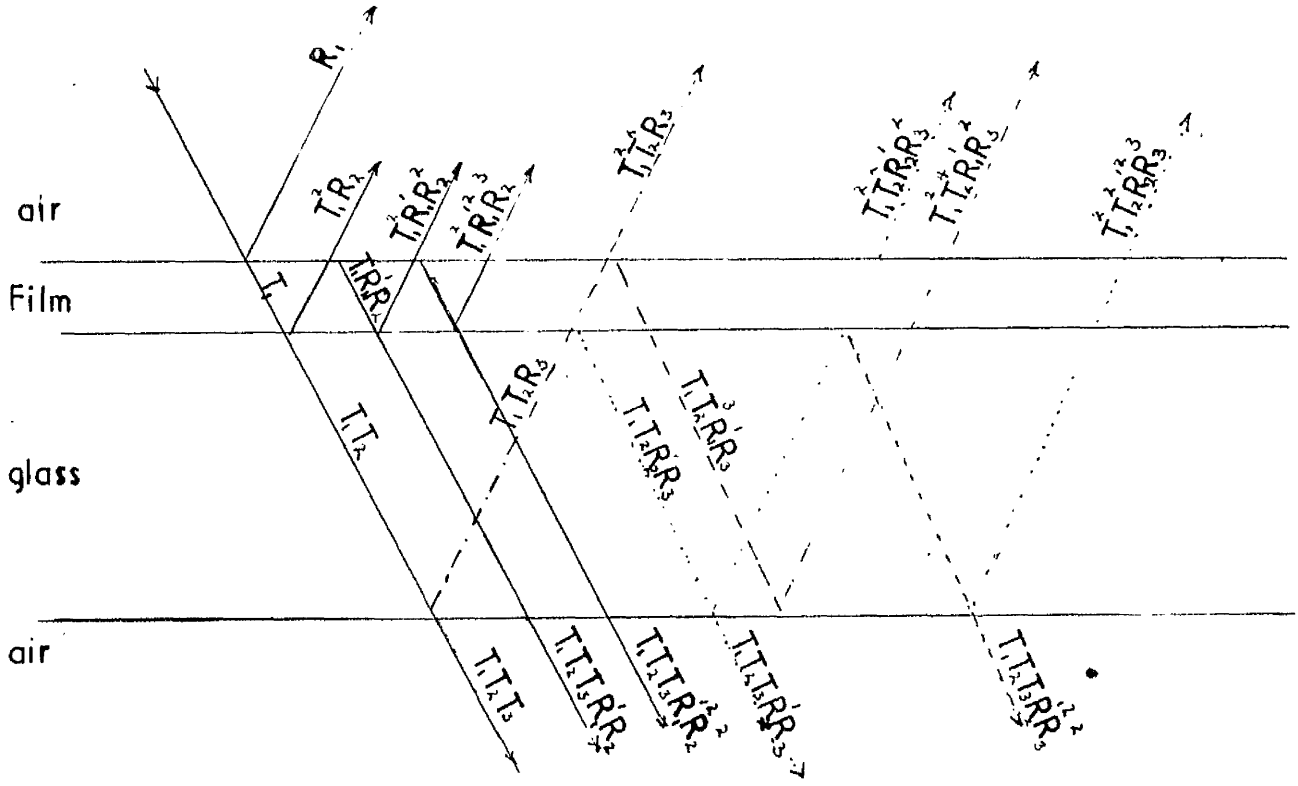

Fig. 3.8. Multiple reflections occurring in a film on a thin non-absorbing substrate.

The validity of the approximations used in deriving equations (3.3.), (3.4.) and (3.7.) has been examined using trial values and the difference between the exact form of the required expressions and their respective approximations was never found to be greater than 1% which was of the same order as the experimental accuracy. A further check was made by depositing a film simultaneously onto a glass slide and also onto a wedge-shaped glass substrate. The multiple reflections occurring in the wedge-shaped substrate were separated from those occurring in the film and the required quantity was that measured directly. A comparison of results from both substrates confirmed the validity of the approximations.

3.6.) Polarization Measurements.

A polarization spectrometer was constructed based on a design due to Tronstad(3.11.). A diagram of the spectrometer is shown in fig. 3.9. A high pressure mercury vapour lamp acted as a source. The light was filtered to pass only the 5461 A mercury green line. The incident beam was collimated and a stop was inserted to reduce scattered light. Before striking the film surface the light beam passed through a polarizer which could be set to any desired azimuth. The beam then passed through a quarter wave plate for the relevant wavelength which is fixed in azimuth $\pi/4$. The linearly polarized light was thus converted into an elliptical vibration whose azimuth and ellipticity could be set to any desired values. The elliptically polarized beam was reflected from the surface of the

metal film at some determined angle of incidence and in so doing underwent modification of its components parallel and perpendicular to the plane of incidence. This modification is dealt with in detail in the section on polarimetry. In short the amplitude reflection coefficients of the p and s components, i.e. the components parallel and perpendicular to the plane of incidence respectively, are different, and there also takes place a change in the phase of each component which is generally different for each. The ratio of the amplitude reflection coefficients is termed the amplitude ratio and the difference between the phase changes on reflection is termed the differential phase change. As shown in Section 3.8. with the aid of the Poincaré Sphere an incident elliptically polarized light can be generated which on reflection from the metal surface becomes linearly polarized light. The linearly polarized light is detected by the analyzer shown in the diagram. The azimuth of the analyzer can read off a graduated scale and hence the azimuth of the emerging linearly polarized light can be determined. In the original Tronstad apparatus the eye was used as a detector of linearly polarized light, high accuracy in azimuth reading being obtained with the aid of a half-shade device. Due to the difficulty of obtaining half-shade components an alternative method was employed. In this method a lens of short focal length was placed on the rotating arm after the analyzer. This lens formed an image of the pinhole on a ground glass screen placed immediately in front of a shielded/

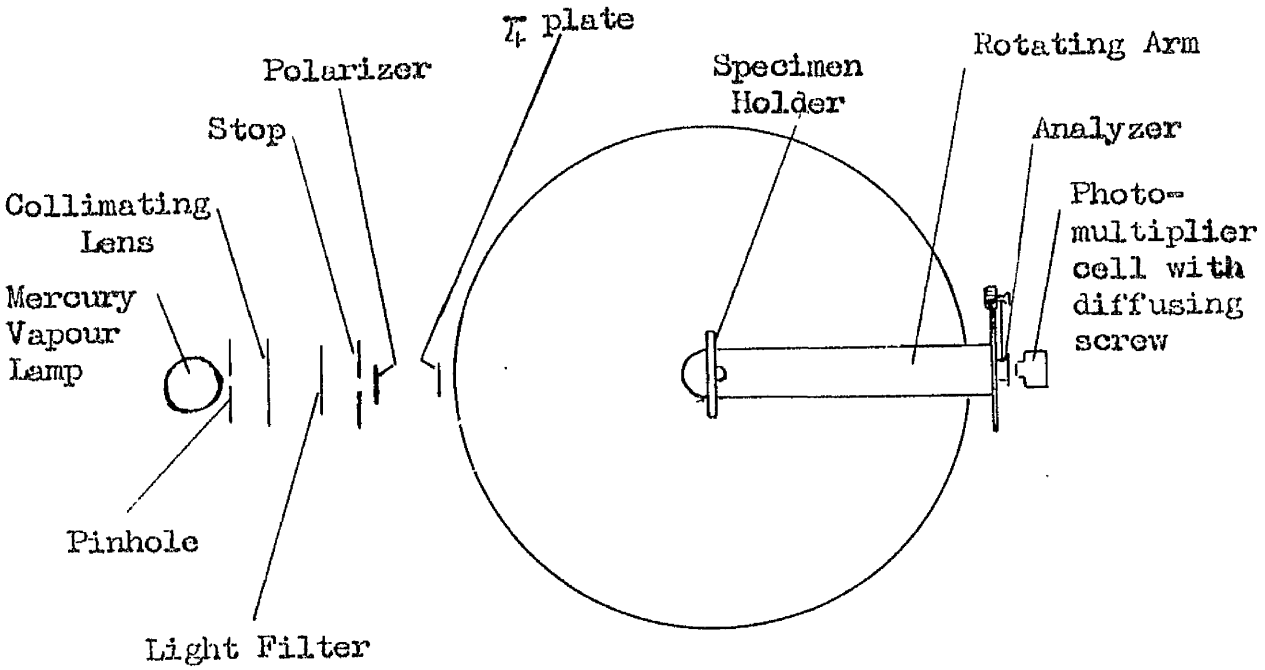

Fig. 3.9. Polarizing Spectrometer.

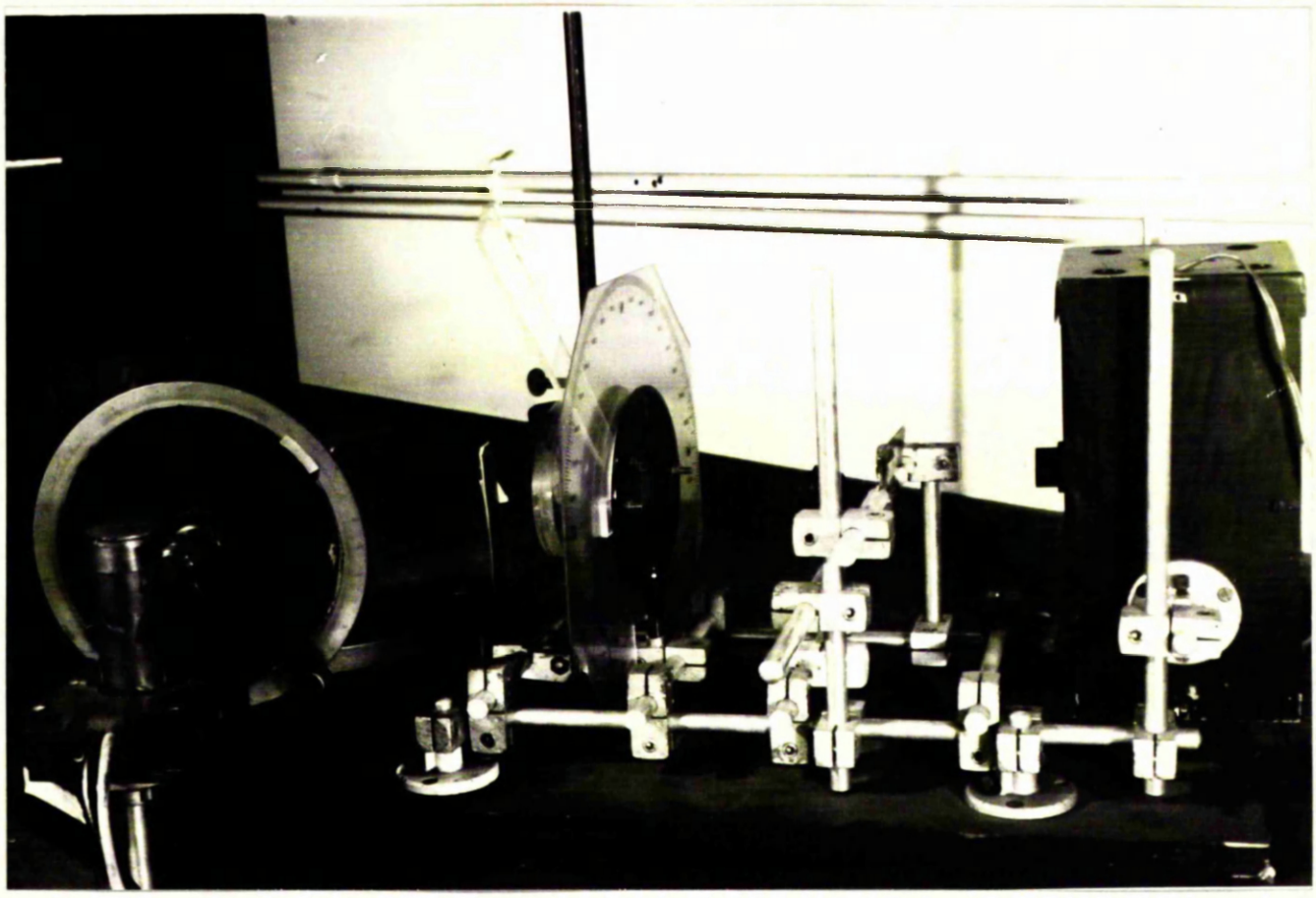

Plate 3.4. Polarizing Spectrometer.

shielded photomultiplier tube similar to that described in Section 3.5. Readings were taken in a darkened room to eliminate extraneous light. In taking a reading the polarizer and analyzer were set to give a minimum reading on the microammeter and then the analyzer was kept fixed in the minimum position while the polarizer reading was altered to give a small reading above the minimum. This polarizer reading was noted and then it was moved to the other side of its minimum position to give the same microammeter reading. The reading was again noted. The first off-minimum position of the polarizer was repeated to detect variation in photomultiplier output if any. The mean of the two off-minimum polarizer positions was taken as the setting for that particular angle of incidence. This process was repeated varying the analyzer about its minimum reading position while the polarizer was set for minimum. By this means an accuracy of 0.2° was obtained for the polarizer and analyzer setting. Plate 3.4. shows a photograph of the polarizing spectrometer.

In Section 2.6. it is shown that the relation between observed extinction settings of polarizer and analyzer for any angle of incidence ϕ are

$$\sin \Delta = \cos P$$

$$\tan \psi \tan A = 1$$

where Δ = Differential Phase Change

$\tan \psi$ = Amplitude Ratio

P = Azimuth of Polarizer

A = Azimuth of Analyzer

3.7.) Vacuum Polarization Spectrometer (V.P.S.).

The evaluation of the optical constants of the surface of an opaque metal film is complicated by the presence of an oxide layer in most cases. The rate of oxidation of various metals has been studied by many workers. In general for the metals studied here an oxide layer some tens of Angstroms thick was formed within several minutes of exposing a film to the atmosphere (3.12.).

In order to evaluate the film constants of the pure metal the effect of this film must be determined.

Two approaches to this problem have been attempted. In the first an existing deposition chamber was adapted to give polarimetric observations of freshly evaporated films without destroying the vacuum. A diagram of this vacuum polarising spectrometer is shown in fig. 3.10. and photographs of the apparatus appear on plates 3.5.a. & b. The original construction of the deposition chamber was such that the angles of incidence for which polarization measurements could be made were limited to 15°, 30° and 45°. In effect the sensitivity of the method falls off very rapidly with decreasing angle of incidence due to the denominator term $\cos\Delta \sin 2\psi$ in equation (2.29.). Consequently only the readings for an angle of incidence of 45° were used. Readings were taken within seconds of an opaque film being formed. It was considered that oxidation would be retarded sufficiently at the operating pressure which was 10^{-5} m.m. Hg. for the observation to be regarded as one on a pure metal film. In this connection it might be /

be noted that at a pressure of 10^{-5} m.m. Hg. there are 5×10^{15} molecules of oxygen striking each square centimetre of surface every second in the chamber. The optics and detection system of vacuum polarizing spectrometer are similar to those of the ordinary polarizing spectrometer previously described.

After the first measurements on the freshly formed film the specimen was allowed to age for 30 hours at atmospheric pressure when a second V.P.S. reading was taken. The specimen was then immediately transferred to the other polarizing spectrometer and a set of readings for a series of angles of incidence for 30° to 80° was taken.

The second approach to the determination of the optical constants of a pure metal film involves a method of trial and error. The form of the Drude equations derived by Tronstad(3.11.) and shown in Section 2.5. is used here. Δ and ψ are the quantities derived from measurements in air on the polarizing spectrometer. Values of n and k of the pure metal film are assumed and from these $\bar{\Delta}$ and $\bar{\psi}$ are calculated. n_1 and L are then calculated using equations (2.33.) and (2.34.). This process is repeated for various angles of incidence. When the calculated values of n_1 and L are the same for a range of angles of incidence the values of n and k used are taken to be the correct ones for those of the pure metal film. This is a tedious process, however using the values of n and k for 45° angle

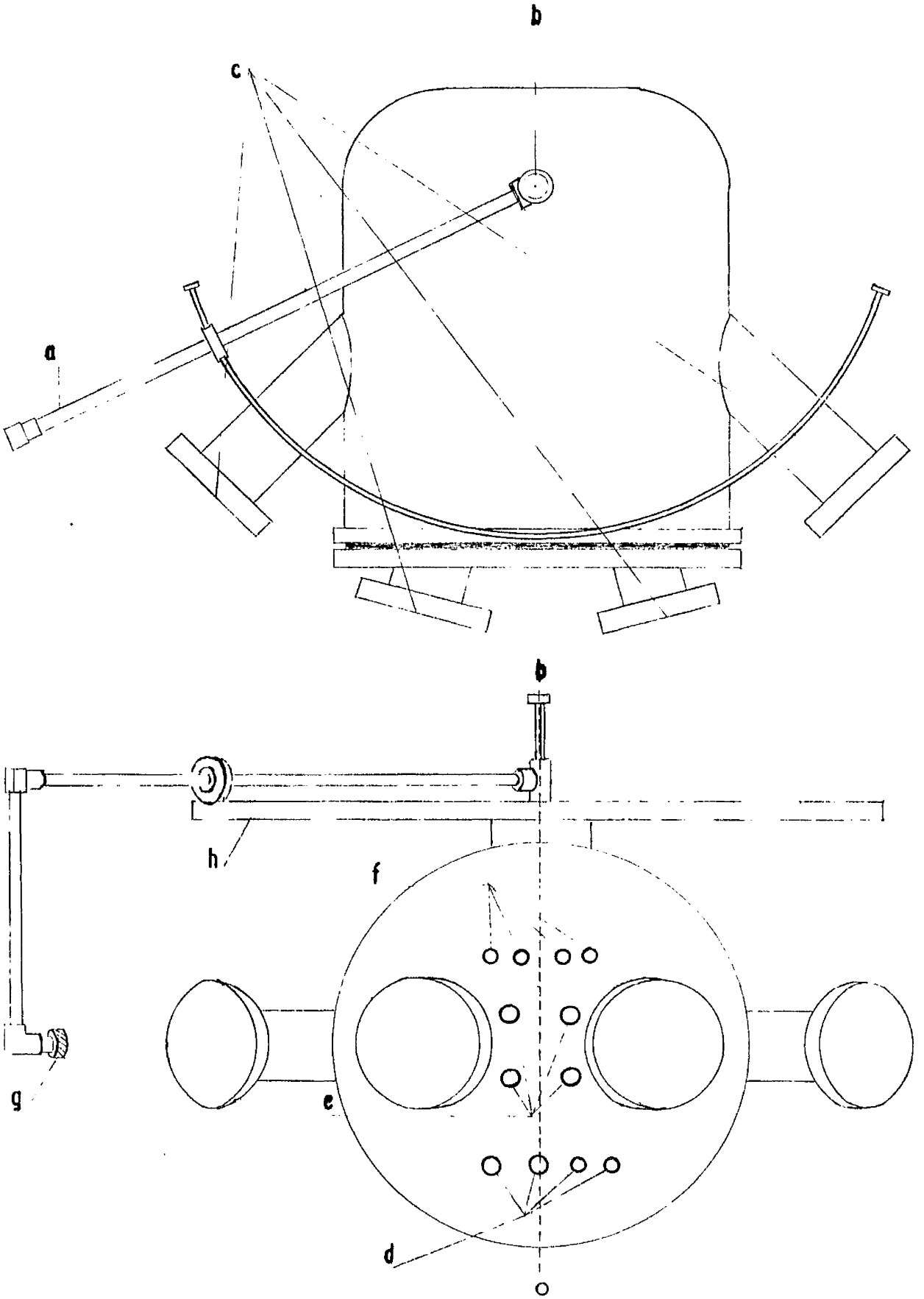

Fig. 3.10. Vacuum Polarizing Spectrometer.

(a) Rotating arm free to rotate about axis oo'. (b) Rotating vacuum sealed rod supporting specimen holder. (c) Observation ports. (d) Vacuum connections for leak valves and gauges. (e) Insulated terminals for evaporation plant. (f) Insulated terminals for miscellaneous electrical connections. (g) Optical compensator holder. (h) Guide rail carrying compensator support arm (a).

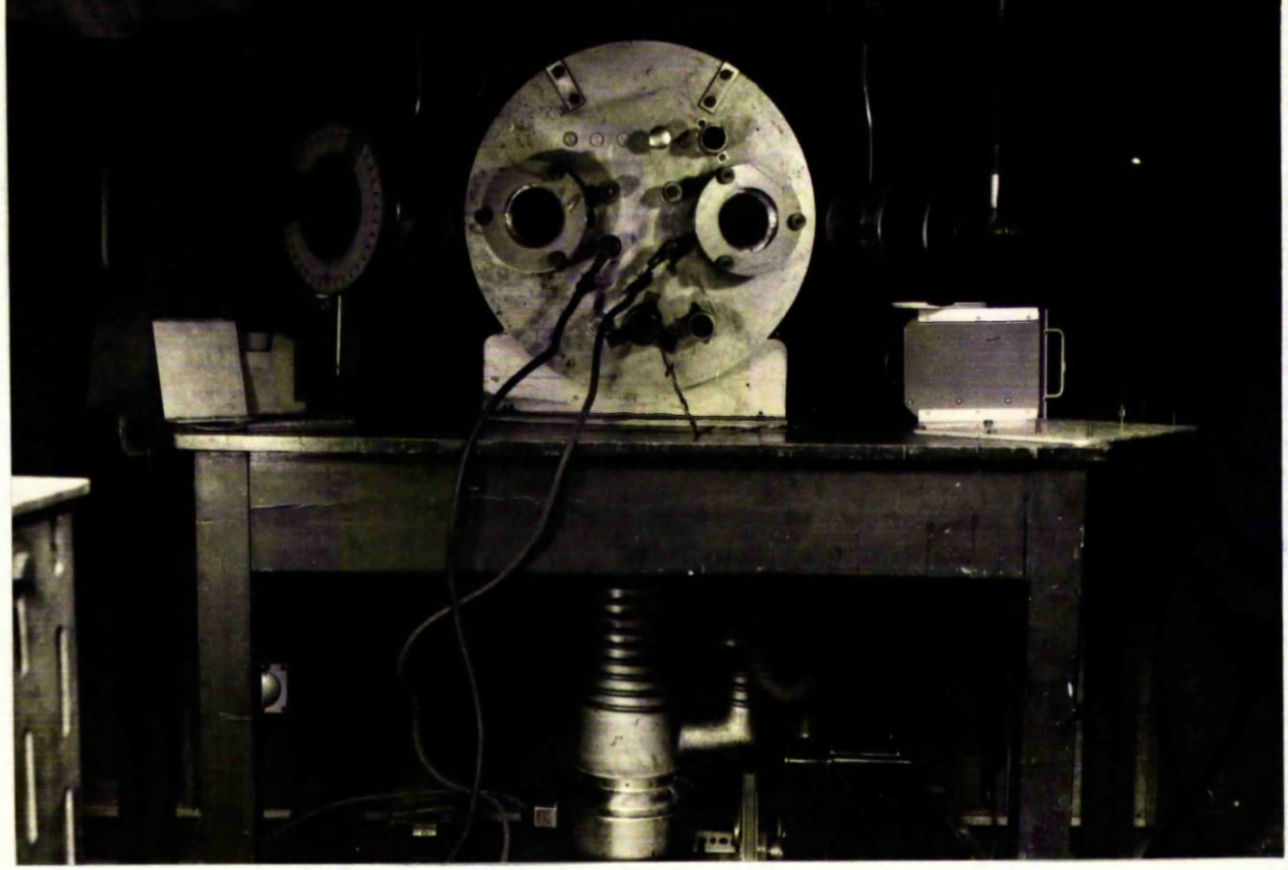

a

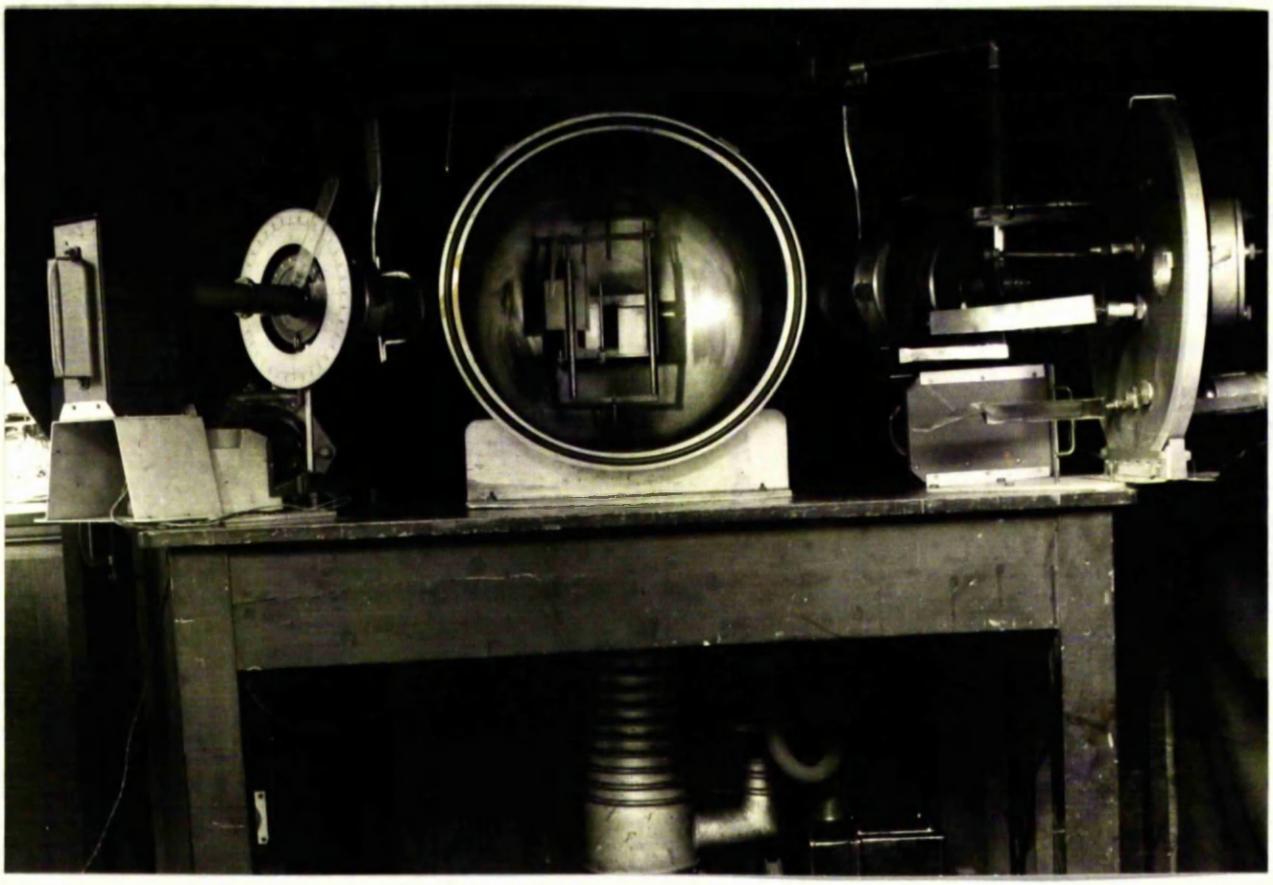

b

Plates 3.5.a & b Vacuum Polarizing Spectrometer.

angle of incidence obtained with the V.P.S. under vacuum as a guide and a digital computer to perform the calculations much of the labour was removed.

3.8.) Phase Change Measurements.

3.8.1.) Rouard Method.

Two separate methods of measuring the phase change on reflection at a metal film were employed. The first is due to Rouard(3.13.). In this method the film to be examined forms one plate of a Fabry-Perot interferometer etalon. In the process of forming the film a strip shield forms an unmetallized channel approximately 1 m.m. wide. Referring to fig. 3.11. a low pressure mercury discharge lamp illuminates a pinhole P and lens L_1 forms a quasi-point image of the pinhole in the clear channel. Circular Haidinger fringes form rings localized at infinity. Lens L_2 forms an image of the ring system on the slit of the spectrograph which lies in the focal plane of L_2. To make a phase change measurement firstly the ring system due to reflection in the channelled region is measured, then the etalon is traversed across the beam to bring the spot onto the metallized region and the modified ring system is observed. Due to the poor fringe visibility Rouard and other workers required to use photography to obtain measurable rings. In this work a modification of the second plate of the etalon permitted direct visual measurement of the ring diameters using a micrometer eyepiece on the spectroscope. As shown below this modification which /

which consists of a partially reflecting metal film on the second interferometer plate has no effect on the measured phase change due to the metal film under investigation. Plates 3.6.a. and 3.6.b. show photographs of the system employed for phase change measurement and the interferometer etalon respectively. In plates 3.7.a. and 3.7.b. are shown the ring systems formed in the spectroscope; plate 3.7.a. refers to the case where the reflecting surface of plate I of the etalon is uncoated, and plate 3.7.b. shows the increase in contrast obtained by using a partially reflecting film on the surface of plate I.

Figures 3.12.a. and 3.12.b. show the relations between the phases of the component parts of a ray passing through the interferometer etalon. Since all phase displacements due to transmission through an interface happen equally to the direct ray and the reflected ray such phase displacements have not been indicated in the figure.

Consider a ray incident normally on the etalon as shown in fig. 3.12.a. For clarity the figure shows the ray as non-normal. Since etalon plate II has the channelled region in the beam initially this means that a phase advance of $\lambda/2$ is experienced by the reflected portion of the beam, where λ is the wavelength of the light. On reflection at etalon plate I the phase change may be written as β, where β is an undetermined fraction of a wavelength. We have therefore that the path difference between the rays (1) and (2) is

$$\Delta_0 = 2nd - \lambda/2 - \beta$$

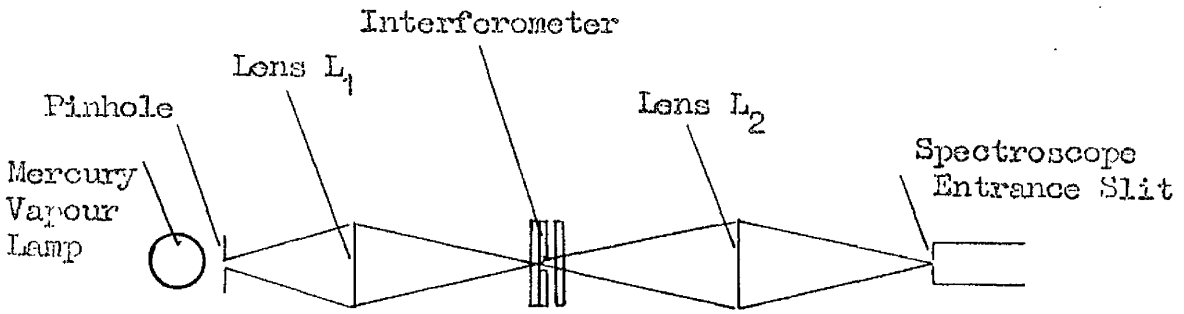

Fig. 3.11. Phase Change Measurement Apparatus.

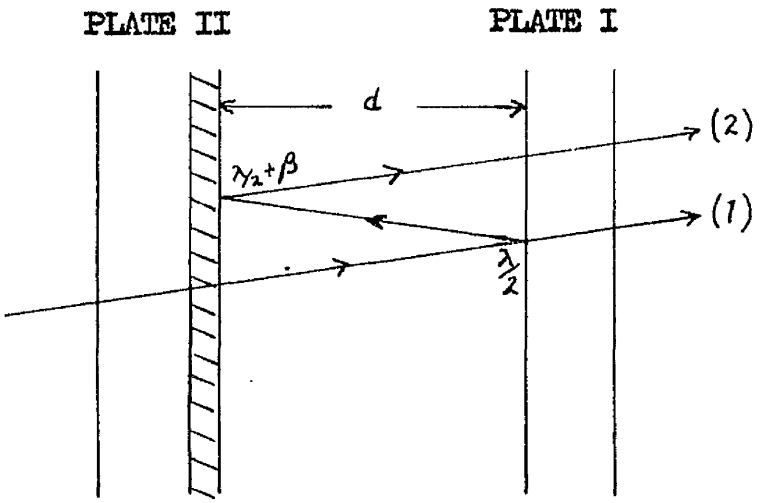

Fig. 3.12.a.

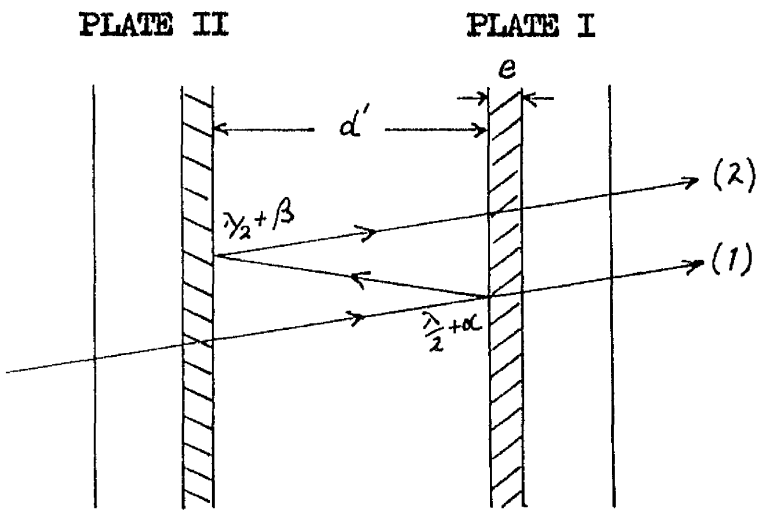

Fig. 3.12.b.

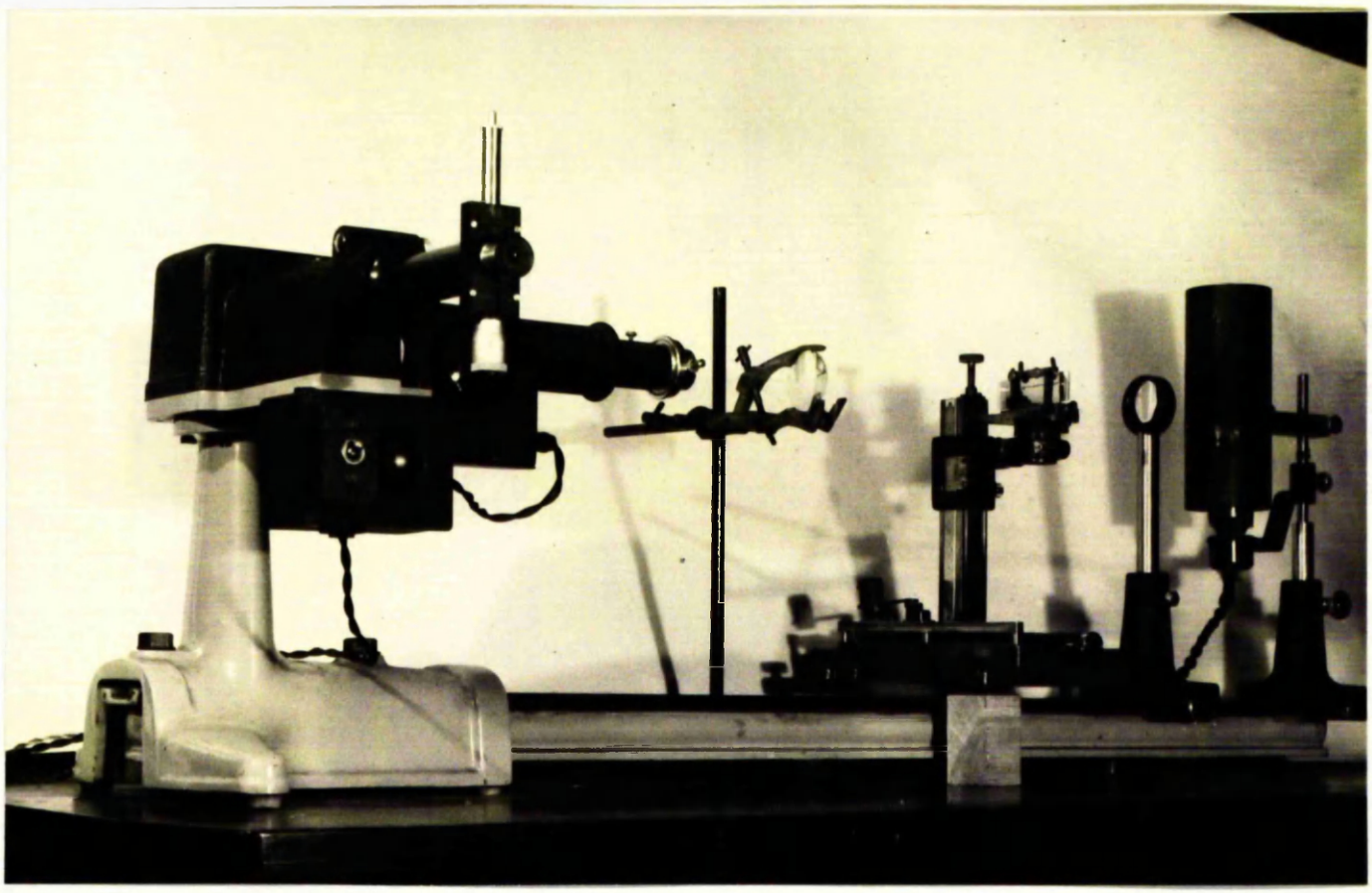

a

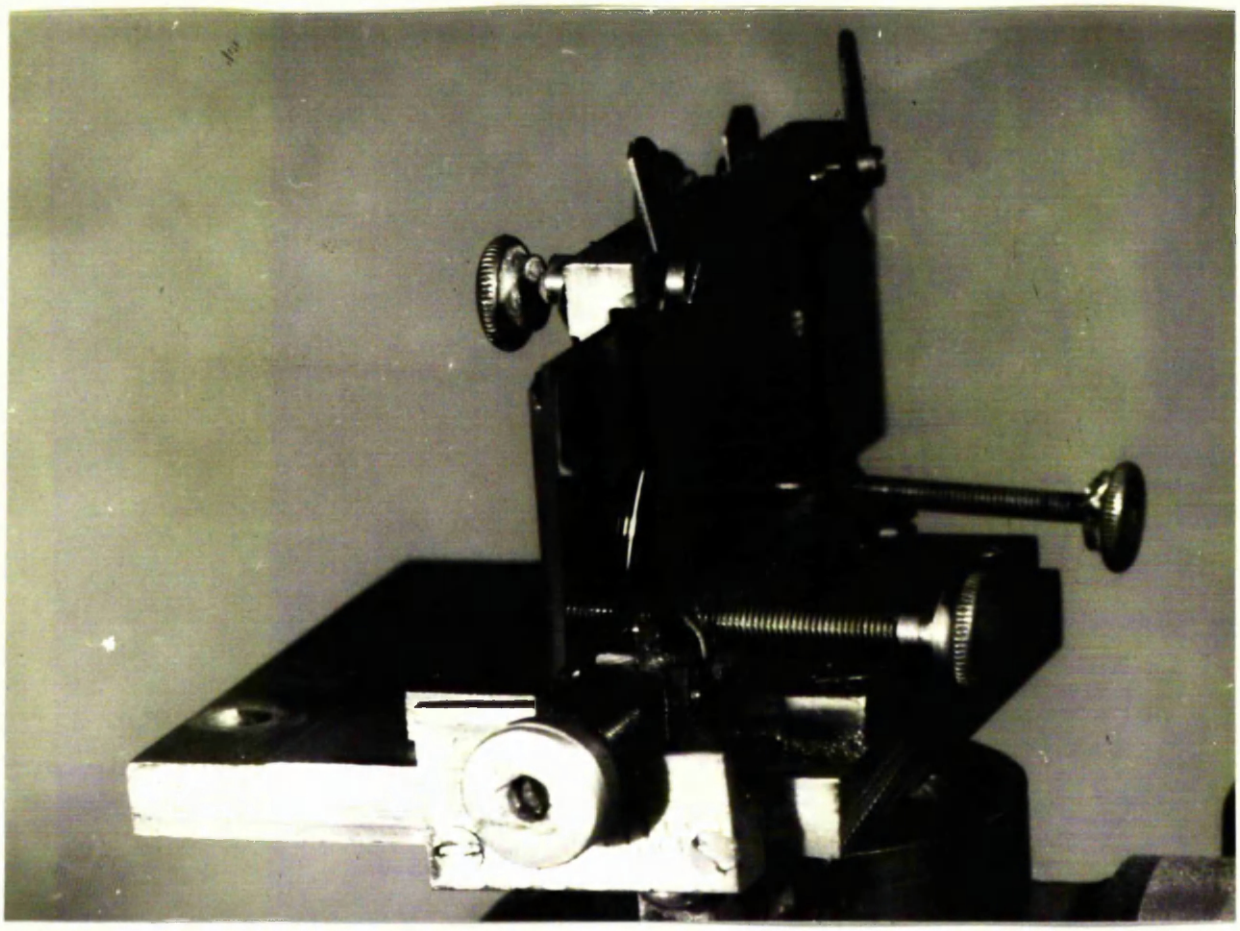

b

Plates 3.6.a & b Phase Change Measurement Apparatus and Interferometer Etalon.

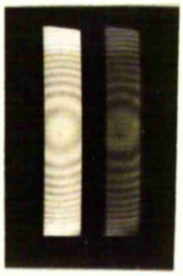

a

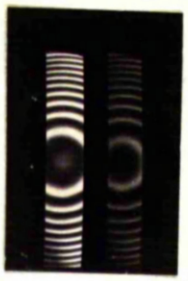

b

Plates 3.7.a & b Ring Systems formed in Spectroscope.

Plate 3.7.a Shows the contrast obtained when one plate of the interferometer is coated and the other is plain glass.

Pla te 3.7.b Shows the contrast obtained when both plates are coated.

We employ here the convention that a phase advance is equivalent to a decrease in path length. The distance between the etalon plates is d and n is the refractive index of the medium separating the plates.

In general Δ_0 will not equal an exact number of wavelengths. It may therefore be written as $(K_0 + \varepsilon_0)\lambda$ where K_0 is an integer and ε_0 is a fraction.

i.e. $\Delta_0 = 2nd - \lambda/2 - \beta = (K_0 + \varepsilon_0)\lambda$

For small angles of incidence the path difference is

$$\Delta = 2nd \cos r - \lambda/2 - \beta$$

Here r is the angle of refraction in the air gap and it is assumed that the phase changes on reflection at plates I and II do not change sensibly for small deviations from normal incidence. When Δ is a whole number of wavelengths reinforcement occurs and a bright ring results.

i.e. For a bright ring $\Delta = K\lambda$

Now by Snell's Law $n = \frac{i}{r}$ for i and r small.

$$\therefore \Delta = 2nd\left(1 - \frac{r^2}{2}\right) - \frac{\lambda}{2} - \beta = K\lambda$$

$$\text{i.e. } \Delta = 2nd\left(1 - \frac{i^2}{2n^2}\right) - \frac{\lambda}{2} - \beta = K\lambda$$

$$\text{i.e. } \Delta = \Delta_0 - \frac{i^2 d}{n}$$

If f is the focal length of lens L_2 then the linear radius in the focal plane of the lens of a ring formed at infinity of angular radius i radians is R = fi

$$\therefore \quad \Delta = \Delta_o - \frac{dR^2}{nf^2} = K\lambda$$

$$\therefore \quad \frac{dR^2}{nf^2} = \Delta_o - \Delta = (K_o - K + \varepsilon_o)\lambda$$

Since $K_o - K$ must be an integer we see that the squares of the radii of successive rings form an arithmetic progression. For the first ring $K_o - K = 0$,

$$R_1^{\,2} = \frac{nf^2}{d}\lambda . \varepsilon_o$$

For the second ring $K_o - K = 1$,

$$R_2^{\,2} = \frac{nf^2}{d}(1 + \varepsilon_o)$$

For the m th ring $K_o - K = (m - 1)$

$$R_m^{\,2} = \frac{nf^2}{d}\lambda\left\{(m - 1) + \varepsilon_o\right\}$$

We may therefore write $_o$ as

$$\varepsilon_o = \frac{R_1^{\,2}}{R_2^{\,2} - R_1^{\,2}} = \frac{D_1^{\,2}}{D_2^{\,2} - D_1^{\,2}}$$, where D_1 and D_2 are the diameters of the first and second rings.

To reduce errors incurred in measuring the rings a common denominator of the form $\frac{D_4^{\,2} - D_1^{\,2}}{3}$ was used in the expression for ε_o.

$$\text{i.e. } \varepsilon_0 = \frac{D_1^2}{\frac{D_4^2 - D_1^2}{3}}, \quad 1 + \varepsilon_0 = \frac{D_2^2}{\frac{D_4^2 - D_1^2}{3}}.$$

A typical set of results obtained for ε_0 was

$\varepsilon_0 = 0.43$

$1 + \varepsilon_0 = 1.47$

$2 + \varepsilon_0 = 2.46$

$3 + \varepsilon_0 = 3.49$

ε_0 is calculated as the mean of the four fractional values thus

$$\varepsilon_0 = \frac{0.43 + 0.47 + 0.46 + 0.49}{4}$$

i.e. $\varepsilon_0 = 0.46$

If we now consider that the etalon has been laterally traversed a distance of approximately 1 m.m. then referring to fig. 3.12.b. let α be the phase change (considered to be an advance) on reflection at the metal film on plate II. Δ_0' for the normal ray may be written as

$$\Delta_0' = 2nd' - \alpha - \beta,$$

where d' is the new distance separating the film surfaces.

We may write Δ_0' as

$$\Delta_0' = 2nd' - \alpha - \beta = (K_0 + \varepsilon_1)\lambda.$$

Also Δ' for the non-normal beam giving a bright ring may be written as

$$\Delta' = 2nd'\left(1 - \frac{i^2}{2n^2}\right) - \alpha - \beta = K\lambda$$

As before,

$$\Delta' = \Delta'_o - \frac{i^2 d'}{n} = \Delta'_o - \frac{d' R^2}{nf^2} = K\lambda .$$

$$\therefore R^2 = \frac{nf^2}{d'}(K_o - K + \varepsilon_1)\lambda .$$

and ε_1 the phase at the centre can be obtained.

The phase change on reflection can be expressed in several ways :-

(a) The Apparent Phase Change which we define as

ϕ app. $= \varepsilon_o - \varepsilon_1$

(b) The Relative Phase Change which we define as

ϕ rel. $= \varepsilon_o - \varepsilon_1 - \frac{2e}{\lambda}$, where e is the thickness of the film on plate II as determined by the Tolansky method of multiple beam interference.

(c) The Absolute Phase Change which we define as

ϕ abs. $= \pi - (\varepsilon_o - \varepsilon_1 - \frac{2e}{\lambda})$, taking the absolute phase change due to reflection at an air/glass interface as $+\pi$.

In practice it is discovered that the ring system may be clearly observed whilst the etalon plates are not exactly parallel. A research project by Houston(3.14.) supervised by the author showed that the ring system could still be observed when non-parallelism up to 0.28 minutes of arc existed between the plates. This means that an error up to $\frac{\lambda}{3}$ could arise, completely masking any phase change effect. To eliminate this error a series of five readings was /

was taken, viz. one in the centre of the channelled region and two on either side on the metallized regions, at 1 m.m. intervals. These outer readings gave accurately the measure of the non-parallelism and permitted the elimination of its effect.

To eliminate undesired reflections involving the back surfaces of the substrate plates the films were formed on wedge-shaped substrates.

3.8.2.) Thickness Discrepancy Method.

The second method of measuring the phase change on reflection at the air/metal interface of a metal film was that used by Weaver, Hill and MacLeod(3.15.). Referring to fig. 3.13a., an opaque film of metal MI was first deposited with two sharp boundaries at A and C. Next a second film of metal MII, the film whose relative phase change is to be determined, is deposited over step A. MII also has a sharp edge at B. Finally steps B and C are overlayered with an opaque film of silver.

To measure the phase change at reflection of MII the system of thickness measurement using Fizeau fringes due to Tolansky is employed. This method was previously referred to in Section 3.4. Figure 3.13b. shows the step of MII on MI. To the left of the step there exists only the thickness of film MII on the glass substrate while to the right of the step there is the total thickness of MI + MII which is completely opaque. The apparent step height is /

is given by the Tolansky theory as

$$\{2(d - x) - \psi\} - \{2d - \psi'\} = 2x - (\psi - \psi').$$

This is the quantity measured by observing the fringe displacement.

i.e. $F \cdot \frac{\lambda}{2} = 2x - (\psi - \psi')$ ... (3.8.)

where F is the fraction of an order a fringe is displaced by the step. Referring now to the step measurement of MI at B given by the opaque silver overlayer it is seen that no relative phase change is involved and only the true height of MI is given, thus

$$F' \cdot \frac{\lambda}{2} = 2x \qquad \ldots \quad (3.9.)$$

Eliminating 2x from equation (3.8.) using equation (3.9.) we can deduce the value of $(\psi - \psi')$. The interpretation of $(\psi - \psi')$ is simply the phase difference occurring between an opaque and a non-opaque film of the metal. Results for such measurements can not be given as absolute phase change unless the absolute phase change for an opaque metal film is known.

The thickness of MII to which the measured relative phase change applies is obtained by measuring the height of step B.

The reasons for adopting two methods of phase change measurement were :

(a) The laborious adjustment of the interferometer and the poor ring definition for certain thicknesses of film in the Rouard method rendered desirable the adoption of a more convenient method of measurement.

(b) The method of Weaver, Hill and MacLeod, whilst very convenient to operate, required verification in its applicability.

In practice the second method permitted relatively rapid determination of relative phase change by using the Talbot Disc previously referred to. This permitted the simultaneous manufacture of six specimens for phase change measurement while at the same time allowing measurements of R, R' and T on the same specimens. The method of shielding adopted for this is shown in fig. 3.14.

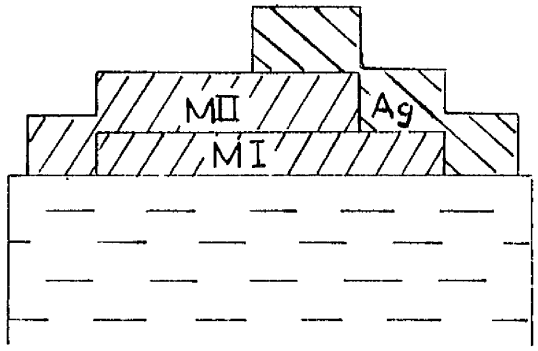

Fig. 3.13.a. Arrangement for measuring phase change on reflection by the method of Weaver, Hill and MacLeod.

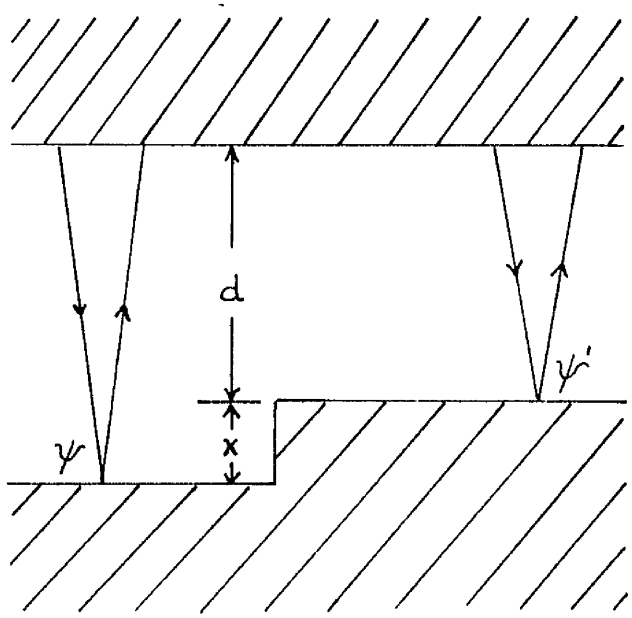

Fig. 3.13.b. Illustrating derivation of the equation for determining phase change.

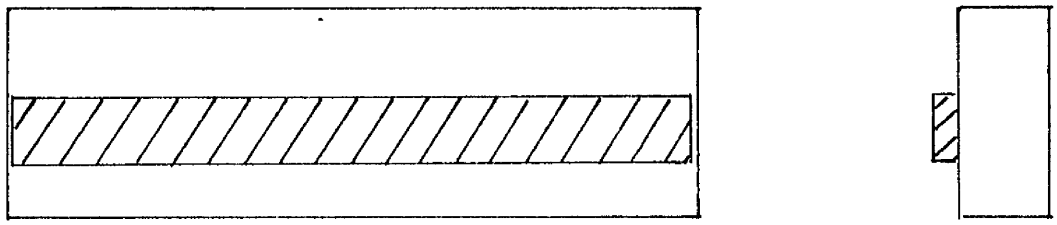

(a) Layer M I (uniform).

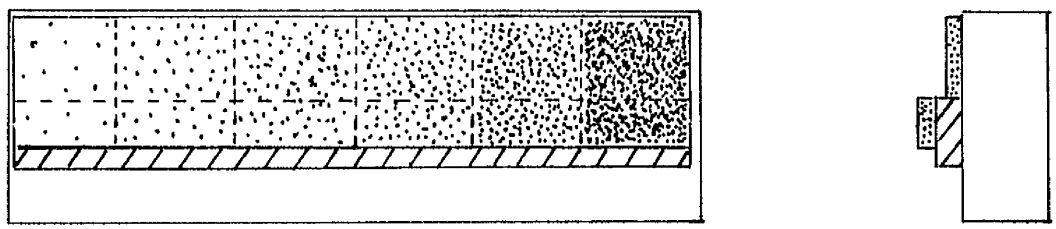

(b) Layer M I (uniform) + M II (6 thicknesses).

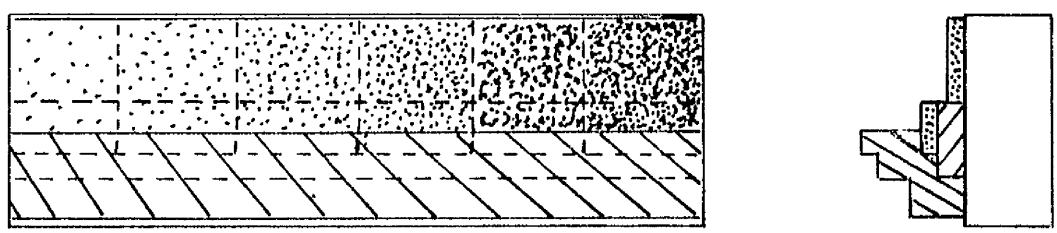

(c) M I + M II with Ag overlayer.

Fig. 3.14.a, b, c. Shielding arrangement for simultaneous preparation of specimens for T, R and R' measurements with phase change measurements.

CHAPTER 3 : REFERENCES.

3.1.) Holland, L., Vacuum Deposition of Thin Films. Chapman and Hall.

3.2.) Male, D., Thesis, University of Paris. Masson et Cie, Paris, 1953.

3.3.)

3.4.) Wiener, O., Wied. Ann., 31, 1887, 629.

3.5.) Tolansky, S., Multiple Beam Interferometry of Surfaces and Films. 1st edition, Clarendon Press (Oxford 1948).

3.6.) Hill, R., Ph.D. Thesis, Glasgow University.

3.7.) Benjamin, P., Ph.D. Thesis, Glasgow University.

3.8.) Heavens, O.S., Optical Properties of Thin Solid Films, Butterworths 1955.

3.9.) Sennett, R.S., and Scott, G.D., J. Opt. Soc. Amer, 40, 1950, 203.

3. Vol. 41, 1951, 9. Soc. Amer.,

.11.) Tronstad, L., Trans. Far. Soc. 31, 1935, 1151.

3.12.) Gulbransen and Andrew, J., Electrochemical Soc.

3.12.) Gulbransen and Andrew, J., Electrochemical Soc., Vol. 104, 1957, p.334.

3.13.) Rouard, P., Ann. de Phys. 7, 1937, p.291.

3.14.) Houston, J.G., Associatoship Thesis, R.C.S.T., Glasgow, 1961.

3.15.) Weaver, C., Hill R.M., and Moleod, J.E.S., Phase Changes on Reflection from Evaporated Chromium Films. J. Opt. Soc. Amer., Vol. 49, No. 10, p.p. 992 - 997, Oct. 1959.

CHAPTER 4 : RESULTS OF POLARIMETRY MEASUREMENTS.

As described in Chapter 3, polarimetry investigations were carried out on opaque films of chromium, copper, tin, manganese, nickel, antimony and aluminium. Figures 4.1. - 4.7. show curves of Δ and ψ as functions of the angle of incidence ϕ for the above-named metals for a wavelength of 5,460 A. Δ is the relative phase change of the p and s components on reflection, and Tan ψ represents the amplitude reduction ratio.

The vacuum polarizing spectrometer gave results for five of the above metals, viz. Cr, Cu, Sn, Mn and Ni. The results were calculated for an angle of incidence of 45° only and the n and k values obtained were then used as a guide in the calculation of the index of refraction and the thickness of the surface film on the metal specimen. Tables 4.1. - 4.5. show the results obtained for each of the five metals. The format of the tables is as follows :-

Table A shows the results obtained from the polarizing spectrometer and the calculated n and k for each angle of incidence using equations (2.29.) and (2.30.). These calculations assume that the boundary at which reflection occurs is a simple plane metal/air boundary. The results in Table A do not show a wide variation with angle of incidence but the results obtained for angle of incidence 45° show a large disagreement with the vacuum measurements and results at the same angle of incidence which are given immediately below Table A.

The vacuum polarizing spectrometer measurements $\bar{\Delta}$ and $\bar{\Psi}$ were made immediately after formation of the film and without breaking the vacuum. It is reasonable to assume therefore that a simple metal/air interface exists although it may not be exactly plane and could be slightly oxidized.

The disagreement of the air and vacuum measurements indicated that allowance should be made for the effect of a surface film and the results obtained in so doing are shown in Table B which is a reproduction of the printout of the computer which showed the best simultaneous constancy in the refractive index and thickness of the assumed surface film. Heading the table are the values assigned to n and k for the metal which gave the best constancy. The first three columns are the results obtained from the polarizing spectrometer, columns 4 and 5 show $\bar{\Delta}$ and $\bar{\Psi}$, calculated from the n and k at the head of the table using equations (2.35.) and (2.36.), and columns 6 and 7 show the values of n_1, the refractive index of the surface film (assumed to be non-absorbing), and L the thickness of the film in Angstrom units. The values of n_1 and L are obtained from equations (2.33.) and (2.34.). Immediately below Table B are shown any published values of oxides of the metal in question if such oxides are stable at room temperature.

Finally Table C shows the values obtained for the refractive index of the metal by both the simple and the sophisticated Drude treatments along with other published values of /

of the refractive index at or near the wavelength used in the present work.

In polarimetry some workers prefer to use the centesimal system of referring to angles, i.e. $2\pi = 400^{\circ}$. In the present work however the sexagesimal system has been retained because of its familiarity; i.e. $2\pi = 360^{\circ}$ throughout.

Except where otherwise stated, the published values of the refractive index of the oxides of the various metals shown under Table B will refer to the wavelength of the sodium D line, i.e. $\lambda = 5,890$ A. The low value of dispersion which commonly applies to these oxides means that the refractive index for $\lambda = 5,460$ A will not be sensibly different from that shown.

Due to the inherent errors in the polarizing spectrometer such as centring and calibration errors, a final accuracy of $\pm$ 0.05 in n and k is estimated and applies to all values of n and k calculated from the polarimetry results obtained in this work.

Chromium :

The results for chromium shown in fig. 4.1. do not agree with those published by Hill and Weaver(4.1.) which are also shown. This is not surprising for the films used by Hill and Weaver had a different appearance, namely there was a definite brownish tinge to the chromium films of these authors which was absent from the films used in this work.

The result obtained for the refractive index of the chromium films neglecting the surface film was clearly different from that obtained when allowance was made for such a film. The value of n changed by about 25% while that of k changed by a much smaller amount. The mean value of 2.51 obtained for the refractive index of the surface layer agrees closely to the published value of the refractive index of Cr_2O_3, viz. 2.5. According to Gulbransen and Hickman(4.2.) at room temperature the oxide of chromium consists entirely of Cr_2O_3. The mean thickness of the surface film of 60 Angstroms is somewhat larger than recent reports of work on other metals would indicate (4.3.) but inconsistencies in film thickness are common. Some workers attribute the discrepancies to the presence of surface roughness in their specimens. Another factor which may cause discrepancies in the values obtained for film thicknesses is that of the considerable penetration of the oxidation into the metal so that below the homogeneous oxide film there exists a mixed zone of metal and oxide extending in depth for some hundreds of Angstroms. The existence of this oxide phase has been detected by different techniques (4.4.) - (4.6.).

Copper :

The values of Δ and ψ obtained for five opaque copper films showed a variation from one specimen to the other, particularly in the ψ values. The various opaque specimens also showed slight variations in reflectivity at normal incidence. This fact will be /

be referred to again in Chapter 5. Instead of taking a mean value for all the specimens measured it was decided to adopt the results for the specimen with the highest reflectivity in the belief that this would best enable a comparison with the refractive index results obtained by the Malé method. Figure 4.2. shows the Δ and ψ results obtained for the copper specimen selected. Also shown are the results obtained on copper films by Avery(4.7.); Lowery, Wilkinson and Smare(4.8.); and Winterbotton(4.9.). It can be seen that the Δ values obtained agree well with those obtained by Avery and Lowery, et al, but not with the value obtained by Winterbotton. In the case of the ψ values there appears to be good agreement with Avery's results up to an angle of incidence of 55°. Beyond 55° there is some variation between the results of the present work and those of Avery. There is fairly good agreement with the ψ value obtained by Winterbotton for an angle of incidence of 60°.

In Table 4.2. it can be seen that the results obtained for the calculation of n and k both show a noticeable change when the effect of the surface film is allowed for. The mean value of 2.69 obtained for the refractive index of the surface film lies fairly close to the published values of 2.84 for Cu O and 2.7 for Cu_2 O. Although the value obtained for the refractive index of the surface film is almost equal to that of Cu_2 O this is probably fortuitous as according to Valensi(4.10.) at room temperature the form of the oxide of copper is Cu O.

Tin :

The calculated values of n = 1.40 and k = 3.63 obtained from Table A become n = 1.99 and k = 4.32 when allowance is made for the effect of the surface film as shown in Table B. It may be noted that the k value obtained using the simple Drude treatment lies fairly close to the k value quoted in Landolt and Bornstein for an evaporated tin film at wavelengths of 5,400 A and 5,500 A. All other published values are for bulk specimens and comparison is less satisfactory.

The mean value of 2.10 obtained for the refractive index of the surface film agrees well with that of 2.05 for $Sn\ O_2$ which is the form of tin oxide at room temperature according to Finch and Quarrell(4.11.). The mean thickness of the film was determined to be 58 A.

Manganese :

The calculated values of n = 2.38 and k = 2.23 obtained using the simple Drude treatment became n = 3.05 and k = 2.30 when the effect of the surface film was taken into account. The n value of 2.38 obtained using the simple Drude treatment lies fairly close to the only other n value available for an evaporated film, viz. the value of n = 2.46 for λ = 5,461 A quoted in Landolt and Bornstein. However there appears to be little agreement between the k values.

The mean value of 2.31 obtained for the refractive index of the surface film agrees closely with that of 2.30 quoted for the mean refractive index of Mn_3O_4. Gurnick and Baldwin(4.12.) investigated the proportions of Mn O and Mn_3O_4 present on a specimen of Mn over a temperature range of 400°C. to 1,100°C. They found that below 800°C. the oxide consisted entirely of Mn_3O_4. It is therefore reasonable to assume that below 400°C. the oxide will continue to be Mn_3O_4. The mean thickness obtained for the surface film on manganese was 58 A.

Nickel :

When the presence of the surface film on nickel is taken into account the calculated n value became 3.60 instead of 2.31 as obtained with the simple Drude treatment. The calculated k value showed a less noticeable change from 3.07 to 3.42. No published values for the refractive index of evaporated nickel films could be found but the published values for specimens prepared in other ways showed a tendency towards a lower n value than that obtained in this work. The published k values generally agreed with those obtained in this work.

The value of 2.17 for the refractive index of the surface film showed good agreement with the published value of 2.18 for Ni O. According to Kubachewsky and Hopkins(4.3.) the oxide of nickel at room temperature is Ni O. The mean thickness obtained for the surface film was 77 A.

In general the results obtained from the air measurements are in agreement with those obtained from the vacuum measurements when allowance is made for the presence of a surface film. In no case is agreement with the vacuum measurements obtained when the surface film is neglected. The refractive index values obtained for the surface films showed good agreement with that of the corresponding metal oxide in every case.

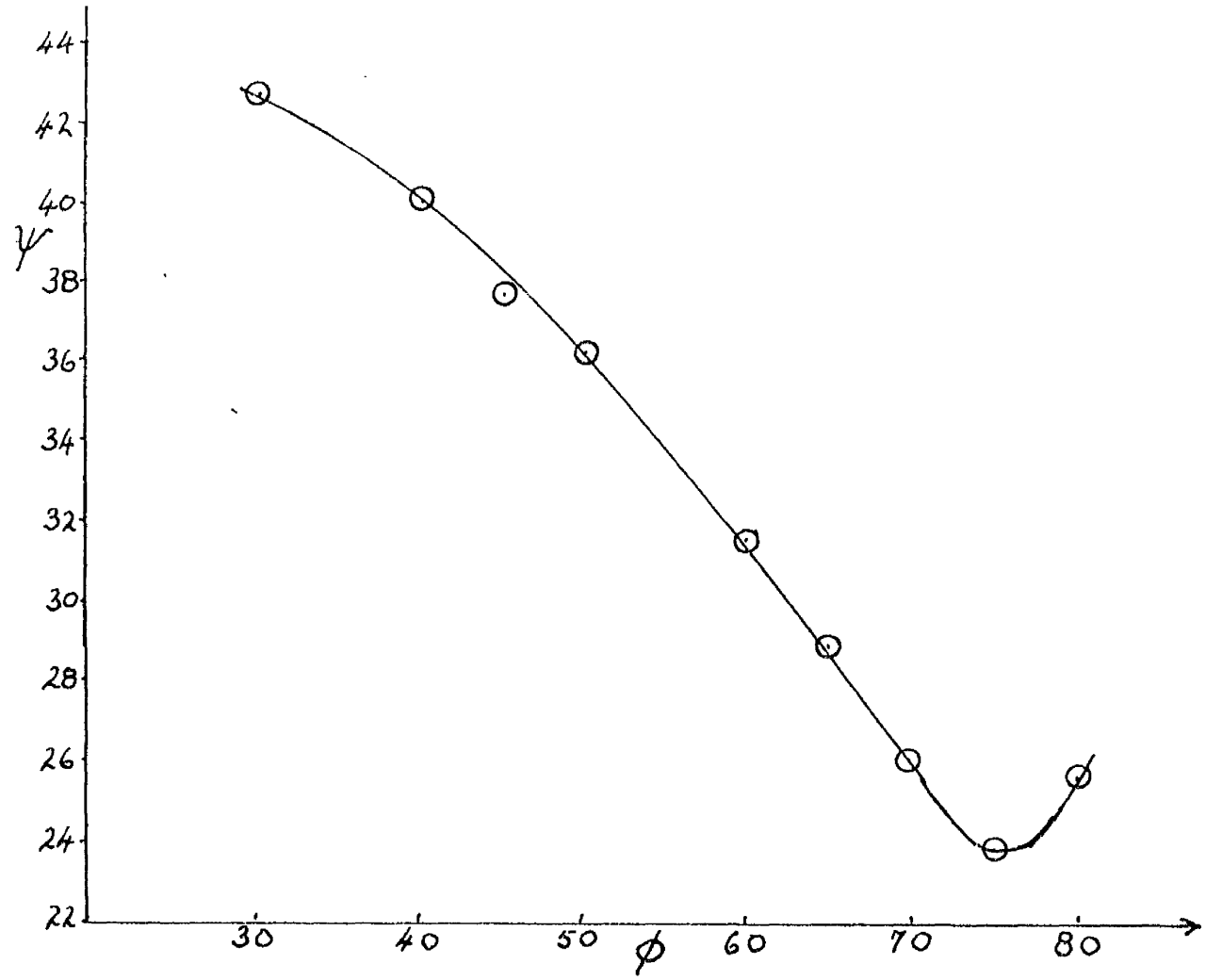

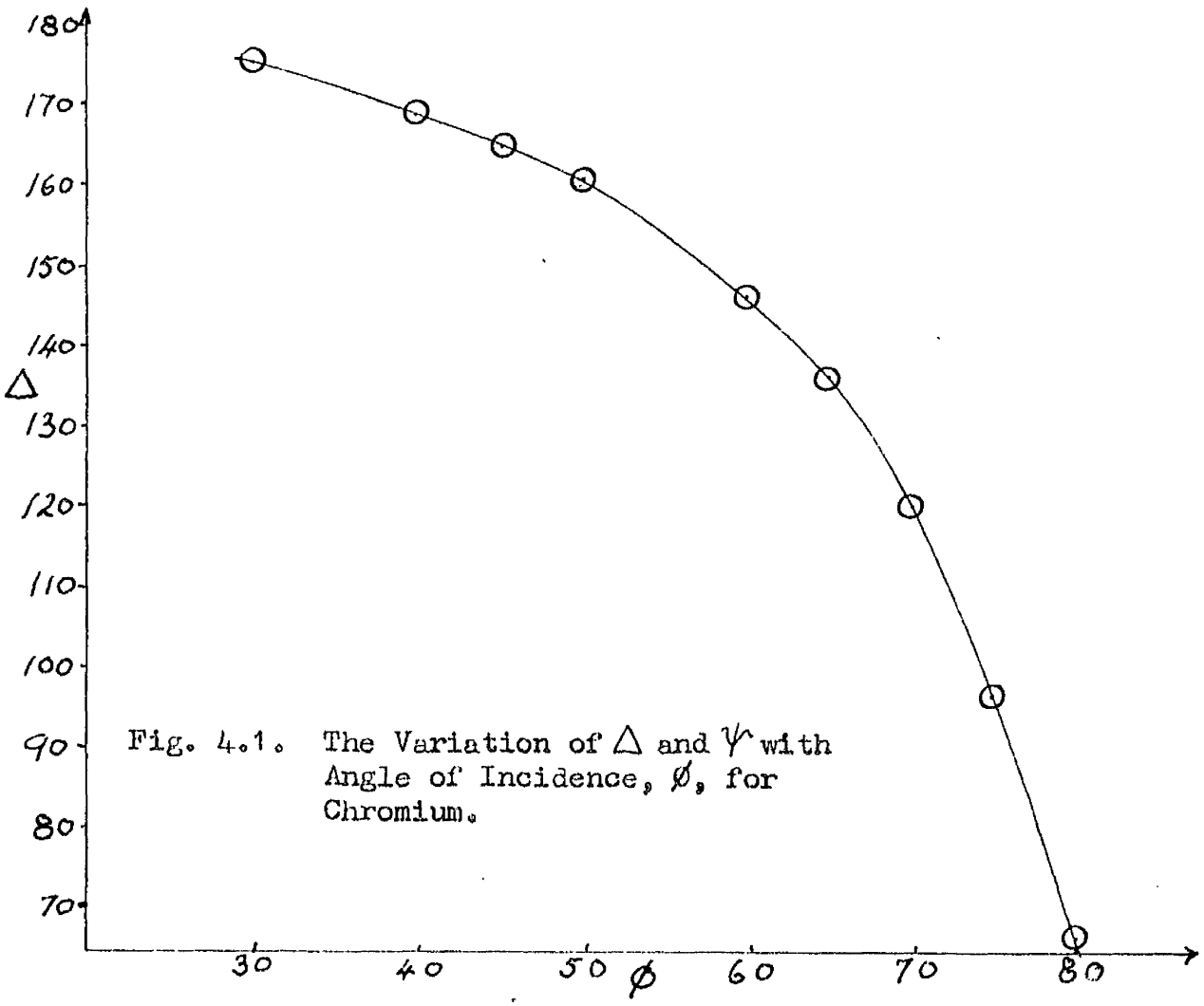

Fig. 4.1. The Variation of Δ and Ψ with Angle of Incidence, ϕ, for Chromium.

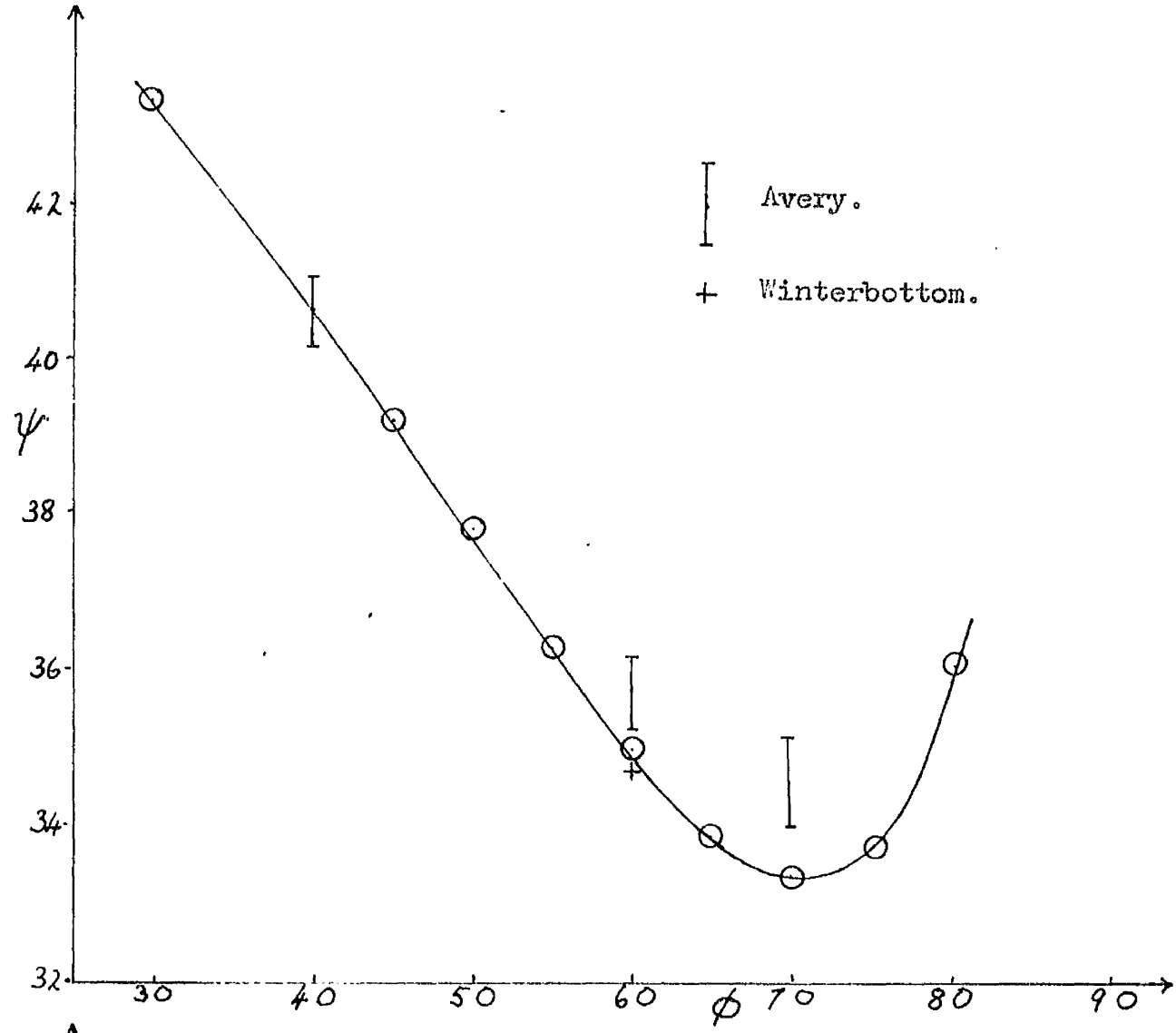

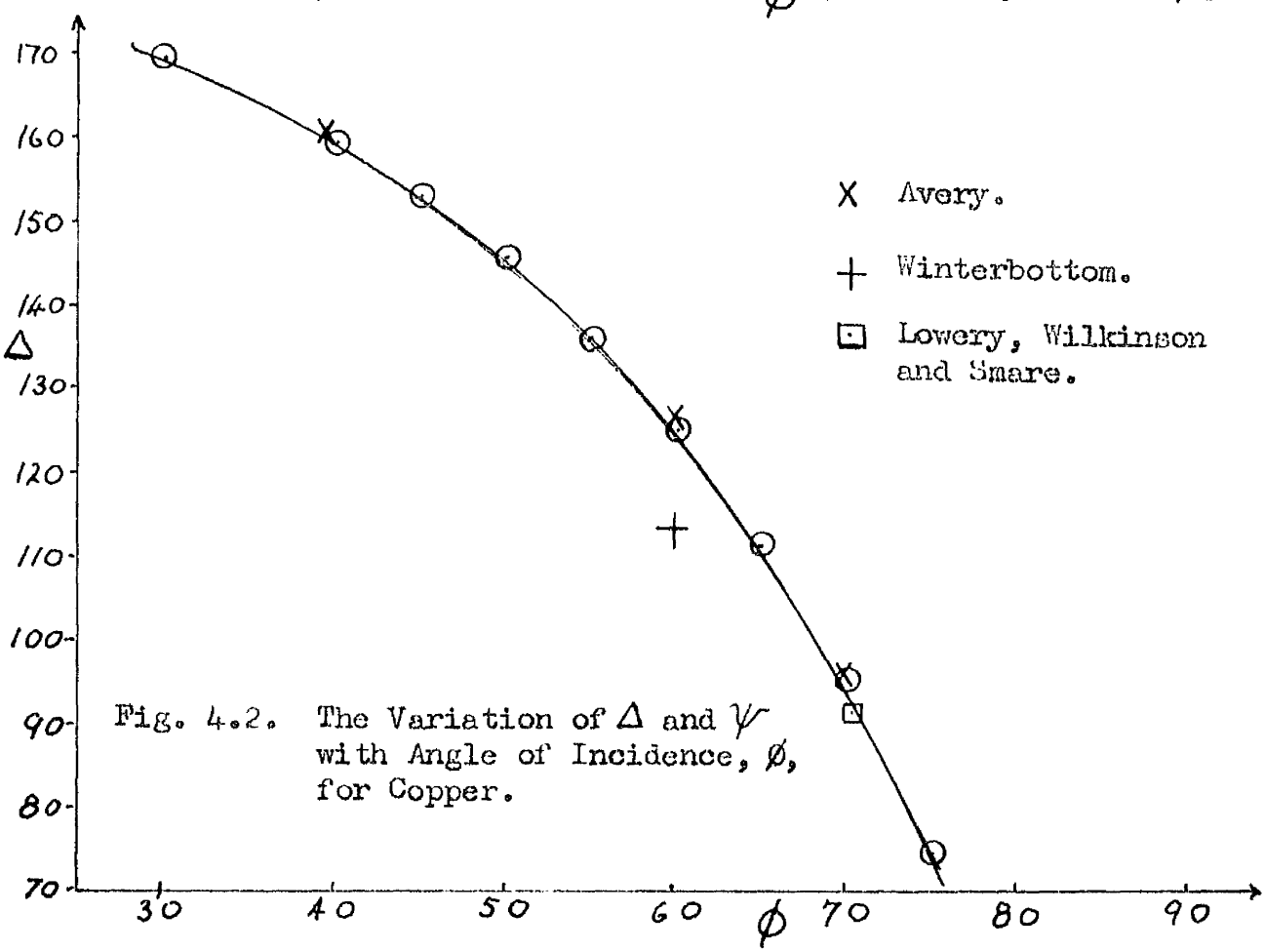

Fig. 4.2. The Variation of Δ and ψ with Angle of Incidence, ϕ, for Copper.

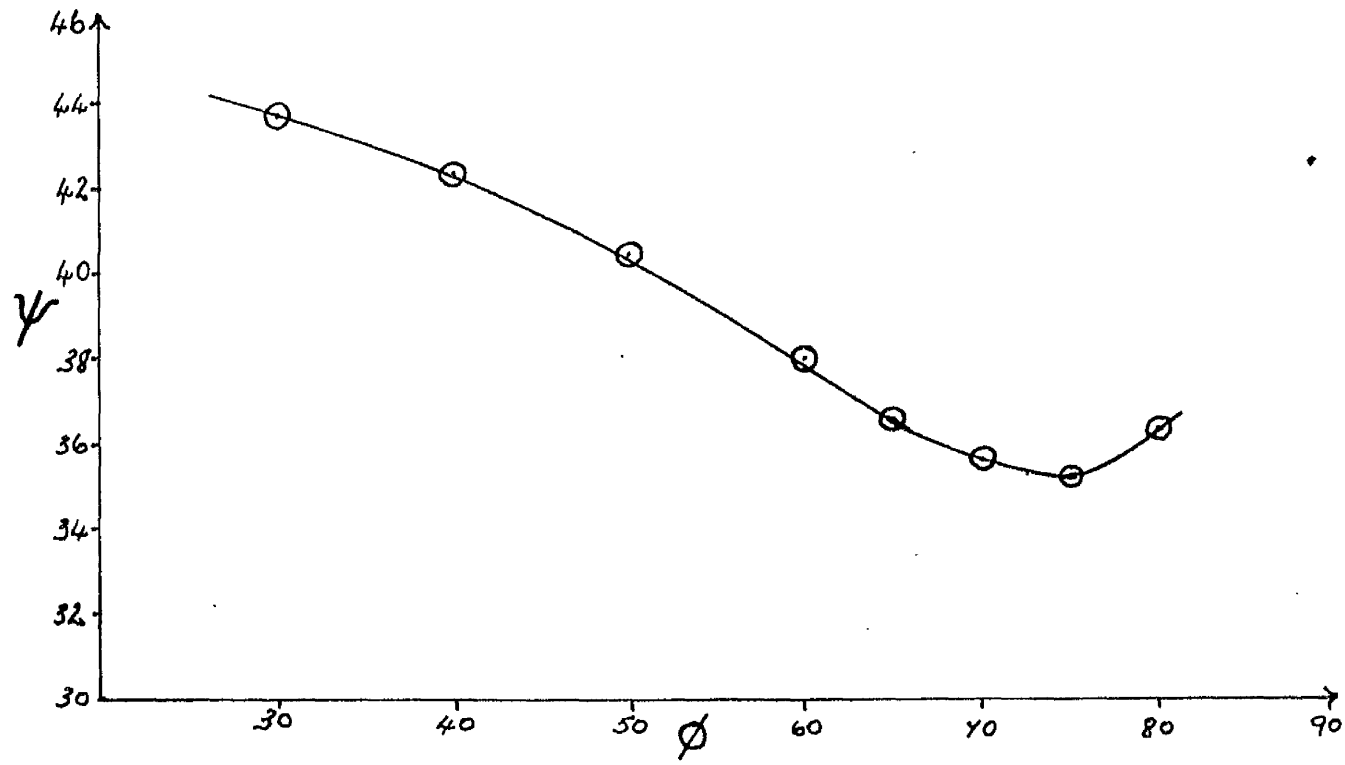

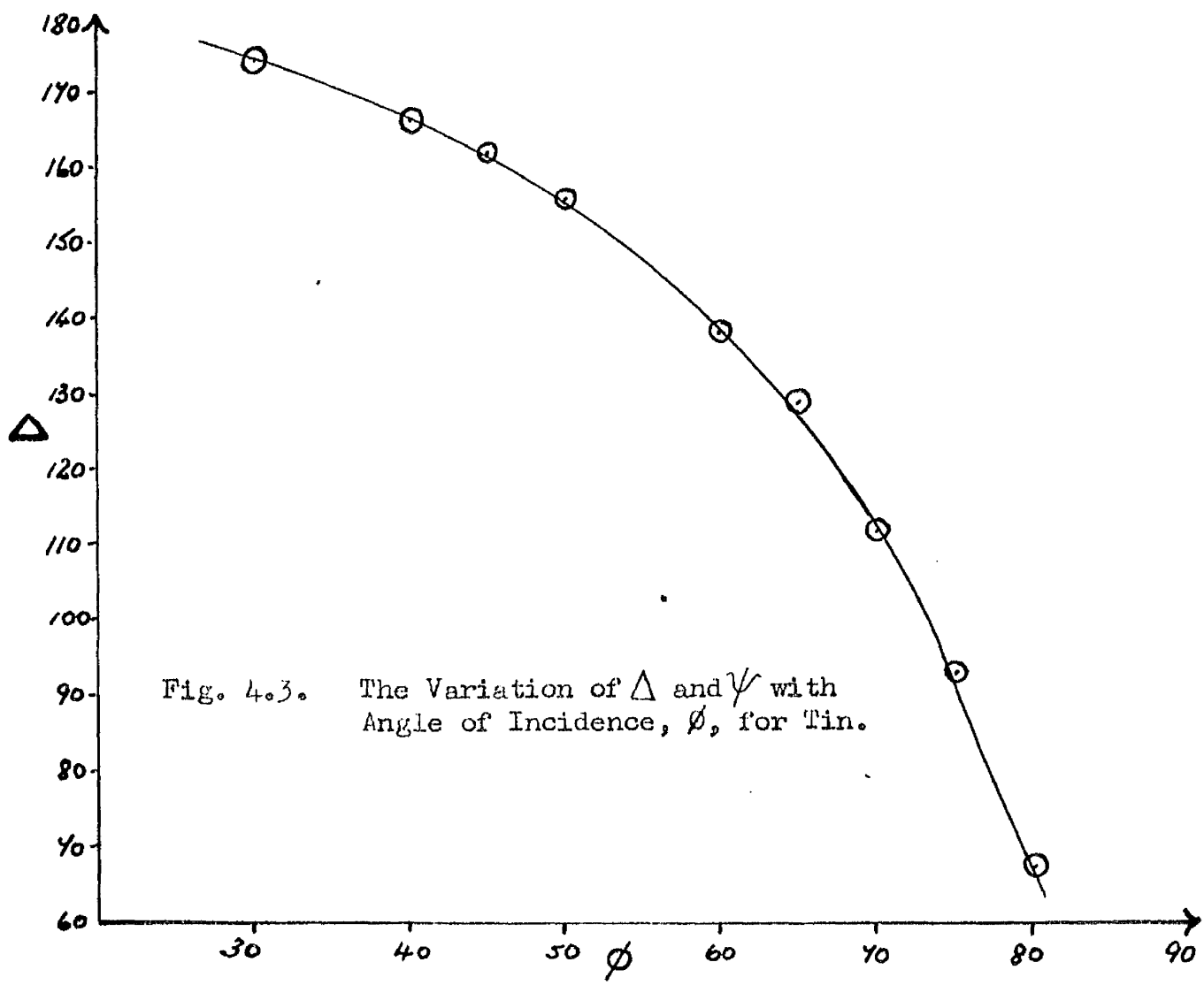

Fig. 4.3. The Variation of Δ and ψ with Angle of Incidence, ϕ, for Tin.

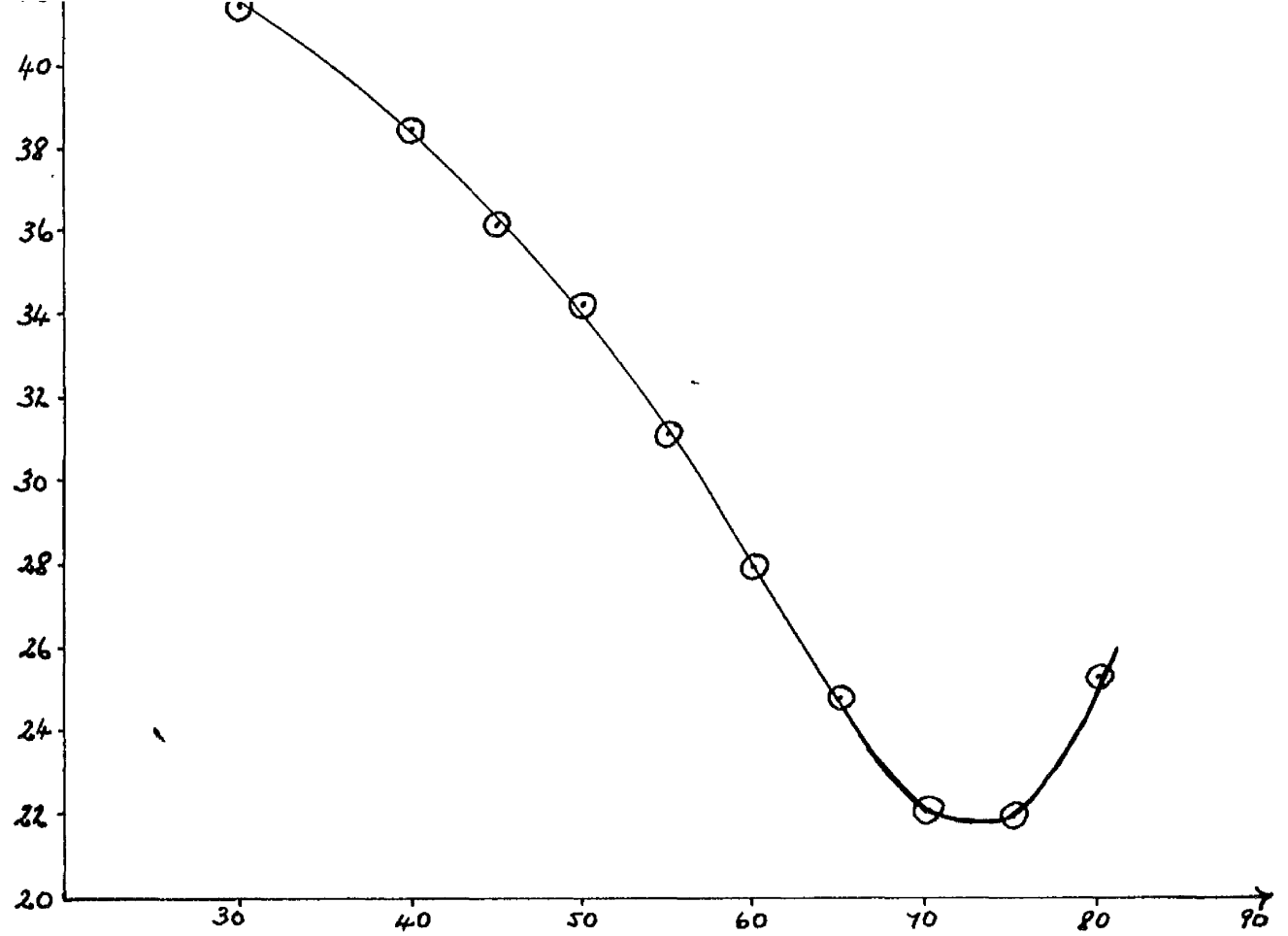

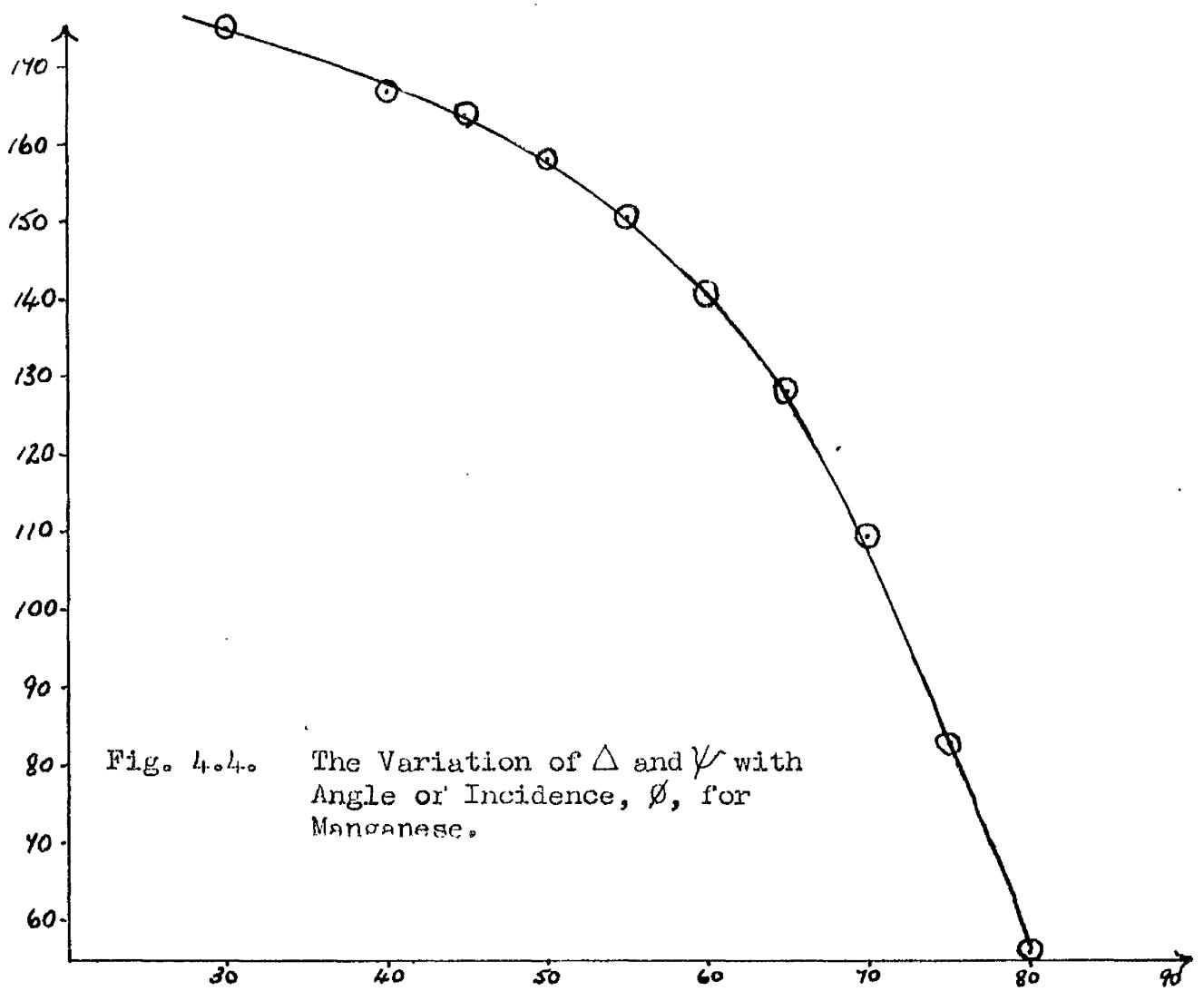

Fig. 4.4. The Variation of Δ and ψ with Angle of Incidence, ϕ, for Manganese.

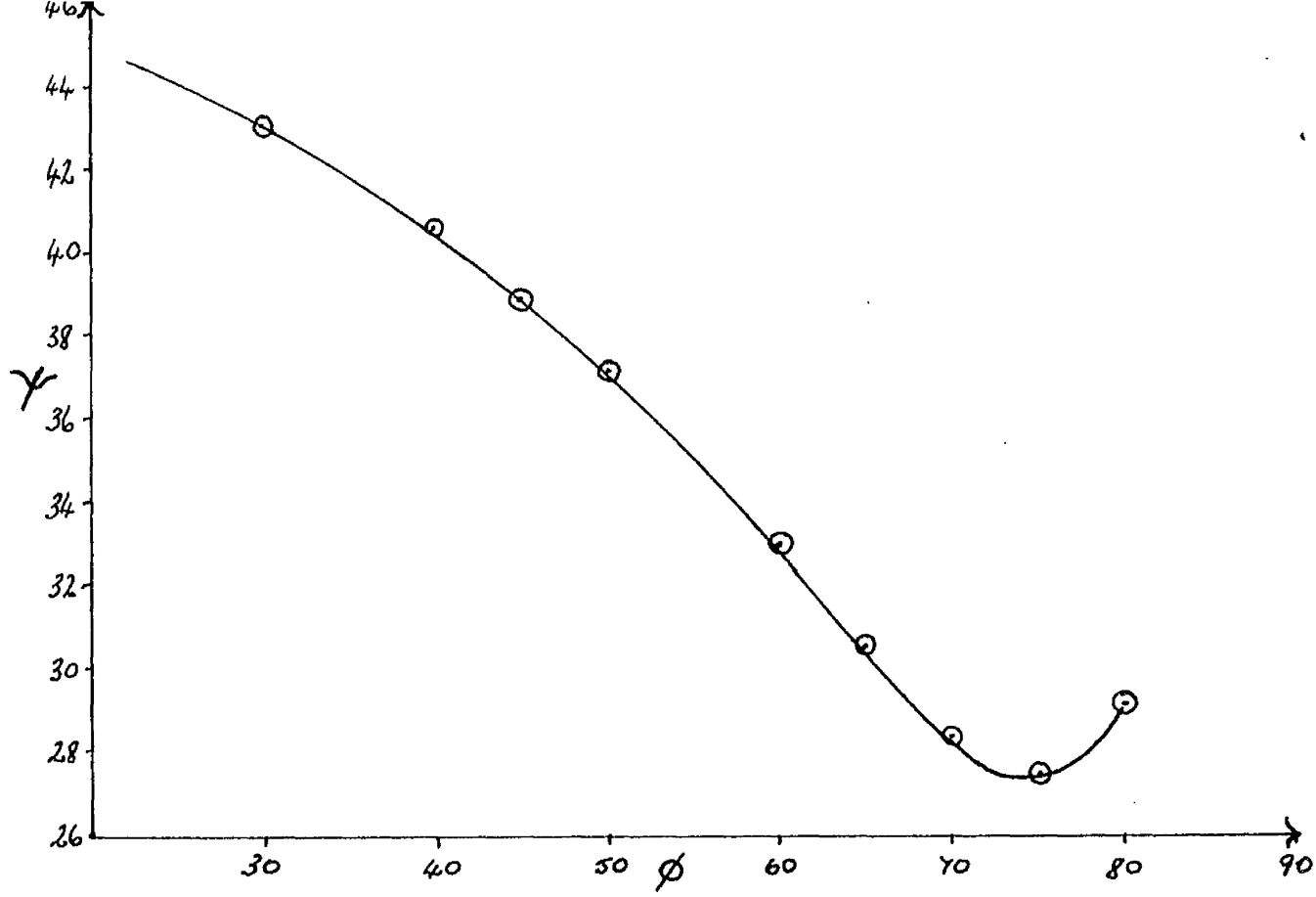

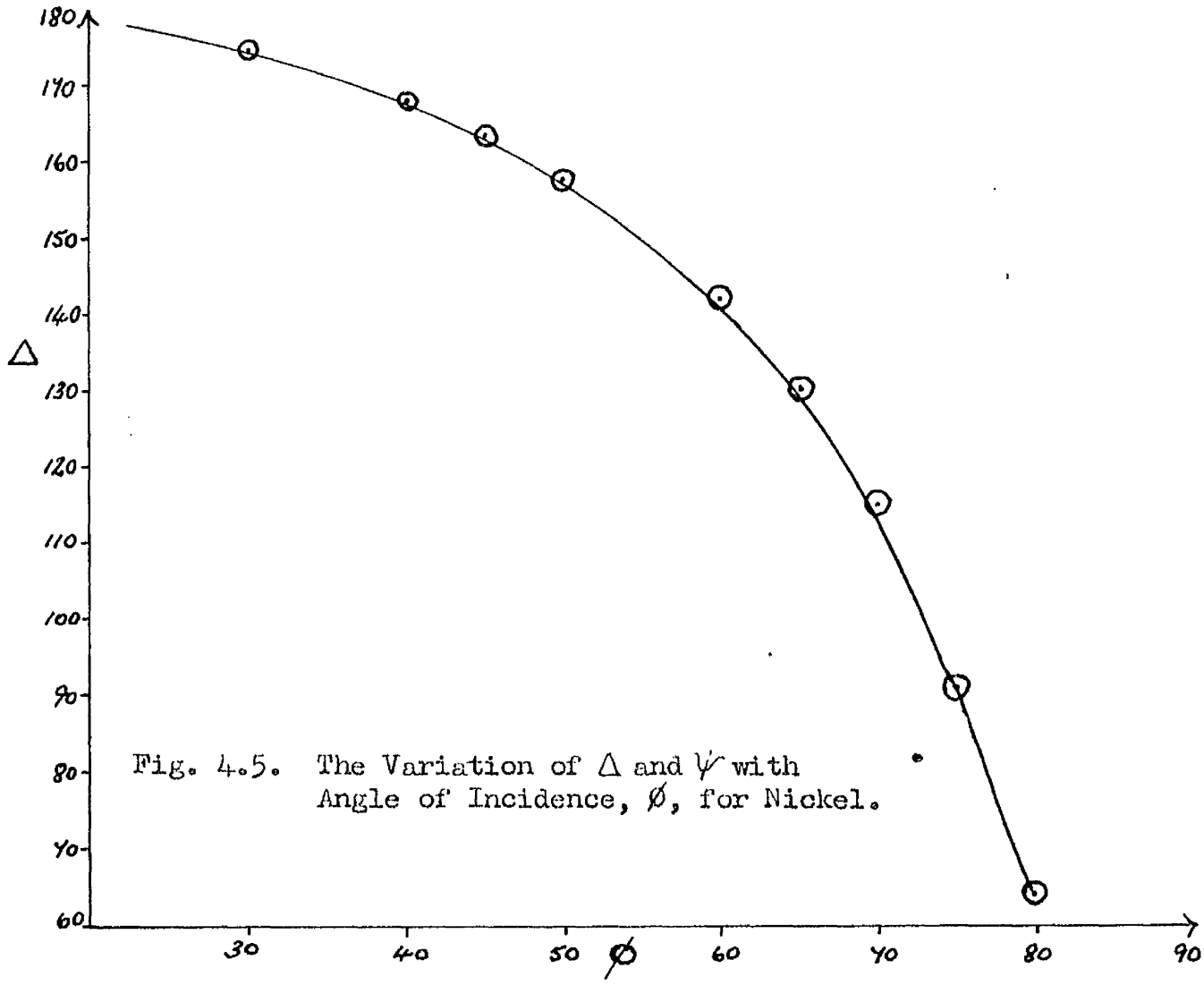

Fig. 4.5. The Variation of Δ and ψ with Angle of Incidence, ϕ, for Nickel.

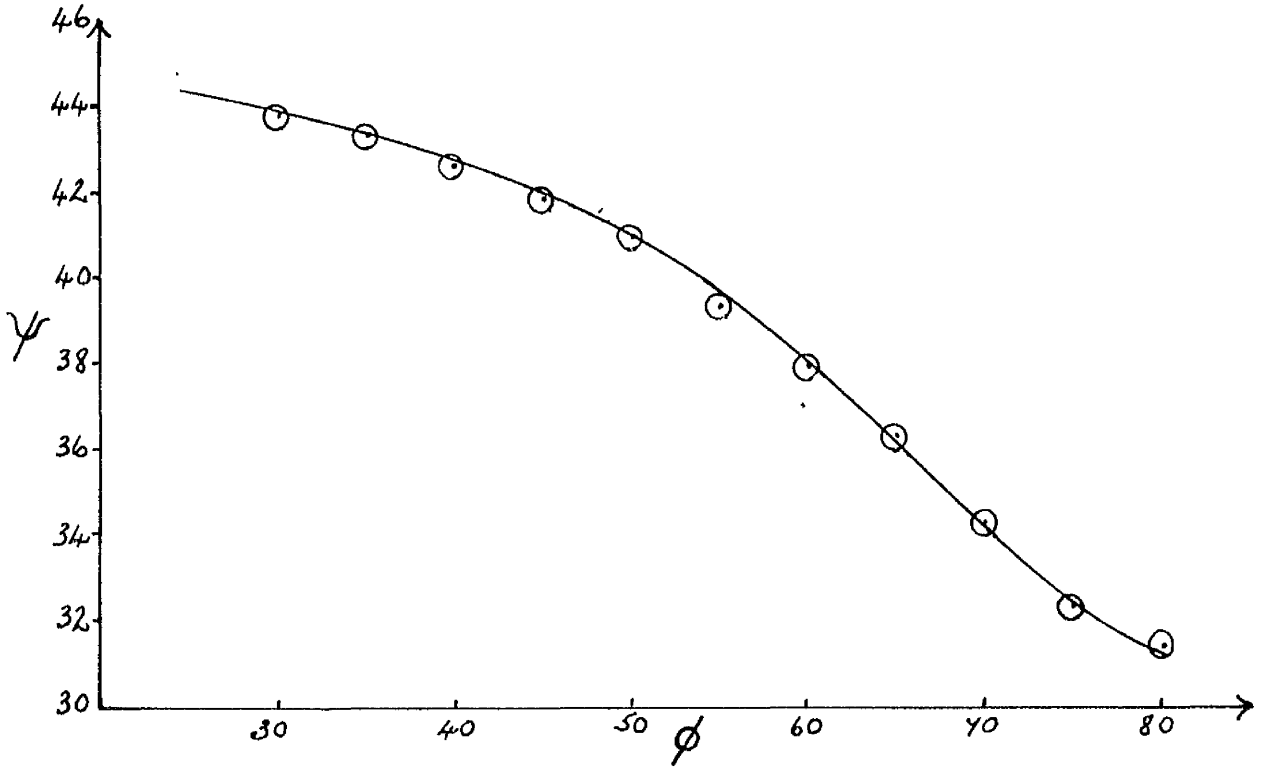

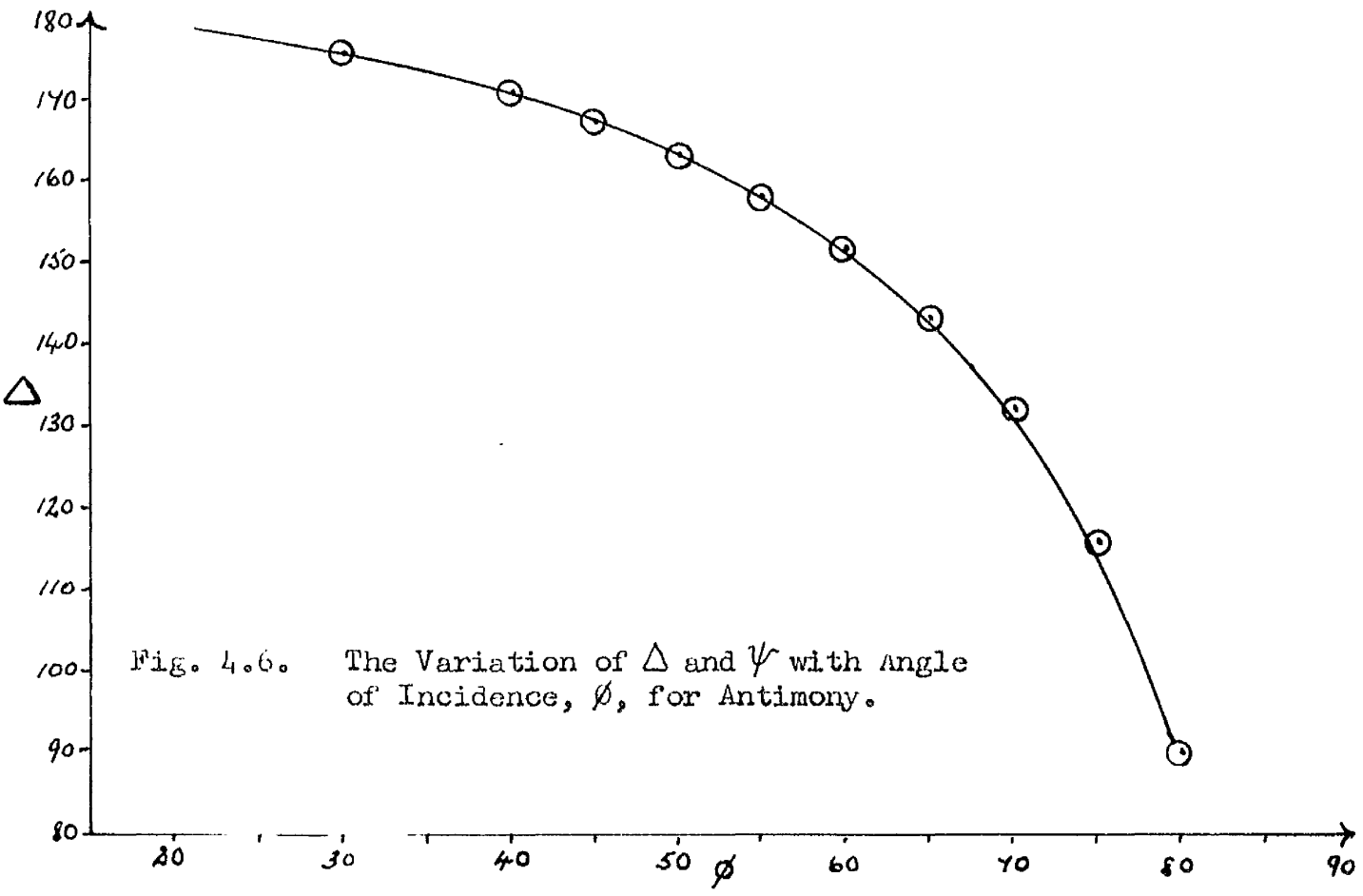

Fig. 4.6. The Variation of Δ and ψ with Angle of Incidence, ϕ, for Antimony.

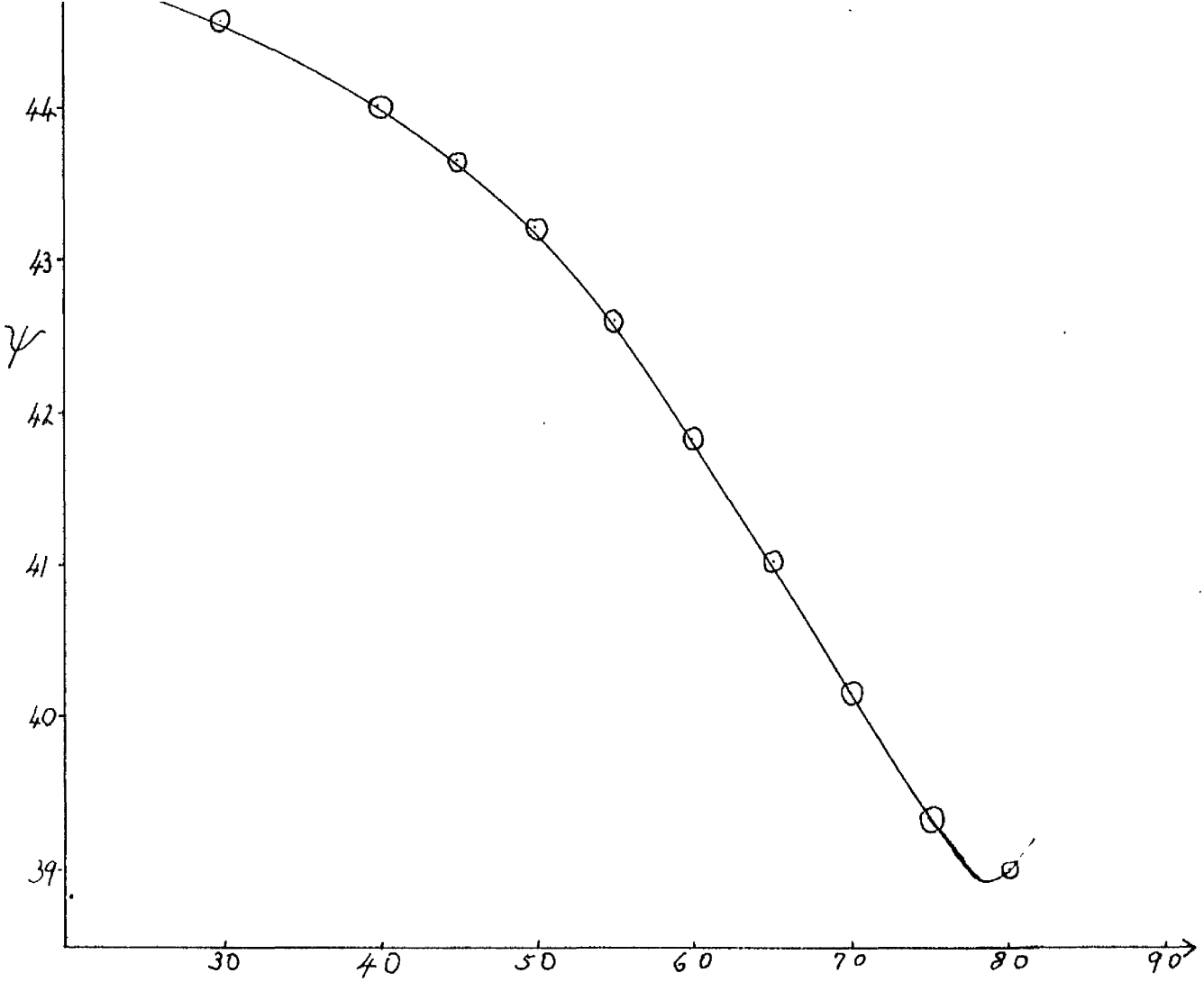

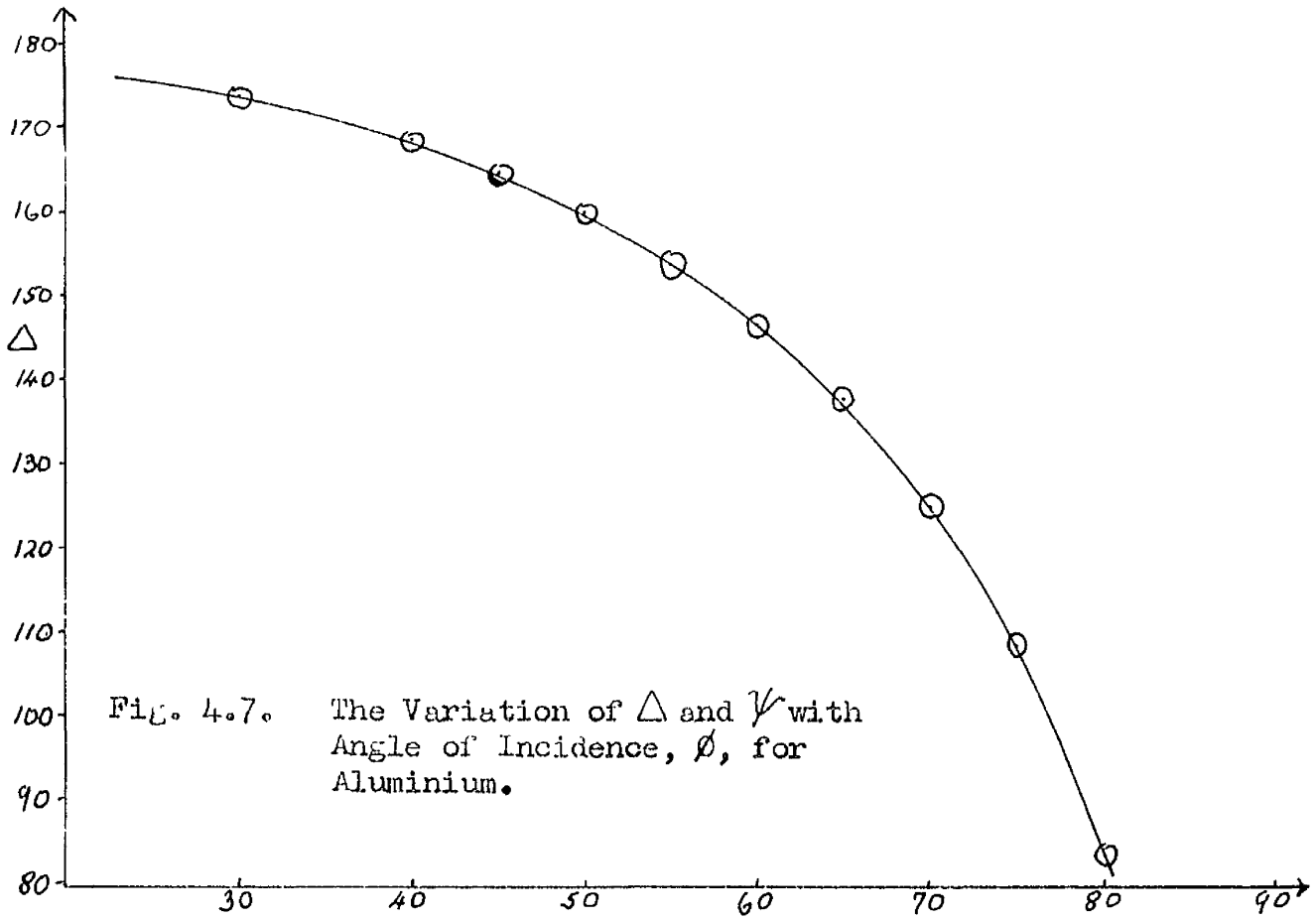

Fig. 4.7. The Variation of Δ and Ψ with Angle of Incidence, ϕ, for Aluminium.

TABLE 4.1. : POLARIMETRY RESULTS FOR CHROMIUM.

Table A : n, k Results Neglecting Presence of Surface Film.

ϕ	Δ	Ψ	n	k
°	°	°		
45	166.00	38.25	2.92	2.94
50	161.00	36.30	2.79	2.90
55	155.00	34.05	2.74	2.88
60	144.00	31.40	2.70	2.86
65	137.20	28.50	2.75	2.88
		Mean Value	2.78	2.89

Vacuum Measurement Result for $\phi = 45^{\circ}$

$\bar{\Delta} = 169.0^{\circ}$ $\bar{\Psi} = 39.2^{\circ}$ $n = 3.68$ $k = 3.43$

Table B : Computer Results Showing Best Constancy in n_1 and L.
$n = 3.95$ $k = 3.00$.

ϕ	Δ	Ψ	$\bar{\Delta}$	$\bar{\Psi}$	n_1	L (A.U.)
°	°	°	°	°		
45	166.00	38.25	170.02	38.57	2.47	51
50	161.00	36.30	167.02	36.76	2.53	58
55	155.00	34.05	163.19	34.58	2.54	62
60	147.00	31.40	158.07	31.91	2.55	65
65	137.20	28.50	150.75	28.62	2.47	63
				Mean Value	2.51	60

Refractive Index of $Cr_2O_3 = 2.5$

Table C : Values of n and k for Chromium.

λ	n	k	Source and Remarks
5460	2.78	2.89	Present Work; simple Drude Treatment.
5460	3.95	3.00	" " ; Drude Method allowing for Surface Film.
5461	2.49	2.30	Abelès; Evaporated Film.
5461	1.18	1.06	Hill and Weaver; Evaporated Film.
5330	3.43	4.85	Landolt and Bornstein; Bulk Specimen.
5790	2.97	4.85	" " " ; " "
5460	3.53	4.41	Physikalisch und Chemische Tabellen.

TABLE 4.2. : POLARIMETRY RESULTS FOR COPPER.

Table A : n, k Results Neglecting Presence of Surface Film.

ϕ	Δ	ψ	n	k
°	°	°		
45	153.50	39.20	1.15	2.51
50	146.00	37.80	1.15	2.51
55	136.20	36.27	1.13	2.48
60	126.00	34.95	1.15	2.54
65	112.00	33.70	1.14	2.54
		Mean Value	1.14	2.52

Vacuum Measurement Result for $\phi = 45^\circ$

$\bar{\Delta} = 159.3^\circ$ $\bar{\psi} = 39.5^\circ$ $n = 1.65$ $k = 3.00$

Table B : Computer Results Showing Best Constancy in n_1 and L. n = 1.59 k = 3.22.

ϕ	Δ	ψ	$\bar{\Delta}$	$\bar{\psi}$	n_1	L (A.U.)
°	°	°	°	°		
45	153.50	39.20	159.83	40.17	2.74	87
50	146.00	37.80	154.02	38.90	2.74	87
55	136.20	36.27	146.83	37.44	2.70	94
60	126.00	34.95	137.78	35.82	2.65	86
65	112.00	33.70	126.08	34.12	2.63	87
				Mean Value	2.69	88

Refractive Index of Cu O = 2.84
" " " Cu_2O = 2.705

Table C : Values of n and k for Copper.

λ	n	k	Source and Remarks
5460	1.14	2.52	Present Work; Simple Drude Treatment.
5460	1.59	3.22	" " ; Drude Method allowing for Surface Film.
5400	1.10 ±.07	2.53 ±0.1	Avery; Evaporated Film; Simple Drude Treatment.
5460	0.93	2.39	Landolt and Bornstein; Bulk Specimen.
5461	0.71	3.19	" " " ; Sputtered Film.
5461	0.87	2.74	" " " ; " "
5500	0.72	-	" " " ;
5500	0.80	2.39	" " " ;
5400	1.07	2.41	International Critical Tables.
5400	1.00	2.40	Winterbottom; Bulk Specimen.

TABLE 4.3. : POLARIMETRY RESULTS FOR TIN.

Table A : n, k Results Neglecting Presence of Surface Film.

ϕ °	Δ °	ψ °	n	k
45	161.50	41.40	1.50	3.76
50	155.30	40.40	1.42	3.65
55	148.00	39.25	1.38	3.60
60	139.00	37.99	1.36	3.57
65	127.80	36.65	1.35	3.56
		Mean Value	1.40	3.63

Vacuum Measurement Result for $\phi = 45^{\circ}$

$\bar{\Delta} = 164.4^{\circ}$ $\bar{\psi} = 41.3^{\circ}$ $n = 2.06$ $k = 4.20$

Table B : Computer Results Showing Best Constancy in n_1 and L. n = 1.99 k = 4.32.

ϕ °	Δ °	ψ °	$\bar{\Delta}$ °	$\bar{\psi}$ °	n_1	L (A.U.)
45	161.50	41.40	164.56	41.50	2.04	46
50	155.30	40.40	160.10	40.54	2.09	56
55	148.00	39.25	154.57	39.40	2.14	60
60	139.00	37.99	147.54	38.06	2.13	63
65	127.80	36.65	138.30	36.48	2.11	63
				Mean Value	2.10	58

Refractive Index of polycrystalline $Sn\ O_2$ = 2.05

Table C : Values of n and k for Tin.

λ	n	k	Source and Remarks
5460	1.40	3.63	Present Work; Simple Drude Treatment.
5460	1.99	4.32	" " ; Drude Method allowing for Surface Film.
5460	1.73	5.33	International Critical Tables.
5330	0.89	3.92	Landolt and Bornstein; Bulk Specimen.
5880	1.12	4.51	" " " ; " "
5400	-	3.74	" " " ; Evaporated Film.
5500	-	3.75	" " " ; " "
5400	1.0	4.2	Hedges and Homer; Bulk Specimen.

TABLE 4.4. : POLARIMETRY RESULTS FOR MANGANESE.

Table A : n, k Results Neglecting Presence of Surface Film.

ϕ °	Δ °	ψ °	n	k
45	163.50	36.35	2.49	2.27
50	157.80	34.00	2.42	2.26
55	151.00	31.20	2.44	2.24
60	139.50	28.05	2.27	2.19
65	127.00	24.86	2.32	2.19
		Mean Value	2.38	2.23

Vacuum Measurement Result for $\phi = 45^{\circ}$

$\bar{\Delta} = 166.5^{\circ}$ $\bar{\psi} = 36.6^{\circ}$ $n = 2.95$ $k = 2.30$

Table B : Computer Results Showing Best Constancy in n_1 and L.
$n = 3.05$ $k = 2.30$.

ϕ °	Δ °	ψ °	$\bar{\Delta}$ °	$\bar{\psi}$ °	n_1	L (A.U.)
45	163.50	36.35	167.00	36.70	2.24	46
50	157.80	34.00	163.03	34.42	2.22	53
55	151.00	31.20	157.86	31.72	2.34	54
60	139.50	28.05	150.79	28.55	2.34	70
65	127.00	24.86	140.42	24.90	2.39	66
				Mean Value	2.31	58

Refractive Index of Mn O = 2.16
Mean Refractive Index of $Mn_3 O_4$ = 2.30

Table C : Values of n and k for Manganese.

λ	n	k	Source and Remarks
5460	2.38	2.23	Present Work; Simple Drude Treatment.
5460	3.05	2.30	" " ; Drude Method Allowing for Surface Film.
5460	1.83	3.17	Landolt and Bornstein; Bulk Specimen.
5461	2.46	3.04	" " " ; Evaporated Film.
5320	1.85	3.28	International Critical Tables.
5780	2.49	3.88	" " "

TABLE 4.5. : POLARIMETRY RESULTS FOR NICKEL.

Table A : n, k Results Neglecting Presence of Surface Film.

ϕ	Δ	ψ	n	k
°	°	°		
45	164.00	38.90	2.47	3.15
50	158.00	37.20	2.30	3.08
55	151.00	35.24	2.23	3.04
60	143.00	33.00	2.26	3.05
65	132.00	30.50	2.27	3.05
		Mean Value	2.31	3.07

Vacuum Measurement Result for $\phi = 45^{\circ}$

$\bar{\Delta} = 168.00^{\circ}$ $\bar{\psi} = 39.3^{\circ}$ $n = 3.40$ $k = 3.50$

Table B : Computer Results Showing Best Constancy in n_1 and L. n = 3.60 k = 3.42.

ϕ	Δ	ψ	$\bar{\Delta}$	$\bar{\psi}$	n_1	L (A.U.)
°	°	°	°	°		
45	164.00	38.90	168.68	39.16	2.19	63
50	158.00	37.20	165.31	37.53	2.17	78
55	151.00	35.24	161.04	35.56	2.16	83
60	143.00	33.00	155.40	33.17	2.17	81
65	132.00	30.50	147.51	30.26	2.17	80
				Mean Value	2.17	77

Refractive Index of Ni O = 2.18

Table C : Values of n and k for Nickel.

λ	n	k	Source and Remarks
5460	2.31	3.07	Present Work; Simple Drude Treatment.
5460	3.60	3.42	" " ; Drude Method Allowing for Surface Film.
5461	1.59	3.27	Landolt and Bornstein; Bulk Specimen.
5461	1.81	2.85	" " " ; Sputtered Film.
5461	1.76	3.44	" " " ; Electrolytically Deposited.
5400	1.63	3.21	International Critical Tables.
5800	1.73	3.43	" " "

CHAPTER 4 : REFERENCES.

4.1.) Hill, R.M. and Weaver, C., Trans. Far. Soc., Vol. 54, 1958, 1140.

4.2.) Gulbransen, E.A., and Hickman, J.W., Trans. Amer. Inst. Min. (Metall) Engrs., Vol. 171, 1947, p.306.

4.3.) Kubachewsky and Hopkins; Oxidation of Metals and Alloys. Butterworths 1953.

4.4.) Evans, U.R., and Stockdale, J., J. Chem. Soc., 1929, p.2651.

4.5.) Vernon, W.H.J., et al. Proc. Roy. Soc. (A), Vol. 216, 1953, p.375.

4.6.) Grunberg, L. and Wright, K.H.R., Conf. on Lubrication and Wear. Inst. of Mech. Engrs., 1957, paper 67.

4.7.) Avery, D.G., Phil. Mag., 1950, p.1018.

4.8.) Lowery, Wilkinson and Smare, Phil. Mag., Vol. 22, 1936, p.149.

4.9.) Winterbottom, A.B., Optical Studies of Metal Surfaces. Det. Kgl. Norske Videnskabers Selskabs Skrifter, 1955, No. 1.

4.10.) Valensi, G., Int. Conf. Surface Reactions, 1948, p.156.

4.11.) Finch, G.I., and Quarrell, A.G., Nature, London, Vol. 131, 1933, p.877, and Proc. Roy. Soc., Vol. 141, 1933, p.398.

4.12.) Gurnick, R.S., and Baldwin, W.M., Trans. Amer. Soc. Metals, Vol. 42, 1950, p.641.

CHAPTER 5.

5.1.) Results of Reflectance and Transmittance Measurements.

The metals investigated in this work were Ni, Cr, Sn, Cu, Sb, Al and Mn. The purity of the evaporant in every case was carefully checked and all were found to have less than 2 p.p.m. of impurities.

In all cases thickness measurements were made immediately after deposition. This applied to both weight thickness measurements and to interferometric measurements by the Tolansky method. If the weight thickness specimens were not measured immediately spurious results could arise due probably to the adsorption of water vapour onto the freshly made film. In the case of interferometric measurements it was found that after allowing the specimens to age for a day or two the "step" in the fringes which gives the film thickness becomes indefinite due probably to a diffusion effect. Reflectance and transmittance measurements were made on a specimen after it had aged in a desiccator jar at room temperature for ten days.

The number of specimens made for each metal was at least six. Each specimen contained six sections of different thickness giving at least thirty six sets of T, R and R' measurements. In some cases, viz. Cr and Cu, it was found necessary to manufacture considerably more specimens in the thicker range. This was because /

because it was observed that specimens of these metals could show a drop in reflectivity with additional deposition beyond opacity. This effect was also occasionally observed with some other metals, but to a much less degree. The copper films which showed this effect had a slightly redder appearance than the others and the chromium films for which it occurred had a definite brownish tinge. Electron diffraction showed that these low reflectance films had a proportion of oxide present. This oxidation might be explained by the fact that copper oxidizes very readily and any prolongation of the heat radiation from the evaporation source would promote the oxidation. In the case of the chromium films the heating effect is sufficient to raise the substrate temperature from room temperature of 20°C. to 40°C. Chromium is very difficult to evaporate since a layer of refractory oxide forms quickly around the chromium chips in the heating basket. This oxide layer cuts down drastically the evaporation rate of the chromium. One might attempt to force further evaporation of chromium by superheating but this often results in the failure of the heater. Moreover undue heating of the substrate would occur and one would expect a high proportion of oxide to be carried off with the evaporating chromium, some of which would find its way to the substrate. An alternative is to use multiple heaters so that when one source loses its efficiency another fresh source can be employed. This was the method used.

The literature on evaporated chromium films shows little or no agreement between different authors. In Fig. 5.1. are shown the results obtained by Perrot(5.1.), for evaporated chromium films. The values of R and R' for very thick films are 50% and 26% respectively. Perrot draws attention to the possibility of structural changes that can take place during prolonged evaporation, thus :-

"C'est pour ces fortes epaisseurs que la duree de la vaporisation est la plus grande; il s'ensuit un echauffement prolonge des lames de chrome et peut etre une alteration superficielle du cote air."

The browning of chromium films evaporated under poor vacuum conditions is also remarked on.

Beeching(5.2.) has studied chromium films on glass by electron diffraction and has shown that the thinner films contain an oxide of chromium. Also, for thick chromium films he has shown that a thin covering layer of oxide is present. Chromium was also studied by Abeles and Croignou(5.3.). The reflectivity at the air side for λ 5461 A.U. quoted by these authors for opaque chromium films was 43% whereas the reflectivity finally obtained in this work for opaque chromium films at the same wavelength was 64%. A selection system was adopted whereby all reflectance measurements were rejected in the case of specimens which showed a violent drop in reflectance with increasing thickness.

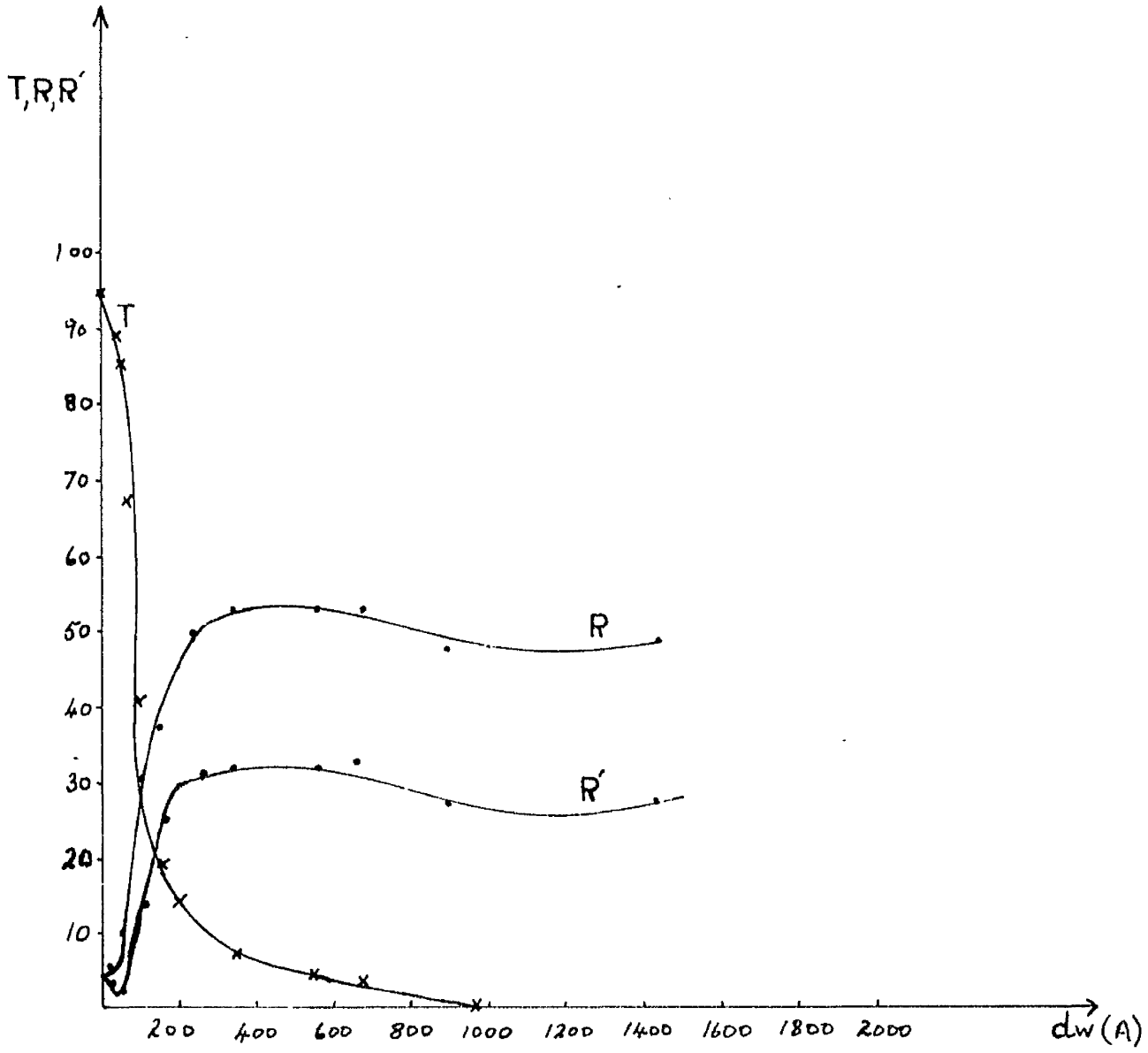

Fig. 5.1. Perrot's Results for the Transmittance and Reflectance of Evaporated Chromium Films expressed as a function of Weight Thickness. λ 5460 A.

The results of the measurement of the transmittance and reflectance for the above-mentioned metals are shown in figures 5.2. - 5.8. The method of presentation, viz. R and R' expressed as functions of T, was adopted for the reason that the most accurately determined measurement of T, R, R' and dw was undoubtedly T. By the use of this method the occurrence of random errors in measurement was reduced. In addition this method allows the use of standard sets of R and R' vs. T curves which are easily constructed from the primary curves calculated by computer. Thus the same sets of curves could be used for different metals, affording a great reduction in the time required to evaluate n and k throughout a range of thickness. There exists a danger in the use of this method in certain cases, e.g. aluminium, where one may obtain for certain wavelengths two thicknesses which give the same T, R or R'. However in the case of the metals studied here a check was made by graphing T vs. d_I, the thickness obtained by interferometry, to ensure that the curve showed no turning points. Curves of T vs. d_I for various metals are shown in fig. 5.9.

In all cases the wavelength used was 5461 A.U.

5.2.) The Wolter Relationship.

When using T, R and R' to determine the optical constants of metal films there occurs a value of thickness below which the method is not applicable. This is because the two curves of n vs. k obtained from T, R and T, R' measurements intersect at a very narrow angle or /

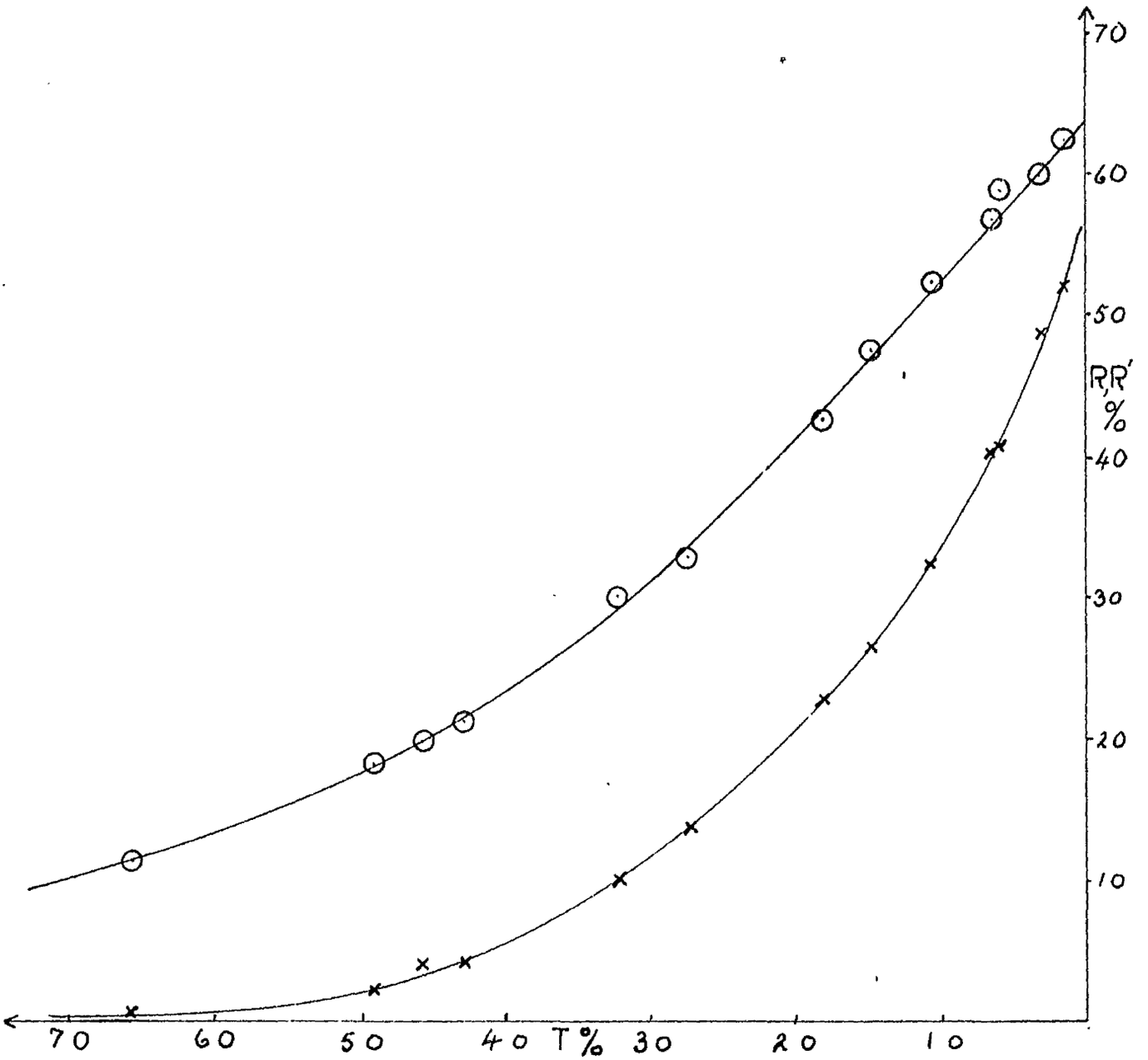

Fig. 5.2. Reflectivity of Evaporated Nickel Films as a Function of Transmittance. λ 5460 A.

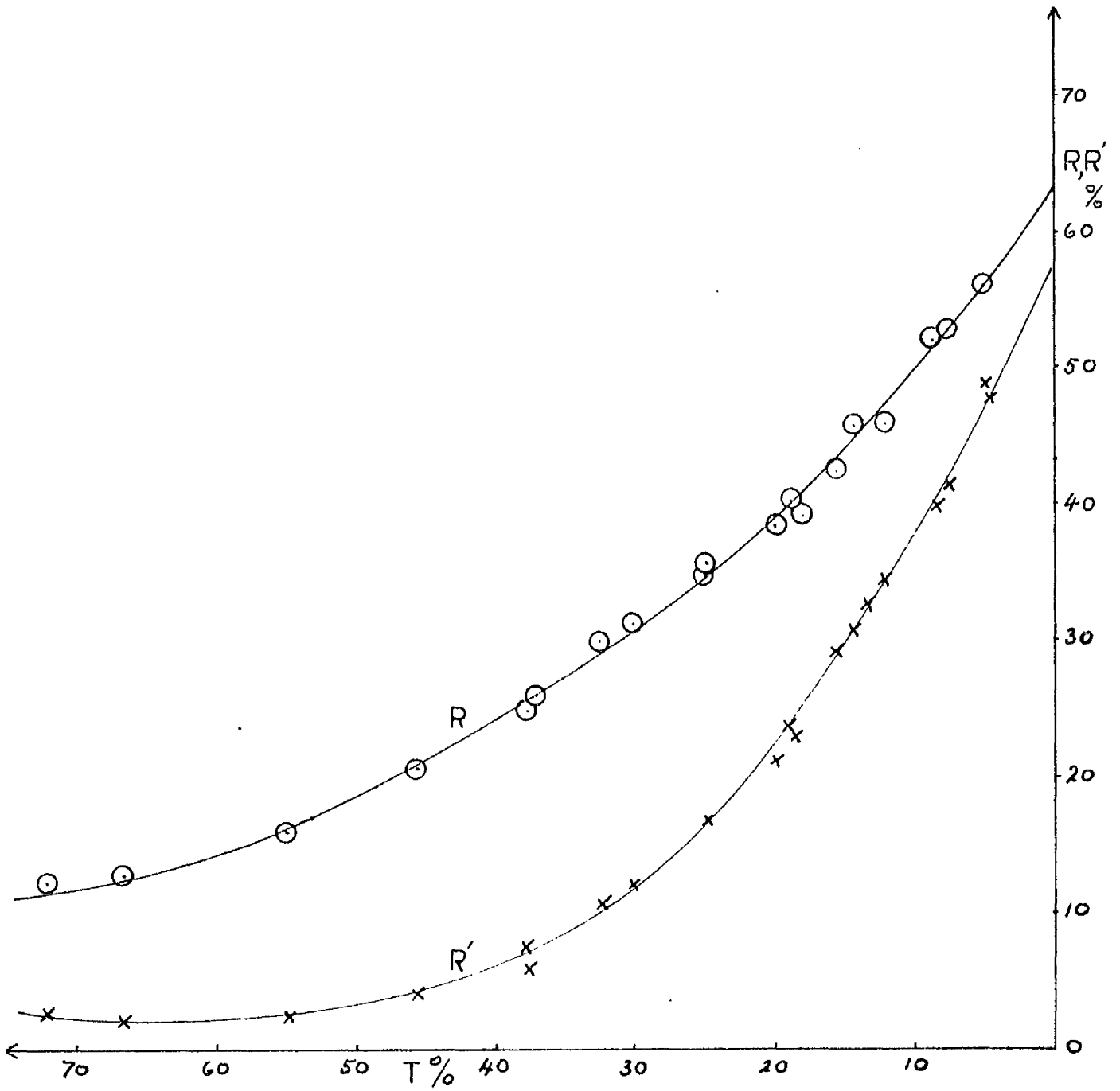

Fig. 5.3. Reflectivity of Evaporated Chromium Films as a Function of Transmittance. λ 5460 A.

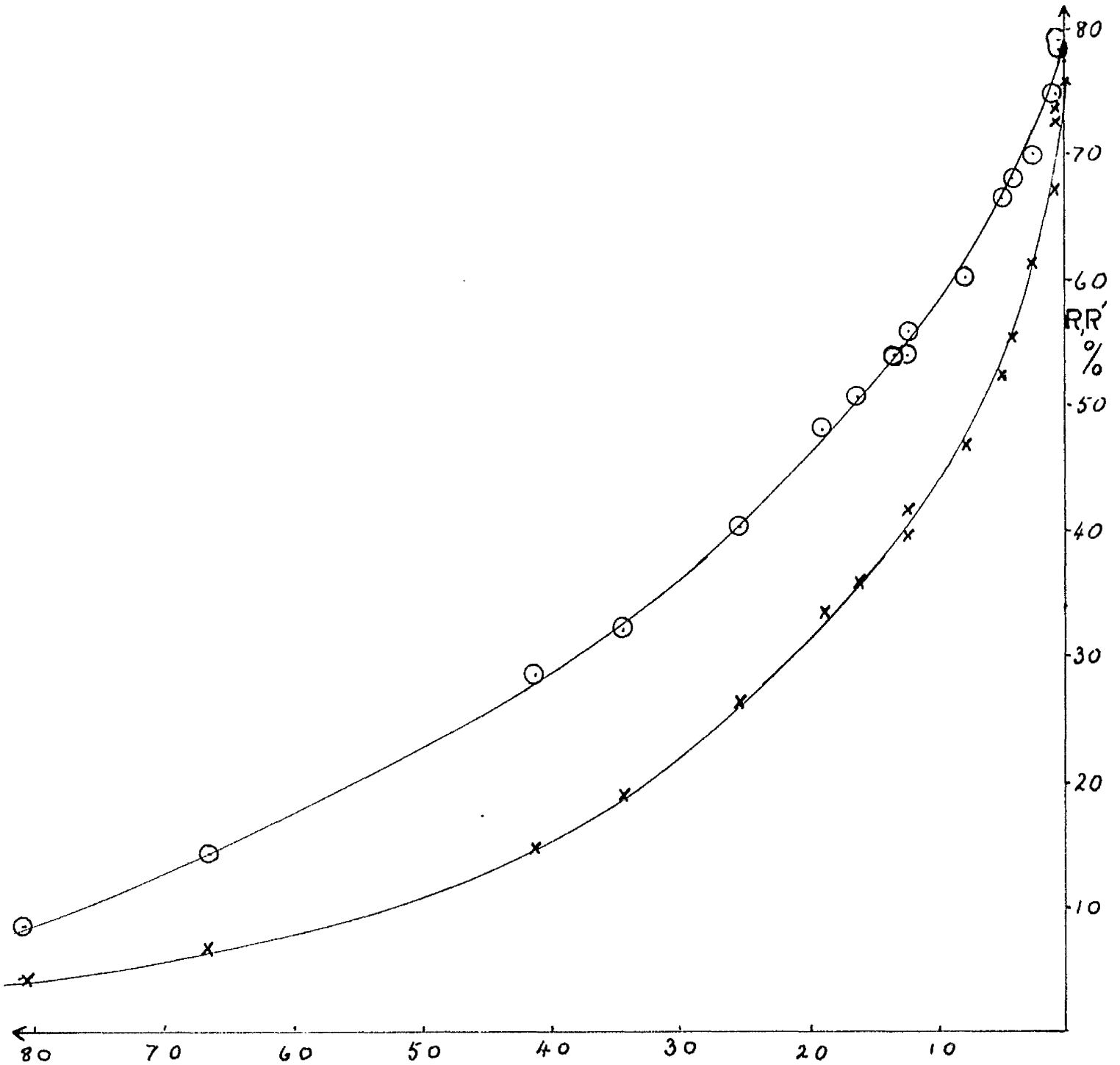

Fig. 5.4. Reflectivity of Evaporated Tin Films as a Function of Transmittance. λ 5460 A.

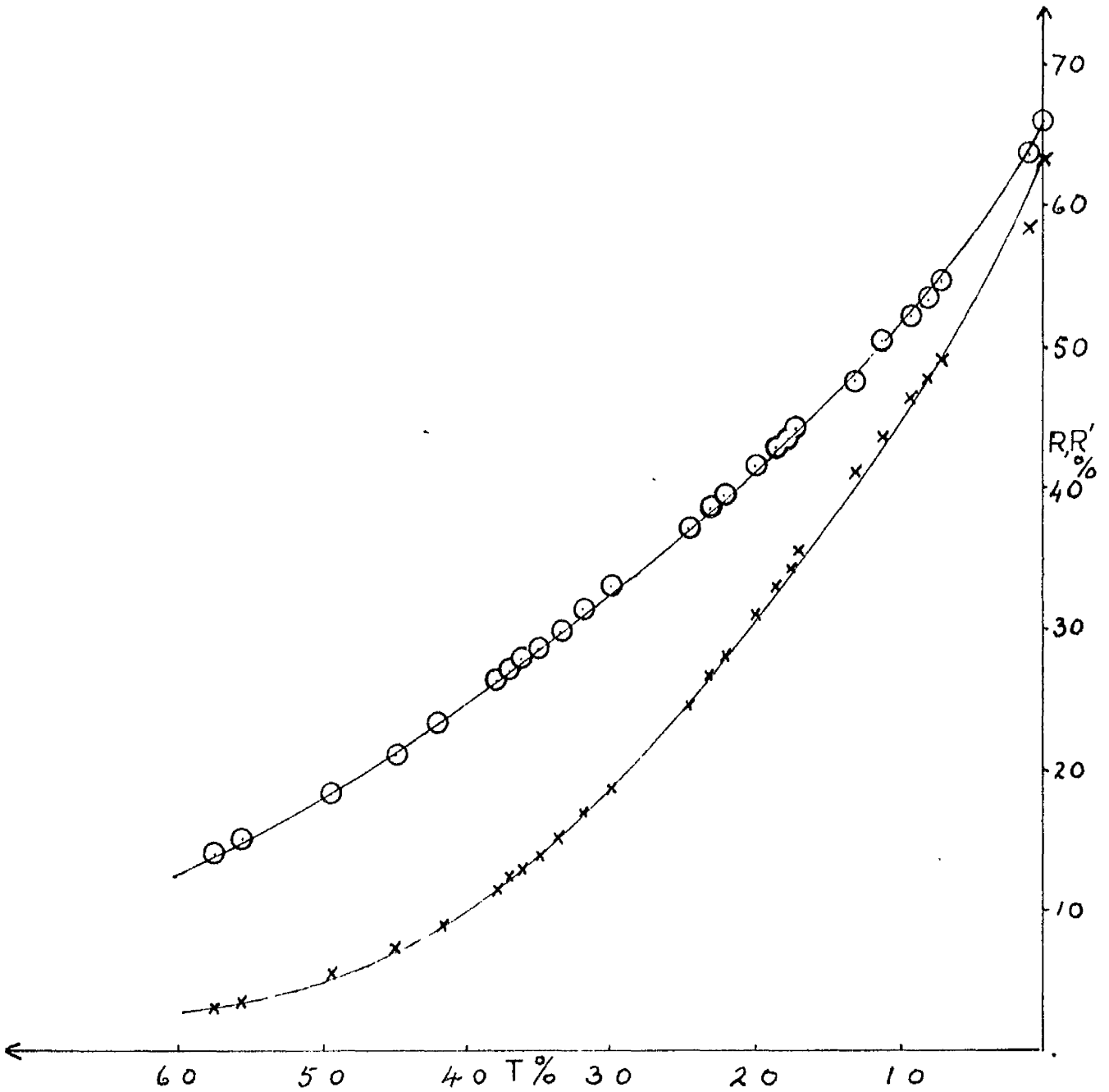

Fig. 5.5. Reflectivity of Evaporated Copper Films as a Function of Transmittance. λ 5460 A.

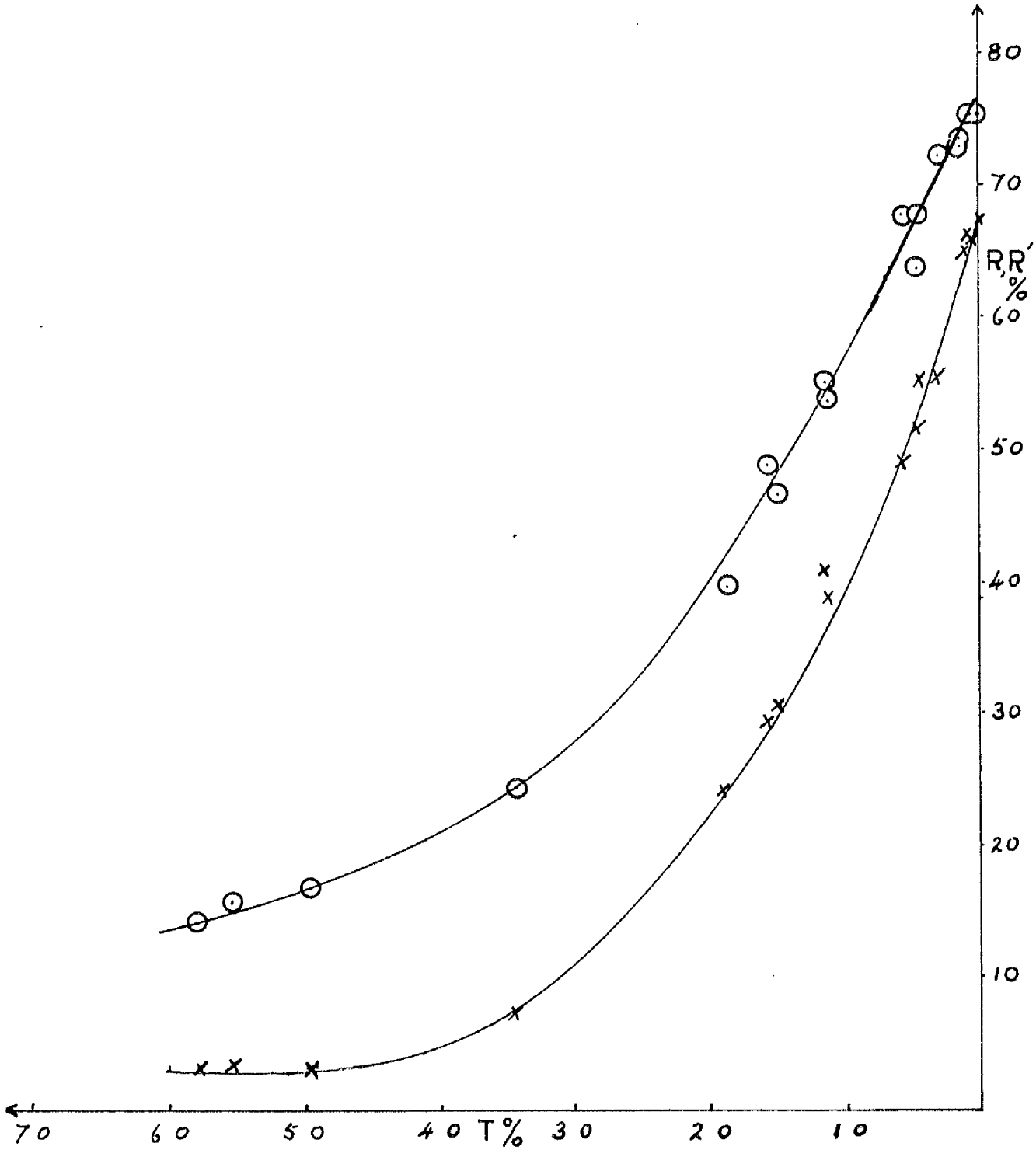

Fig. 5.6. Reflectivity of Evaporated Antimony Films as a Function of Transmittance. λ5460 A.

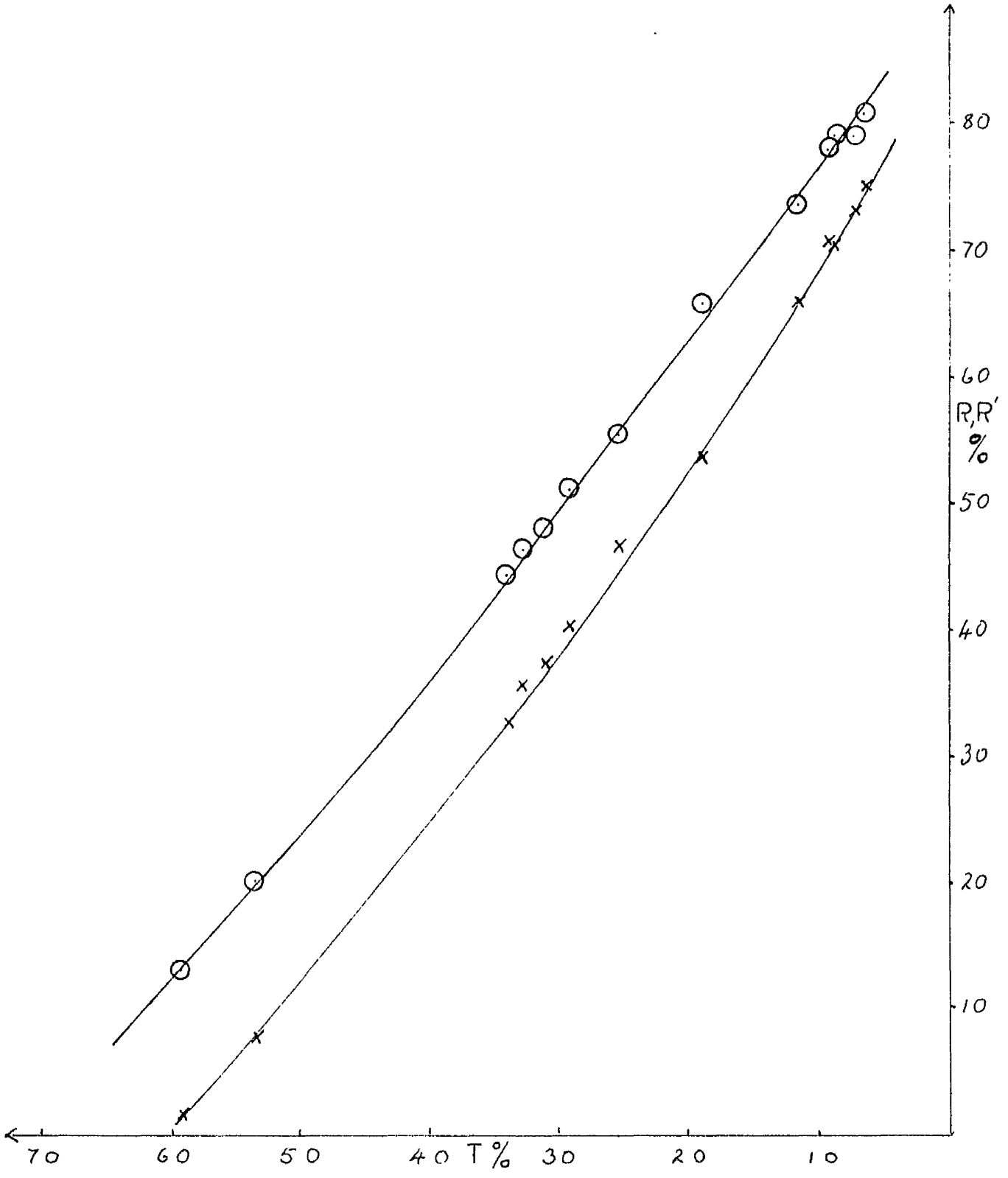

Fig. 5.7. Reflectivity of Evaporated Aluminium Films as a Function of Transmittance. λ 5460 A.

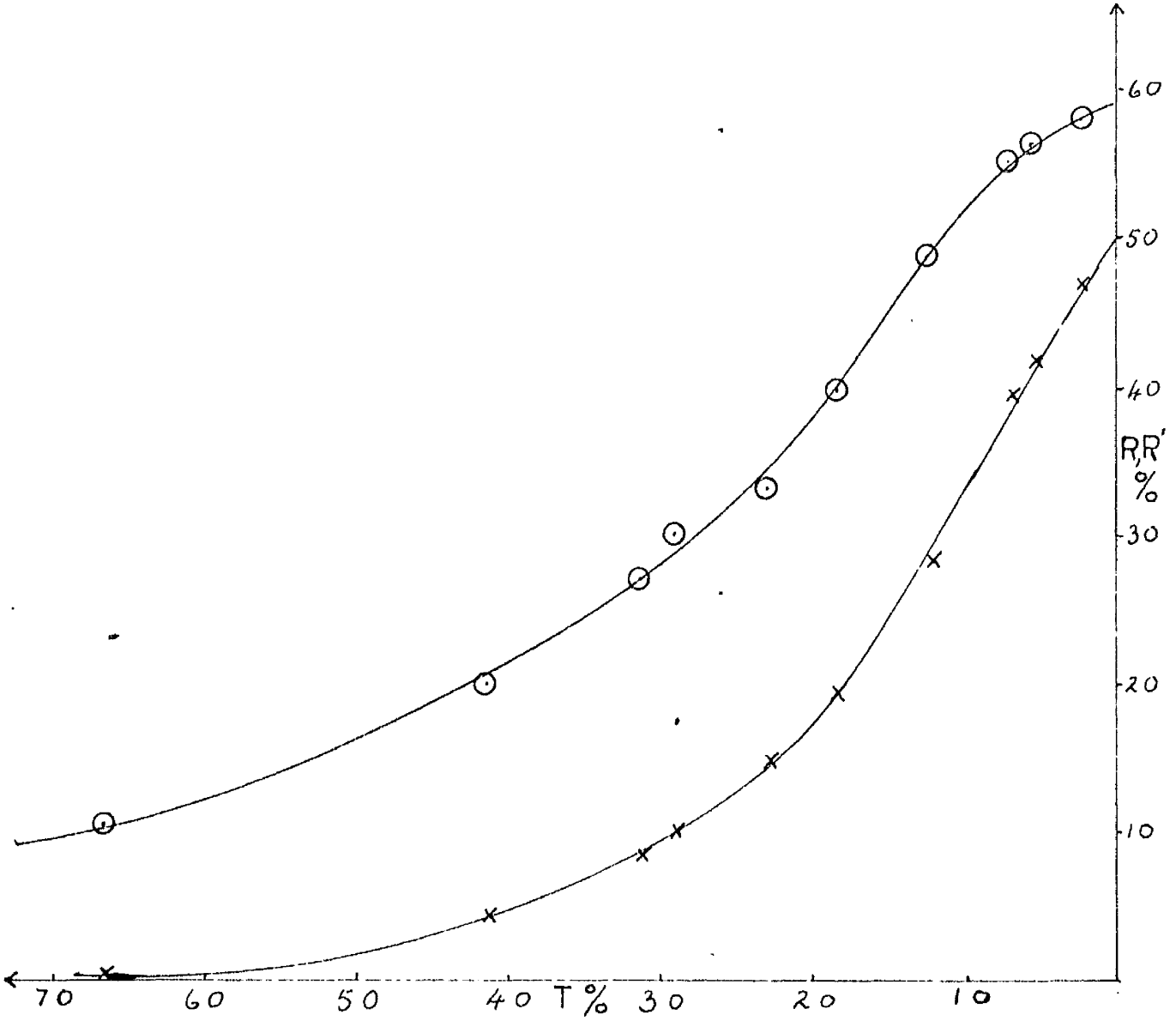

Fig. 5.8. Reflectivity of Evaporated Manganese Films as a Function of Transmittance. λ5460 A.

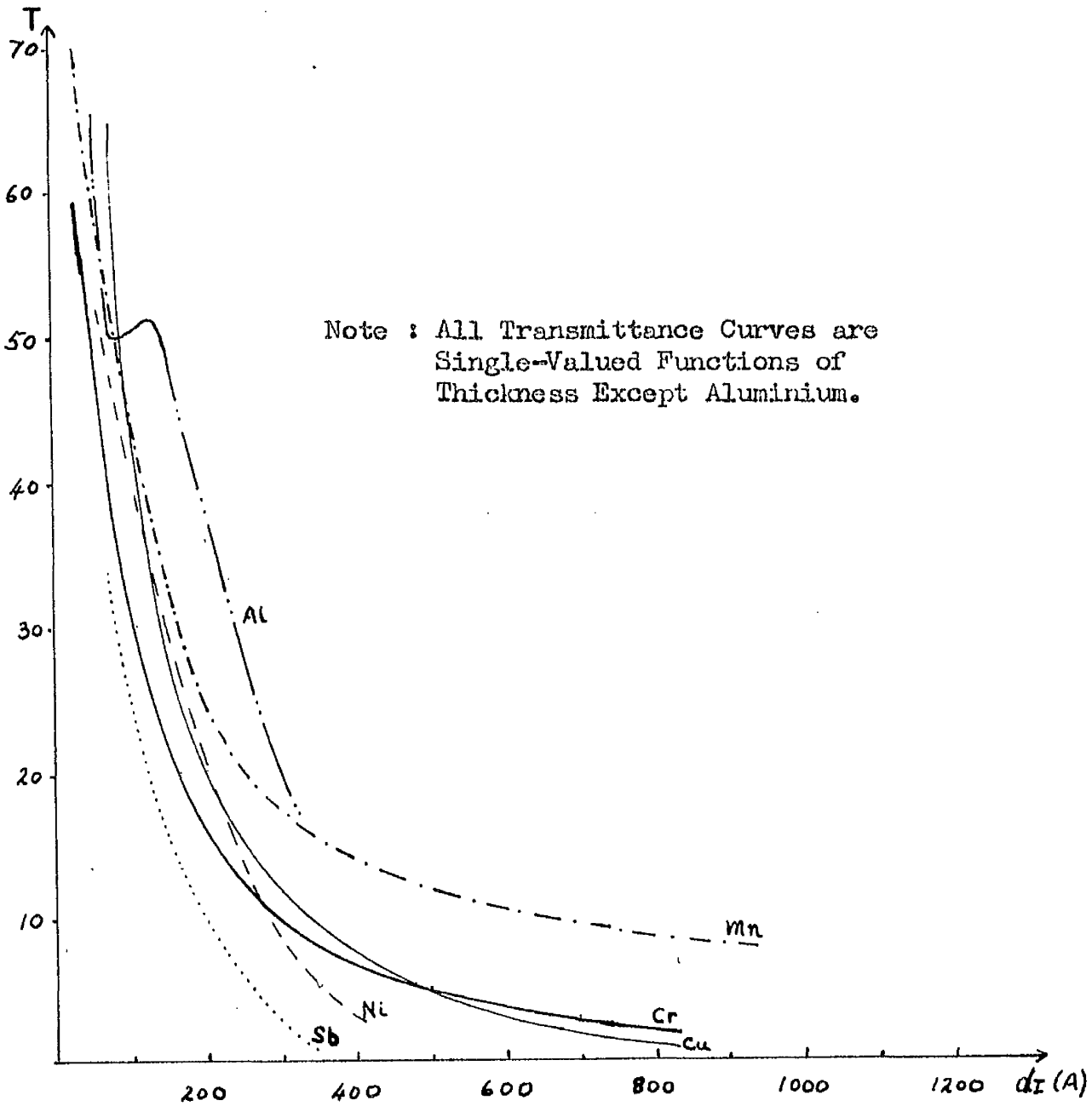

Fig. 5.9. Curves of Transmittance as a Function of Interferometric Thickness for Various Metals. λ5460 A.

or may even be parallel or overlap. When this is the case then the simultaneous evaluation of n, k and dn is either very inaccurate or impossible.

An explanation of this occurrence is to be found in the theory. The method in effect consists of solving graphically three simultaneous equations which are assumed to be independent of each other. These relationships are represented by equations (2.19.), (2.20.) and (2.21.). The three observable quantities are T, R and R' and the three unknowns to be evaluated are n, k and dn. When the final curves are found to be coincident this indicates the existence of a relationship between a pair of the observables. The three equations are now no longer independent and therefore n, k and d cannot be obtained explicitly.

Earlier, Wolter(5.4.) had shown theoretically that under certain conditions there would exist a relationship between T, R and R'. This relationship was obtained by making approximations which were valid in the case of very thin films. Wolter expressed the relationship thus

$$\frac{n_2}{n_o} = \frac{1 - T - R'}{1 - T - R} \qquad \ldots \quad (5.1.),$$

where n_o and n_2 are the refractive indices of the bounding media of the film, viz. air and glass respectively. He also deduced that in general the equation (5.1.) would hold when the film thickness d was such that

$d < 0.027\,\lambda$.

Writing $A = 1 - T - R$ and $A' = 1 - T - R'$, we may regard A and A' as the fraction of incident energy absorbed by the film when the light is incident from the air and glass sides respectively. Equation (5.1.) may then be written as

$$n_2 A = A' \qquad \ldots \quad (5.2.)$$

Equation (5.2.) is termed the Wolter Relationship. When the Wolter Relationship is true in the case of a film then it will not be possible to derive n, k and dn from measurements of T, R and R' alone.

Malé(5.5.) evaluated theoretically the expression $n_2 A - A'$ for certain n, k pairs over a range of d and verified that for $d < 0.027\,\lambda$,

$$n_2 A - A' \doteqdot 0.$$

This was the case irrespective of the choice of n and k. He also found that for certain values of n and k the expression $n_2 A - A' \doteqdot 0$ held even for d values which were quite large. For example, taking $n = 0.2$ and $k = 4.0$, which are nearly the constants of silver in the visible region of the spectrum, it was found that $n_2 A - A' \doteqdot 0$ for all values of d.

In fig. 5.10. are shown determinations of the expression $n_2 A - A'$ as a function of T for a range of n k values. It can be seen from these graphs that the greater the value of the ratio k/n,

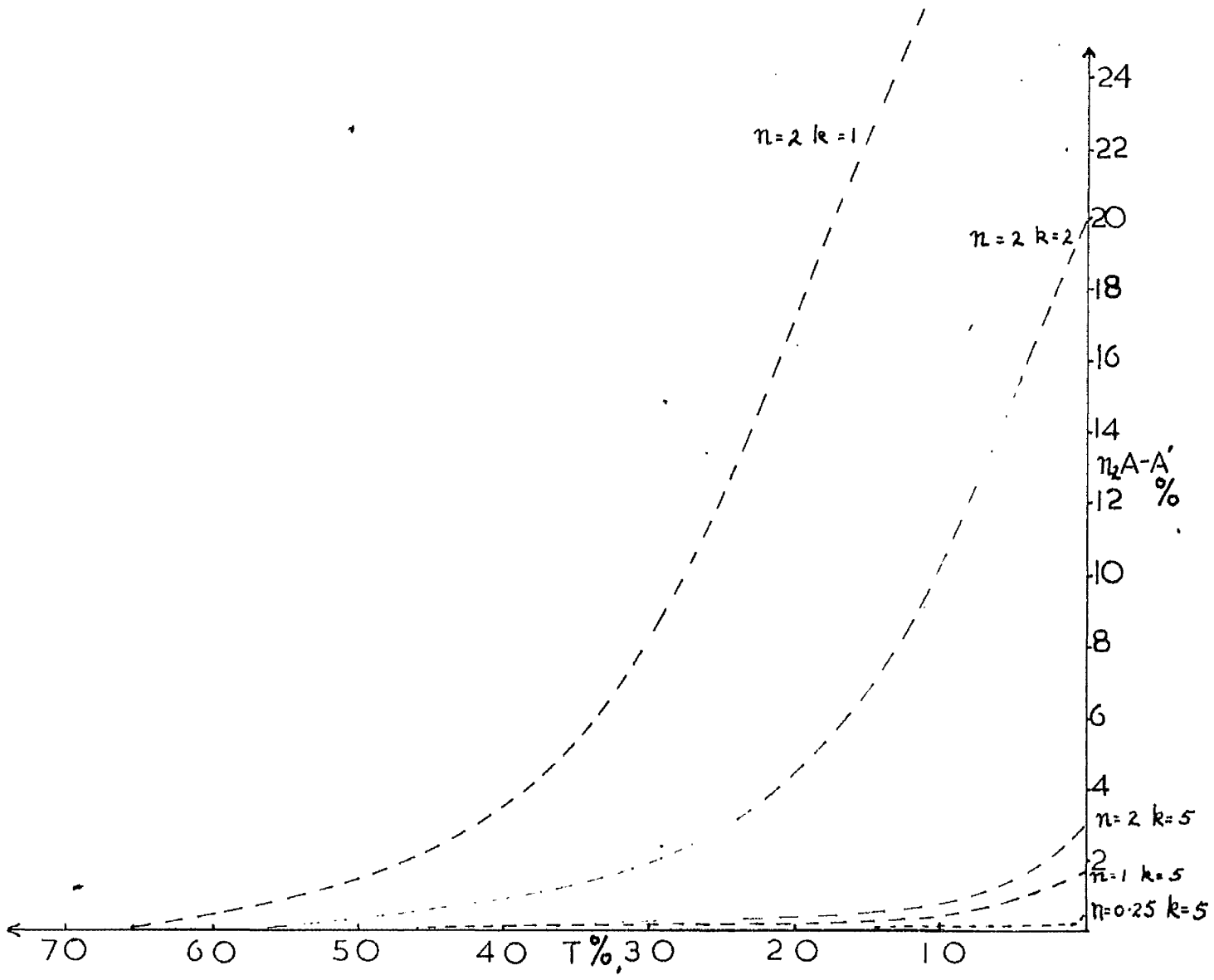

Fig. 5.10. N_2 A - A' vs. T as determined by calculation for a range of n, k pairs.

then the greater is the thickness for which the Wolter Relationship holds. In fig. 5.11. are shown experimental determinations of the expression $n_2A - A'$ vs. T for the metals used in this work. The choice of T for the abscissa is to preserve continuity with the preceding graphs. Attempts have also been made to determine n, k and d for all of these metals down to as low a thickness as possible. Allowing for a possible error of 1% in the observed quantities it was found that generally determination of n, k and d from T R and R' was not possible when $n_2A - A' < 0.03$. This is in good agreement with the observations of Malé and Wolter.

As can be seen from fig. 5.11. it is only in the case of Cr and Cu that the value of $n_2A - A'$ remains at all times above this critical value down to thicknesses of the order of 200 - 300 A.U. These are therefore the only metals of those investigated in this work for which a continuous determination of optical constants with varying thickness could be made using the Malé method.

In fig. 5.11. curves for all the metals studied except Cr and Cu dip to a minimum turning point and thereafter the value of $n_2A - A'$ remains low over most of the working range. The shape of the curves may have some significance in relation to the fact that only Cr and Cu are amenable to the method of evaluation of optical constants and thickness using T, R and R' only. The interpretation of the existence of this turning point is not however apparent.

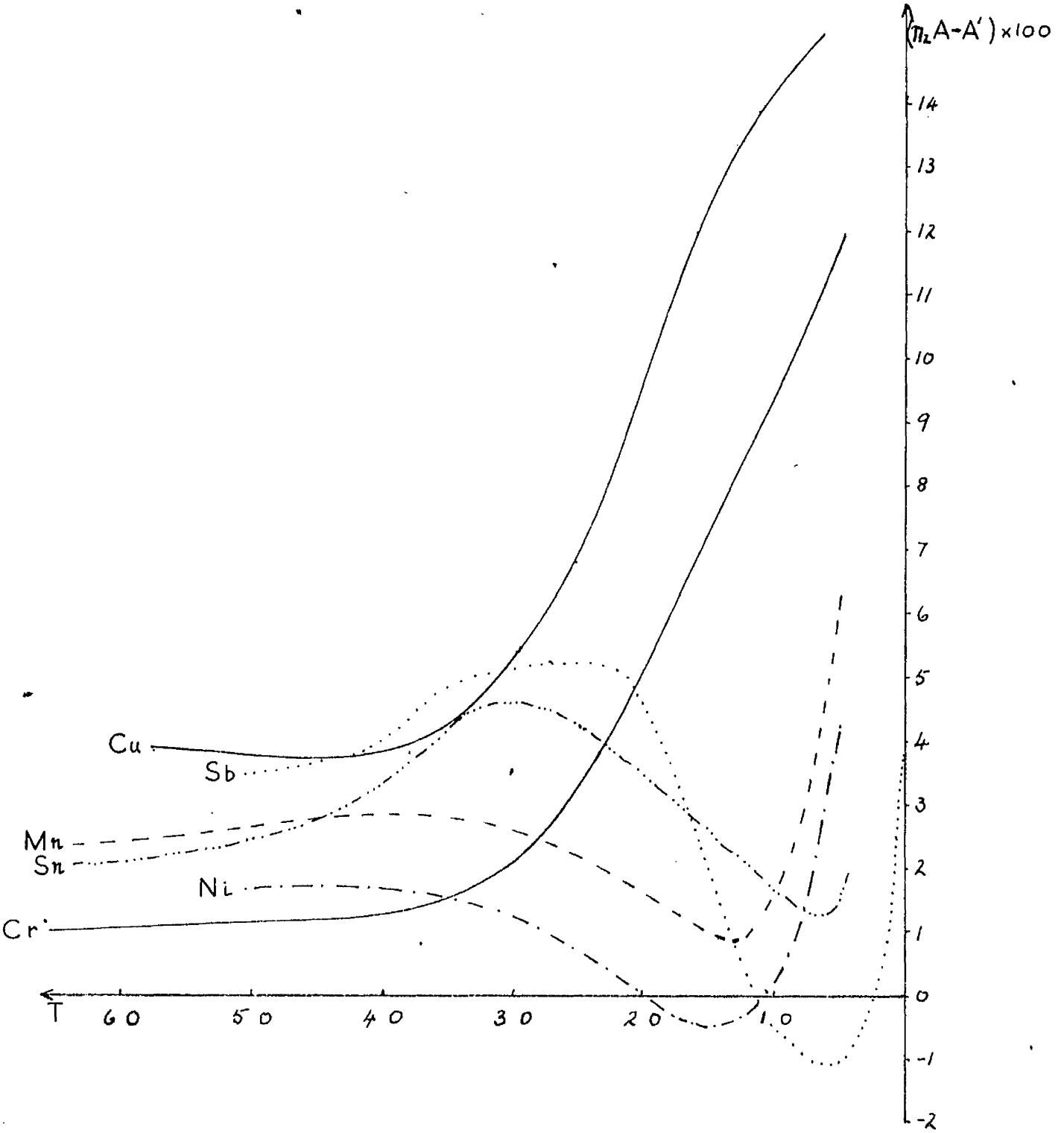

Fig. 5.11. Experimental Determination of $(n_2 A - A') \times 100$ vs. T for Various Metals.

CHAPTER 5 : REFERENCES.

5.1.) Ferrot, M., Thesis, University of Marseilles, 1943.
5.2.) Beeching, R., Phil. Mag., Vol. 22, 1936, p.938.
5.3.) Abeles and Creignou. J. de Phys. (I), April 1954.
5.4.) Wolter, H., Zeit. Phys., Vol. 105, 1937, p.269.
5.5.) Malo, D., Thesis, University of Paris, Masson et Cie, 1953.

CHAPTER 6 : OPTICAL CONSTANTS OF CHROMIUM AND COPPER FILMS.

a) Chromium Films.

Using the curves for chromium shown in fig. 5.2. the optical constants were evaluated using the method of Malé. Results were obtained down to a thickness of 200 A. Below 200 A the Wolter Relationship prevented results from being obtained. In fig. 6.1. are shown the variations of n and k with optical thickness dn. Starting at the lowest thickness for which results were obtained, viz. 195 A, the value of n decreases with increasing thickness until it attains a steady value of 0.57 at a thickness of about 1,100 A. The value of k passes through a rather flat maximum in the region of 350 A and levels off at about 1,000 A to a constant value of 1.8. The maximum is not so distinct as that obtained by Hill and Weaver(6.1.) but the thickness value for which it occurs is about same. The general tendency of the curves agrees with those of other metal films examined by other authors, namely increasing n with decreasing thickness and k tending to zero as the thickness tends to zero.

As a check on the results obtained, selected n, k and d values were used to recalculate T, R and R'. This was done using the graphical method and nomogram devized by Malé(6.2.). In this way a check independent of the calculations performed by the computer was obtained. Comparing the recalculated T, R and R' values with the original ones gave a general agreement to within 1%.

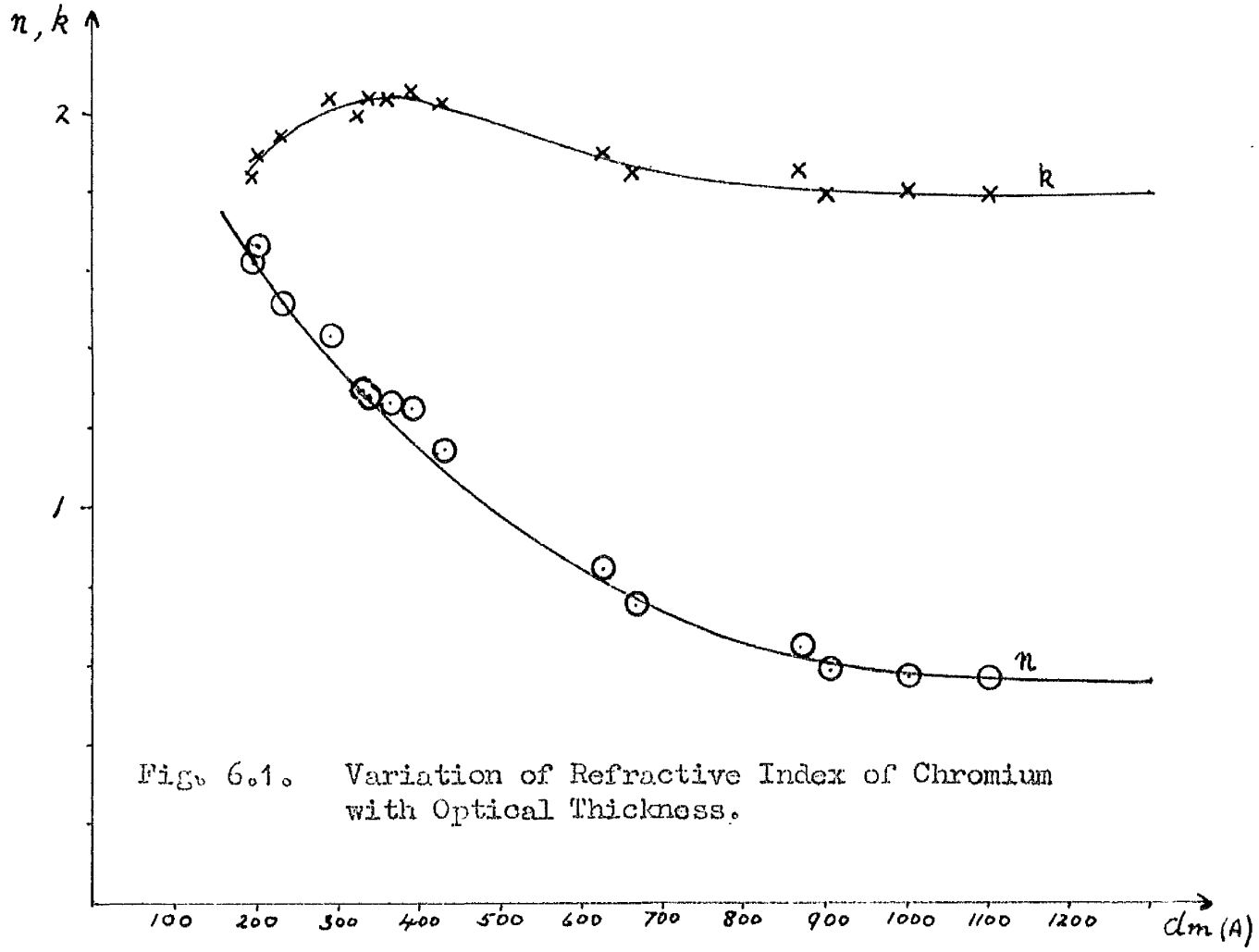

Fig. 6.1. Variation of Refractive Index of Chromium with Optical Thickness.

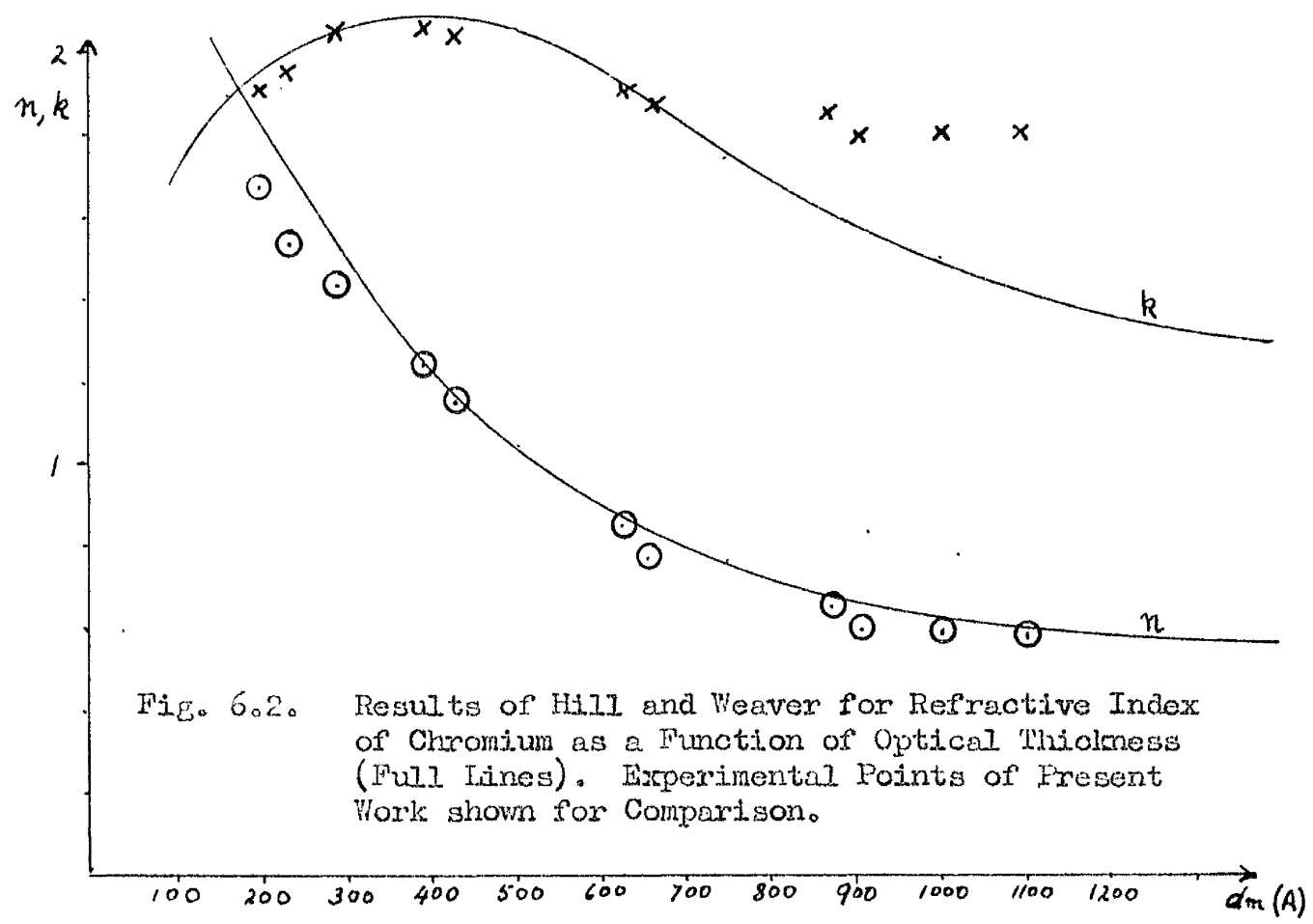

Fig. 6.2. Results of Hill and Weaver for Refractive Index of Chromium as a Function of Optical Thickness (Full Lines). Experimental Points of Present Work shown for Comparison.

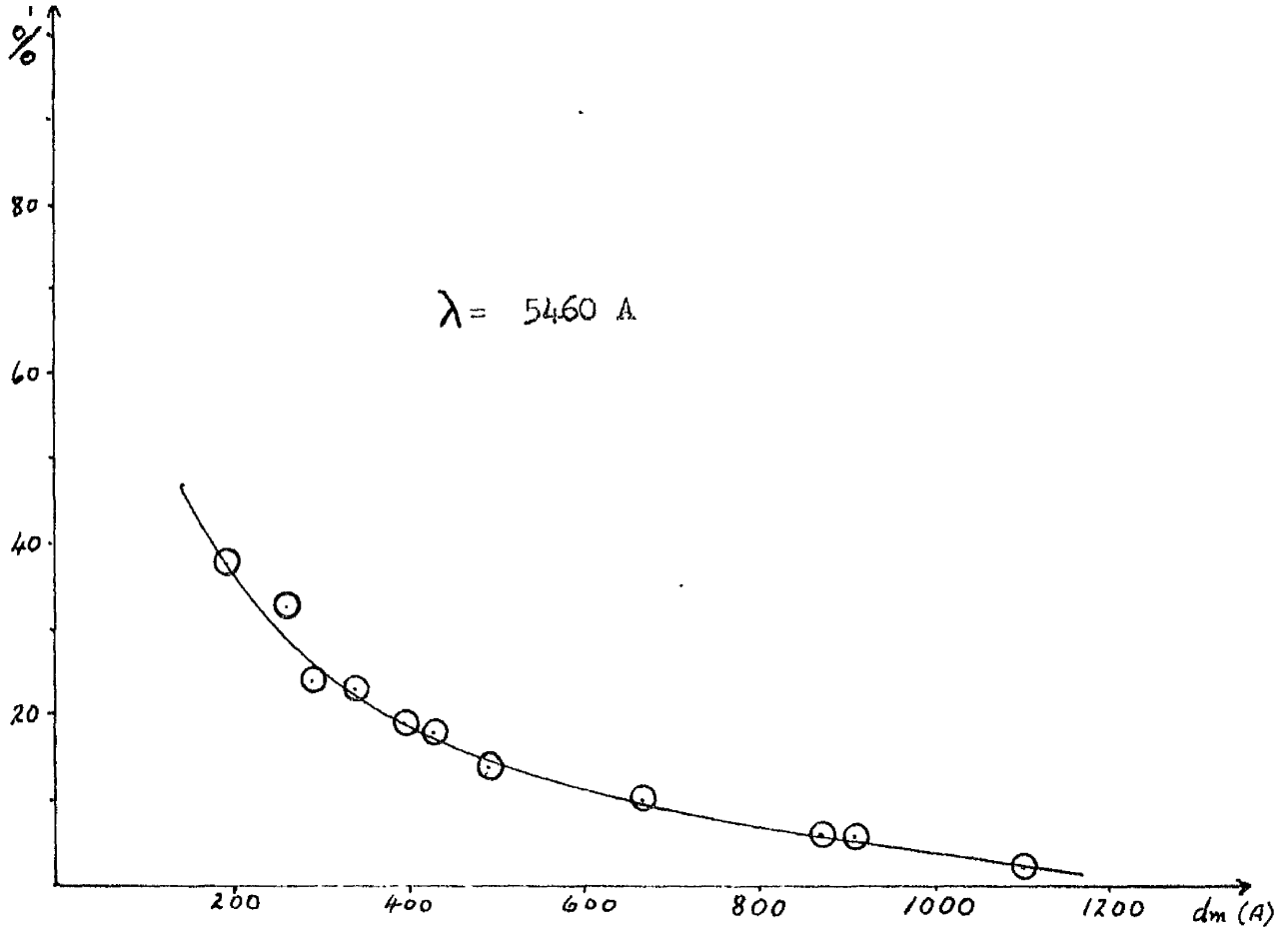

Fig. 6.3. Variation of Transmittance of Chromium with Optical Thickness.

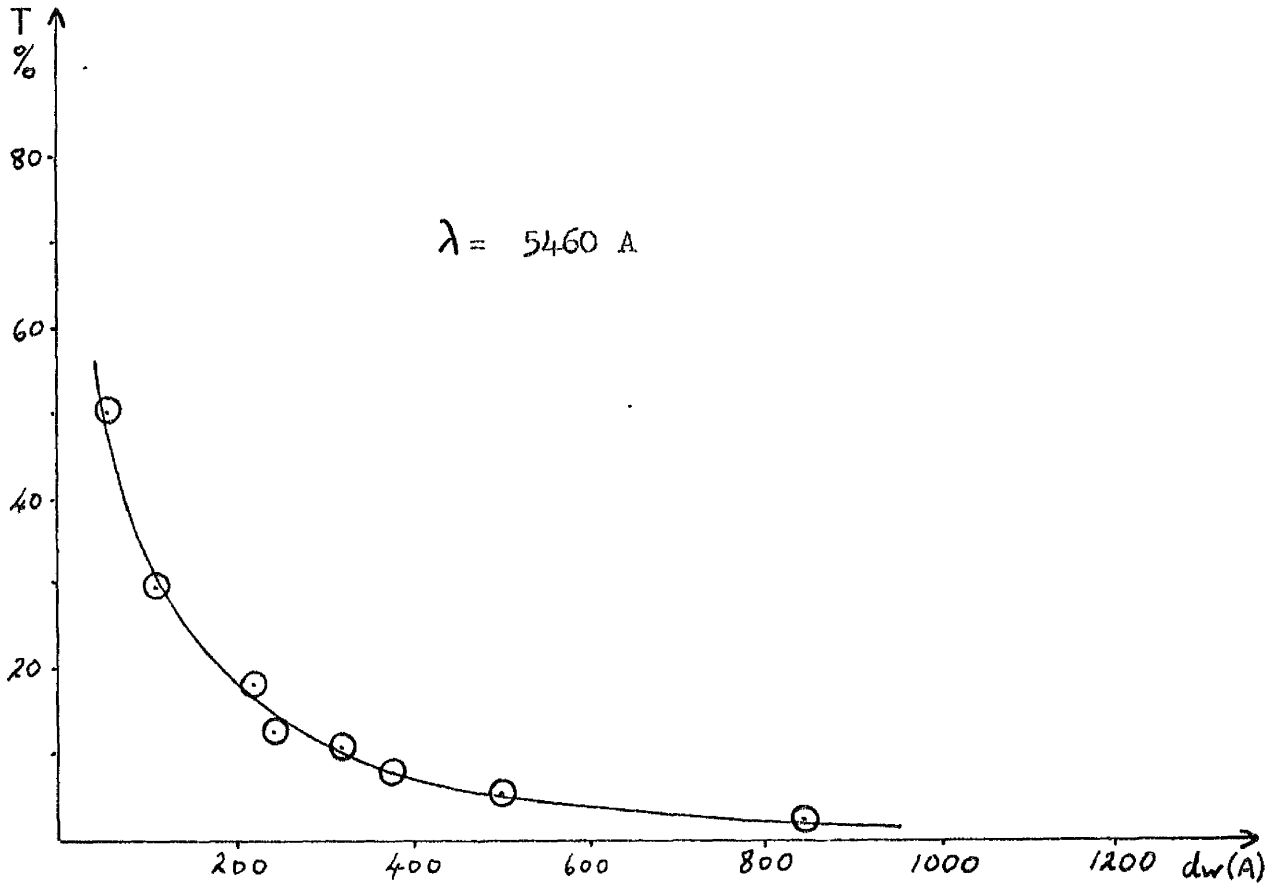

Fig. 6.4. Variation of Transmittance of Chromium with Weight Thickness.

Figure 6.2. gives curves showing the variation of n and k with thickness for chromium films as obtained by Hill and Weaver(6.1.) for the same wavelength. The experimental points obtained in the present work are superimposed and it can be seen that the n values agree well with the curve throughout the thickness range. The k values agree with the curve up to a thickness of about 400 A but above this thickness the experimental points lie above the earlier results. This is more likely to be due to differences between the two sets of specimens rather than experimental errors. Attention has already been drawn in Chapter 5 to the fact that other workers who investigated chromium films did not obtain such high reflectivities for thick films as were obtained in this work. Hill and Weaver(6.1.) do not give the T, R and R' values used in determining the refractive index of chromium films but a recalculation of these quantities using the values obtained for n and k for the thickest films, i.e. n = 0.56, k = 1.29 showed that the reflectance at the air side must have been about 43%.

These films were produced by continuous evaporation using a single heater and it has already been shown that this tends to cause oxidation and browning of the films. Such films have a low reflectivity and in the present work multiple sources were used to avoid this difficulty. Films of low reflectivity were rejected. The differences in k above 400 Å film thickness may therefore be attributed to the differences in reflectivity.

Figures 6.3. and 6.4. show the variation of the transmittence T with dm and dw respectively, dw being the thickness as determined by weighing. Reference has already been made to the necessity of having both methods of thickness measurement when any attempt is made to interpret results of optical constants of films (viz. Chapter 3, Section 4). The aggregation which occurs causes the effective volume Veff. of a film to be greater than the volume obtained by dividing the weight by bulk density of the material, Vw. We define a "Volume Factor" or "Packing Factor", q as the ratio of these two volumes, viz. :

$$q = \frac{Vf}{Vs} = \frac{dw}{dm}$$

Hence using the curves shown in figs. 6.3. and 6.4. we can construct a curve of q vs. dm or q vs. dw. This is done by selecting a value of T and noting the values of dm and dw which correspond to it. Figure 6.5. shows the variation of q with dw for the chromium films studied.

b) <u>Copper Films.</u>

The results obtained for the refractive index of the copper films studied are shown in fig. 6.6. Here again the n value falls with increasing film thickness, although the slope is more gradual. The value of n becomes constant at n = 0.5 beyond a film thickness of about 1,400 A. The k curve rises from 200 A up to about 500 A when it becomes more or less constant at a value of k = 1.5.

In the k curve there is no clear maximum present as there is in the case of the k curve for chromium. The variations of the transmittance with dm and dw are shown in figs. 6.7. and 6.8. respectively, and the variation of the packing factor q with dw is shown in fig. 6.9.

As the film thickness decreases n rises gradually while k remains fairly constant down to about 500 A optical thickness when it begins to fall. This variation of n and k is in agreement with the general tendency of the variation of the refractive index of metal films with thickness.

Malé(6.2.) and Trompette(6.3.) investigating other metals, have obtained a turning point in the n curve at thicknesses which are generally below 100 A optical thickness. The results obtained in this work for chromium and copper did not show a maximum turning point in the n curve in the thickness region studied. No turning point was observed by Hill and Weaver who obtained results for chromium down to 119 A optical thickness. Rouard(6.4.) discussing the results obtained by Malé has postulated that for film thicknesses approaching zero the value of n must tend to unity. He regards a thin metal film as composed of a mixture of metal and air "particles" wherein the proportion of air "particles" increases as the film thickness gets smaller. The value of n therefore tends nearer and nearer to that of air until in the limit for zero film thickness the film is regarded as composed entirely of air "particles" and the /

The refractive index is unity. In the opinion of this author however this theory is open to question for the Malé method yields the refractive index and thickness of a hypothetical uniform continuous isotropic layer whose effect on the incident light is similar to that of the actual metal film. Regarded in this light we must expect the refractive index to be discontinuous at zero thickness, i.e. taking the limiting case with only one metal particle present on the substrate, then if measurements could be made, the effect would be that of a uniform layer of certain thickness and refractive index which would not necessarily be close to unity. The next case is that of no metal particles present when we have no equivalent film and therefore no refractive index to be discussed.

The discussion of the results obtained for chromium and copper is given in Chapter 9.

Fig. 6.6. Variation of Refractive Index of Copper with Thickness.

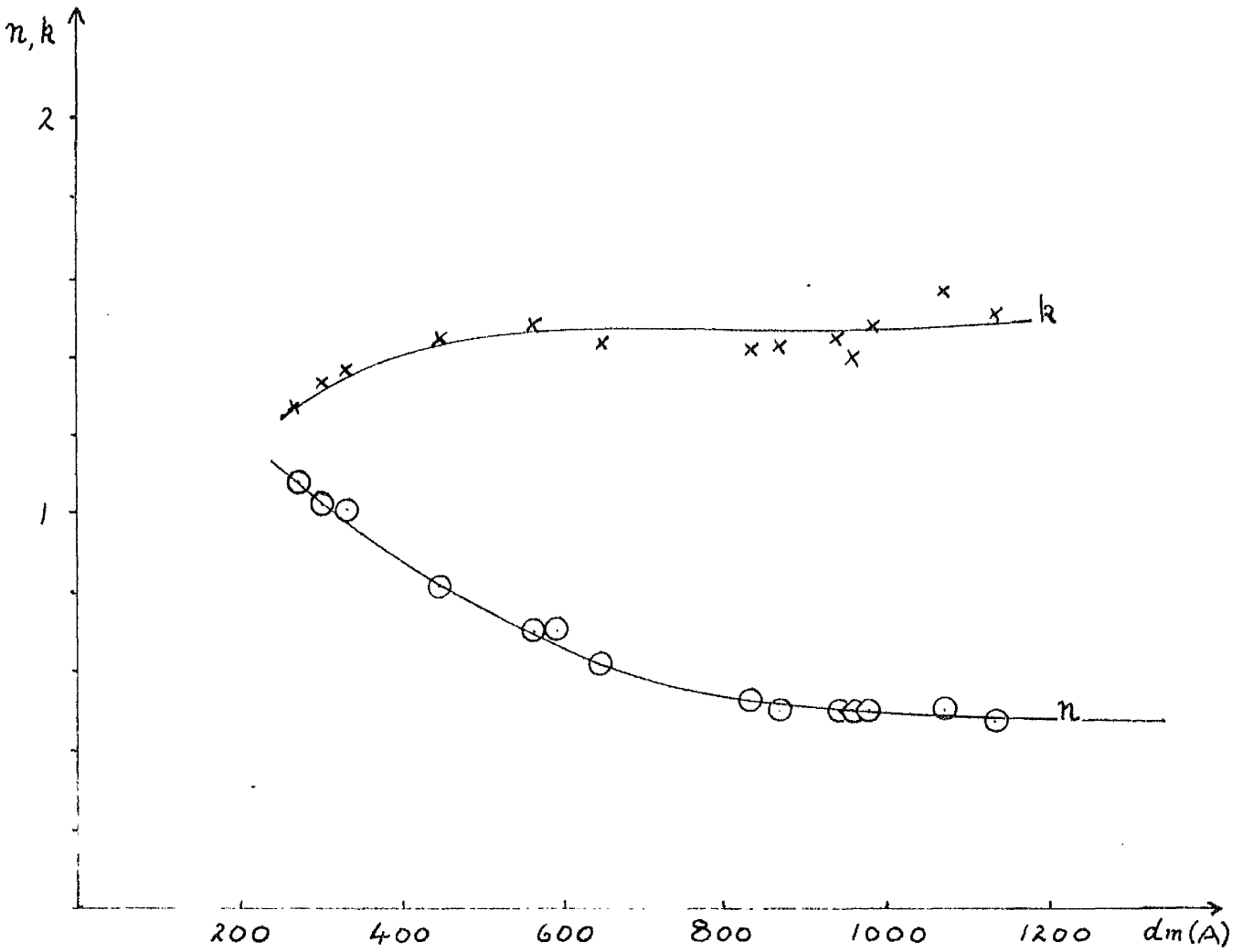

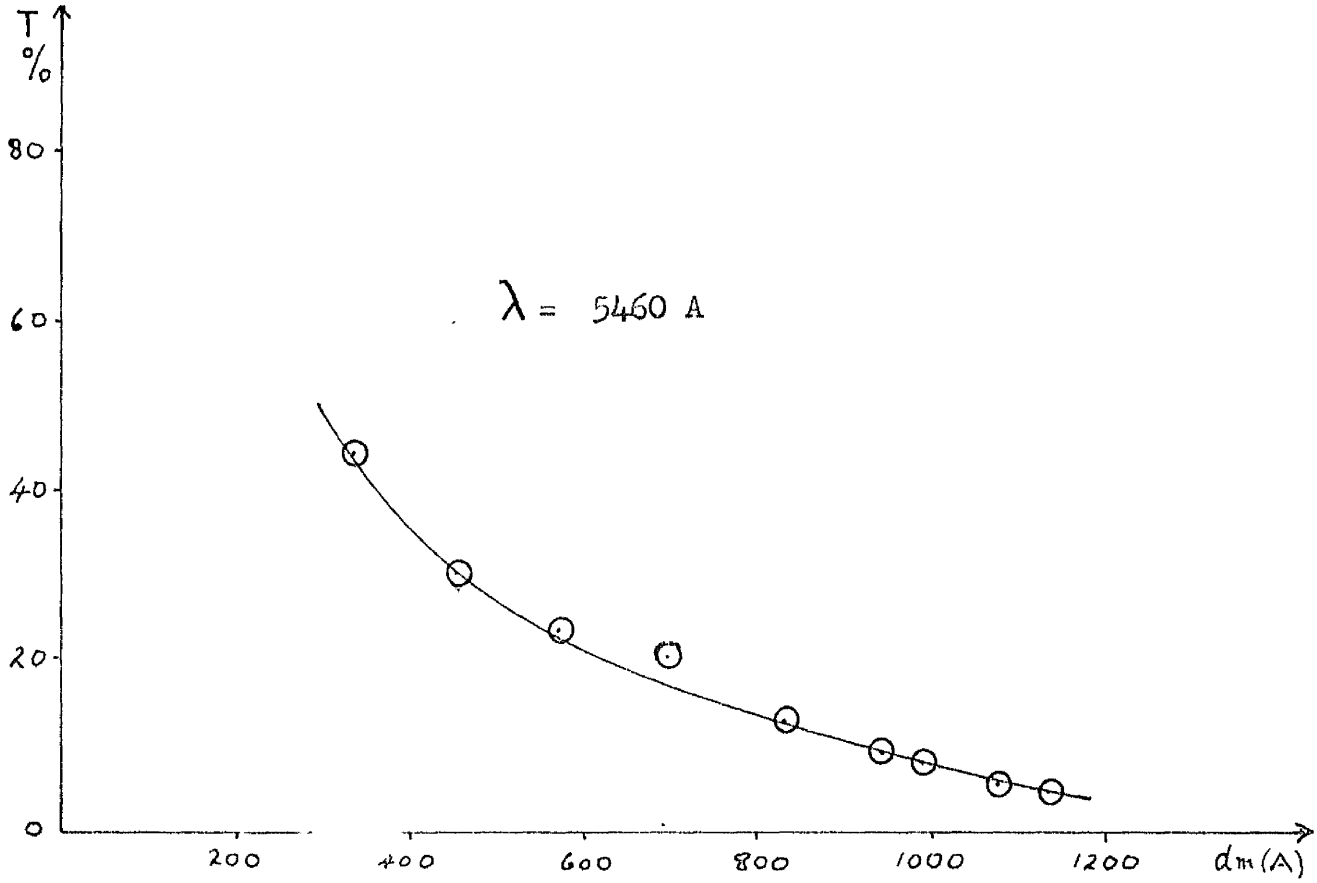

Fig. 6.7. Variation of Transmittance of Copper Films with Optical Thickness, dm.

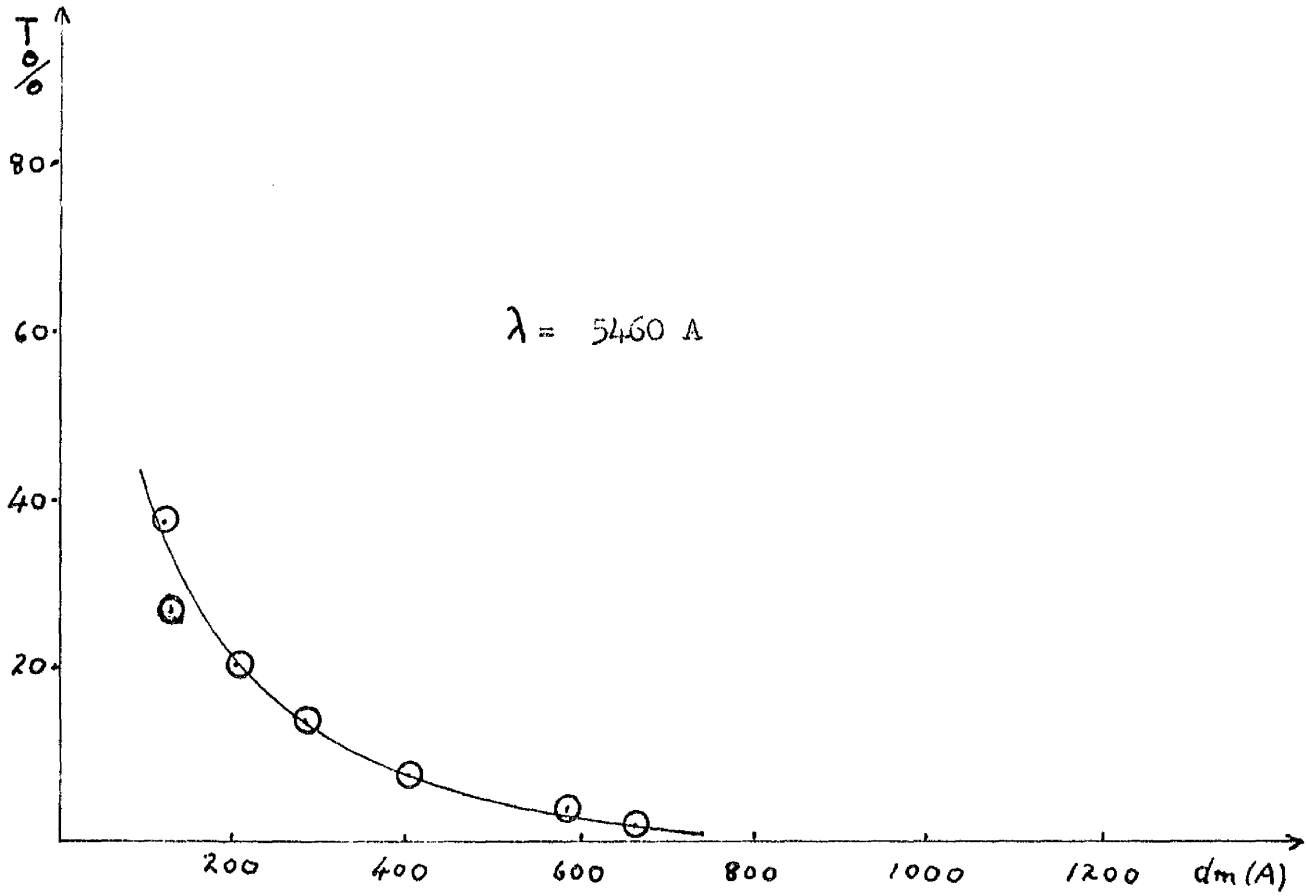

Fig. 6.8. Variation of Transmittance of Copper Films with Weight Thickness, dw.

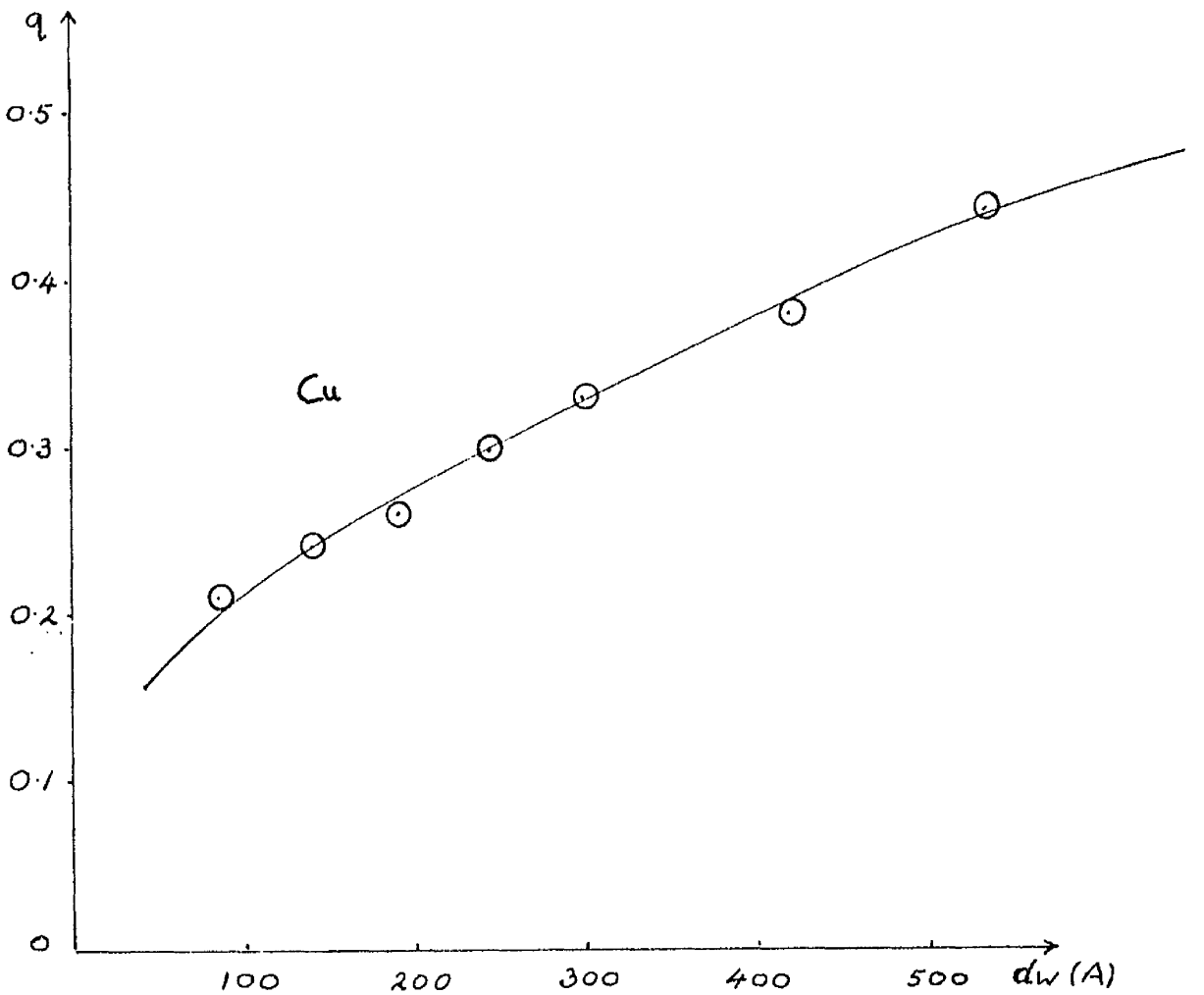

Fig. 6.9. Variation of Packing Factor q with Weight Thickness, dw.

CHAPTER 6 : REFERENCES.

6.1.) Hill, R.M., and Weaver, C., Trans. Far. Soc., Vol. 54, 10, Oct. 1958.
6.2.) Male, D., Thesis, University of Paris, Masson et Cie., 1953.
6.3.) Trompette, J., Thesis, University of Marseilles, Masson et Cie., Paris, 1960.
6.4.) Rouard, M.P., Proprietes Optiques des Lames Minces Solides. Mem. des Sciences Phys., Acad. des Sci. de Paris. Gauthier-Villars, Paris, 1952.

CHAPTER 7 : RESULTS OF PHASE CHANGE MEASUREMENTS.

From the results of the refractive index, $n - ik$, as found by the Malé method and the corresponding weight thickness of the chromium films used, a calculated curve of Absolute Phase Change on reflection, Δr, as defined in Chapter 3.8., was constructed. This was done by using the graphical technique of Malé(7.1.).

Experimental measurements of the absolute phase change on reflection were made by both the methods described in Chapter 3.8. Table 7.1. gives the results obtained by the method of Rouard(3.13.) and table 7.2. gives the results obtained using the method of Weaver, Hill and MacLeod(3.15.). The experimental results obtained by both methods are shown in fig. 7.1. along with the theoretical curve. The method of Weaver, Hill and MacLeod gives the difference in phase change between an opaque film of chromium and a non-opaque film of chromium. In order to reduce these results to absolute phase change values it is necessary to displace the ordinate reference point by the amount of phase change introduced by an opaque chromium film. When this is done it can be seen that both sets of experimental points give a similar measure of agreement with the theoretical curve. The degree of scatter shown by both sets of points is about the same. The presence of scatter is not surprising as in the Rouard method the rings /

rings observed are diffuse and this leads to a corresponding uncertainty in the measured ring diameters. In the case of the second method the fringes obtained when a semi-transparent film acts as one of the reflectors are not as clearly defined as multiple-beam interference fringes obtained with two highly reflecting surfaces and there is again a corresponding uncertainty in the measured fringe displacement.

Within the limits of the experimental error the two different methods of phase change measurement gave results which were in agreement and both methods are valid within a range of 0 to 400 A weight thickness, over which both methods are usable. It may be noted here that for very thin films (dw < 100 A) the method of Rouard is more suitable although one may be obliged to use photography to measure the ring diameters. For the thicker films (dw > 300 A), the method of Weaver, Hill and MacLeod is preferable, the low transmittance of thick films making the use of the Rouard method difficult.

The agreement between the theoretical curve and the experimental measurements tends to confirm the validity of the refractive index as obtained by the Malé method for the conditions under which the measurements are made, viz. normal incidence.

The thickness values used for graphing the experimental results were obtained by measuring the transmittance of the specimens, T, and using the transmittance vs. weight thickness curve of fig. 6.4.

TABLE 7.1.

Phase Change on Reflection by Chromium Films, Δr. Howard Method.

T%	dw	$\varepsilon_0 - \varepsilon$	$2d/\lambda$	r $(\varepsilon_0 - \varepsilon - 2d/\lambda)$	$\pi - \Delta r$ in degrees
34.5	100	0.101	0.037	0.064	157
28.8	120	0.049	0.044	0.050	162
26.8	130	0.163	0.055	0.108	141
20.2	175	0.147	0.064	0.083	150
15.5	233	0.195	0.085	0.110	139.7
15.0	240	0.200	0.088	0.112	139.5
13.5	260	0.206	0.095	0.110	140
9.8	300	0.230	0.110	0.120	137

TABLE 7.2.

Phase Change on Reflection by Chromium Films, Δr. Method of Weaver, Hill and MacLeod.

T %	dw (A.U.)	A Cr I by Ag. (A.U.)	B Cr I by Cr II (A.U.)	C Cr II by Ag. (A.U.)	B - A (A.U.)	ϕ Phase Change °
20	72	540	200	90	- 340	+ 45
32.6	105	820	630	190	- 190	+ 25
44.8	115	540	300	165	- 240	+ 31.6
20.9	170	850	700	280	- 150	+ 20
10	325	900	850	350	- 50	+ 6.6

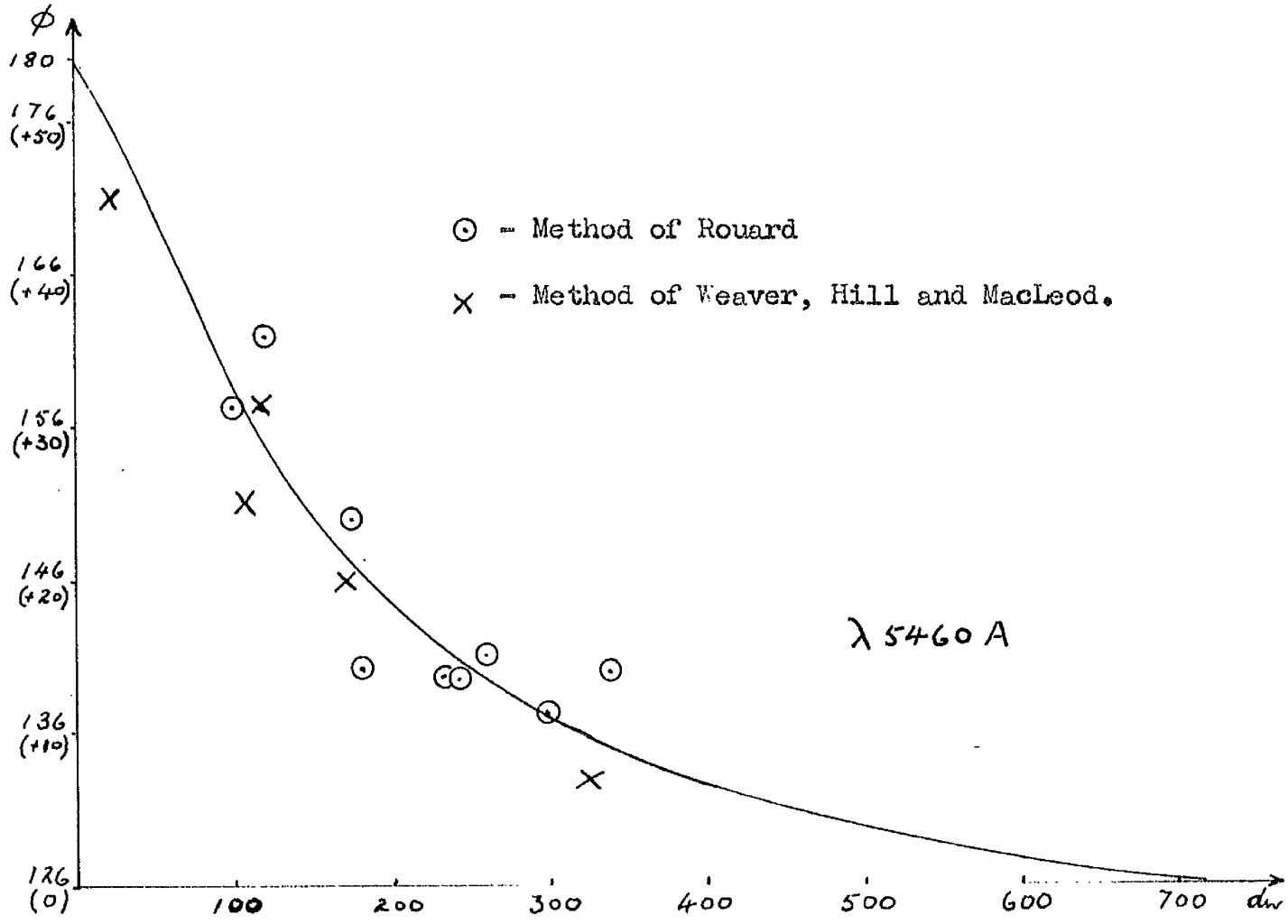

Fig. 7.1. Comparison between Experimental Results and Theoretical Curve of Absolute Phase Change on Reflection at a Chromium Film, ϕ, expressed as a function of Weight Thickness, dw.

CHAPTER 7 : REFERENCES.

7.1.) Malo, D., Thesis. University of Paris.
Masson et Cie, 1953.

CHAPTER 8 : RESULTS OF ELECTRON MICROSCOPY.

Plates 8.1. - 8.5. show the variation of film structure with thickness for films of chromium, copper, manganese, nickel and antimony. The thickness referred to is the interferometric thickness as determined by the Tolansky method.

Generally speaking it can be seen that all the films exhibit an aggregated structure, the degree of aggregation and particle size varying from one metal to another.

The substrate for the electron microscopy specimens as described in Chapter 3, was formed by a film of Formvar about 150 A thick. Sennett and Scott(8.1.) have shown that the structure of metal films on Formvar substrates is similar to that of metal films on glass. Hence conclusions arrived at by inspection of the electron micrographs will be applicable to the specimens formed on glass substrates for optical investigation.

It has been suggested(8.2.) that the aggregated structure observed in thin metallic films may be due to bombardment by the electron beam. Sennett and Scott also investigated this possibility by shadow-casting the specimen before inserting it into the electron beam. The image obtained showed each aggregate in a specimen with its corresponding shadow which proved that the aggregates were unchanged by the electron beam.

The rate of evaporation of a metal film has an influence upon the degree of aggregation of the film. Generally speaking the aggregates are smaller the faster the deposition rate for any given metal. It is therefore important that deposition rates should be known when comparing the structures of metal films.

Chromium :

Examples of the variation of the structure of chromium films with thickness are shown in plates 8.1. The rate of evaporation was about 3 A/sec. The thinnest film with a thickness of 100 A shows that the chromium is continuous with a very fine microstructure. This microstructure persists in the thicker films although it becomes progressively overlayered with larger crystallites with increasing film thickness.

Copper :

In plates 8.2. are shown the structures of copper films of various thicknesses. As in the case of chromium the thinnest film, viz. 165 A shows a continuous microstructure on which are superimposed larger crystallites. Again it can be observed on close examination of the thicker films that the fine microstructure persists up to the thickest film examined. The deposition rate was in the region of 12 - 20 A/sec.

Antimony :

The antimony films shown in plates 8.3. display a definite evolution of structure with increasing thickness. The thinnest specimen consists of isolated crystallites which join up with increasing thickness as is clearly seen in the 120 A specimen. There is no fine grained structure evident here, even for the thinnest specimen, as occurred in the case of chromium and copper. The deposition rate was about 25 A/sec.

Manganese :

The manganese films in plates 8.4. show a fine grained texture at 175 A thickness. The thickest specimen shows a great deal of fissures which may make the film behave as one which is heavily aggregated. The deposition rate was in the region of 10-15 A/sec.

Nickel :

The thinnest nickel specimen shown in plates 8.5. consists of small individual crystallites which are not joined to each other. The seperation of these small crystallites is maintained in the thicker specimen which also shows a number of large crystallites. The deposition rate was about 4 A/sec.

The electron diffraction patterns show that the films are all composed of microcrystallites which are either randomly oriented, or possibly have fibre orientation, with the fibre axes perpendicular to the substrate. Without a provision for tilting the specimen the possibility of such fibre orientation cannot be eliminated.

Summary :

From the results of the electron microscopy examination it appears that the metals chromium and copper have a common feature in their structures and which is not shared by the other metals examined. This is the existence of the continuous microstructure in the thinnest specimens and its persistence into the thicker ones.

Chromium and copper are the only two of the metals examined which were amenable to the evaluation of their optical constants by the Malé method. The Wolter Relationship held for the other metals at relatively high thickness values, and thus prevented the application of the Malé method.

It is worthy of note that the metals where the Wolter Relationship holds all show either high aggregation or fissuring and it may be that these structures have an influence upon whether or not the Wolter Relationship holds for a particular metal film. In general, for all metals, as the thickness of the films /

films gets smaller there comes a stage where the Wolter Relationship holds. Moreover when thin enough specimens are examined all metals generally show a discontinuous structure. This fact coupled with the findings outlined in the summary above would indicate that in addition to the criterion of large values of $^{b}/_{n}$ outlined in Chapter 5, another indication of the applicability of the Wolter Relationship is the existence of a completely aggregated or fissured structure in a specimen.

d = 100 A

Magnification 60,000 X

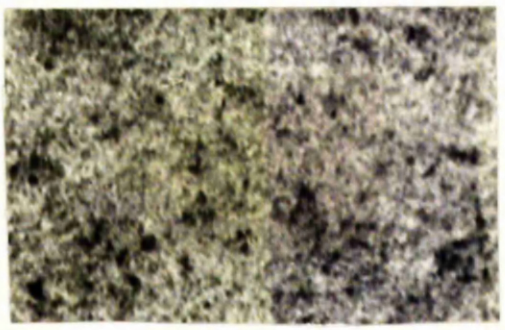

d = 200 A

Magnification 60,000 X

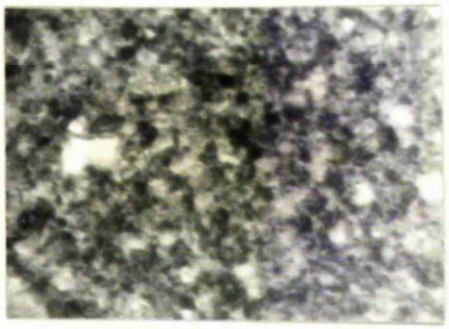

d = 350 A

Magnification 60,000 X

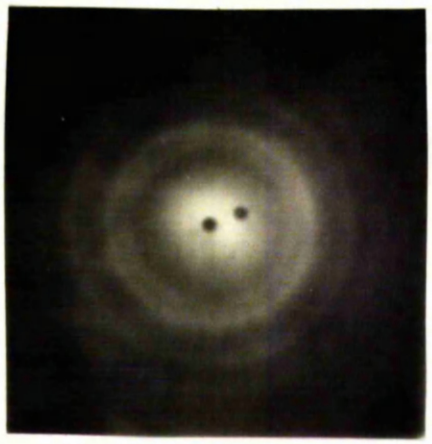

Electron Diffraction
Pattern of 100 A
Chromium Film

Plates 8.1. Electron Micrographs of Chromium Films.

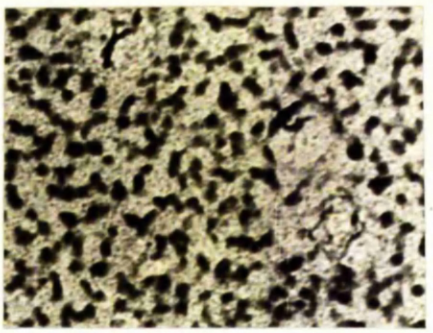

d = 165 A

Magnification 60,000 X

d = 240 A

Magnification 60,000 X

d = 440 A

Magnification 60,000 X

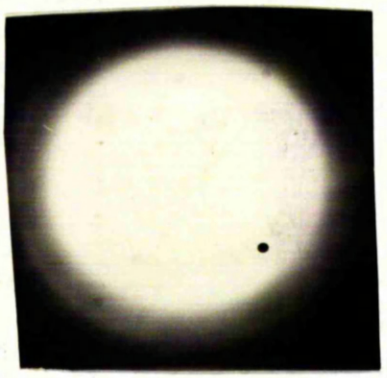

Electron Diffraction
Pattern of 165 A
Copper Film

Plates 8.2. Electron Micrographs of Copper Films.

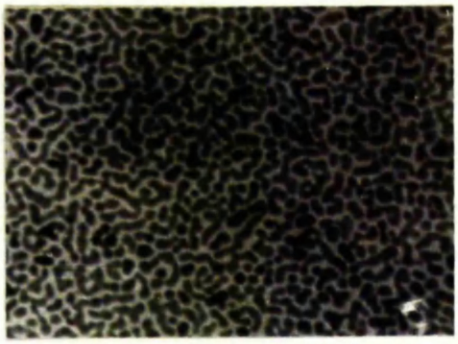

d = 80 A

Magnification 60,000 X

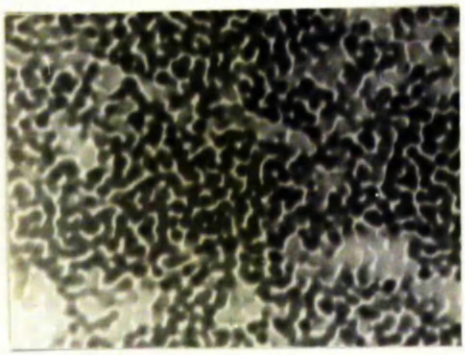

d = 120 A

Magnification 60,000 X

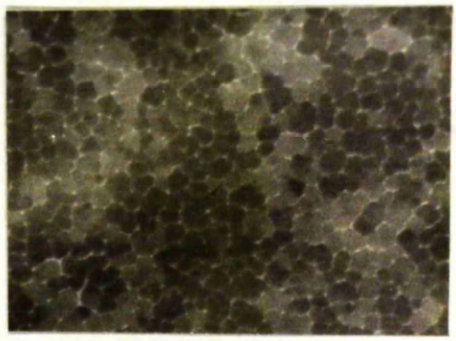

d = 250 A

Magnification 60,000 X

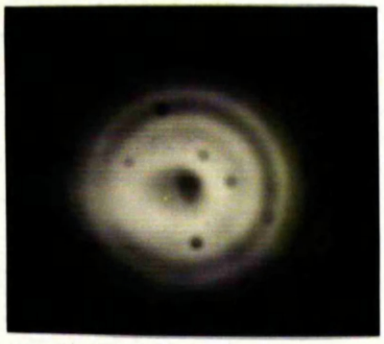

Electron Diffraction
Pattern of 120 A
Antimony Film

Plates 8.3. Electron Micrographs of Antimony Films.

d = 175 A

Magnification 60,000 X

d = 300 A

Magnification 50,000 X

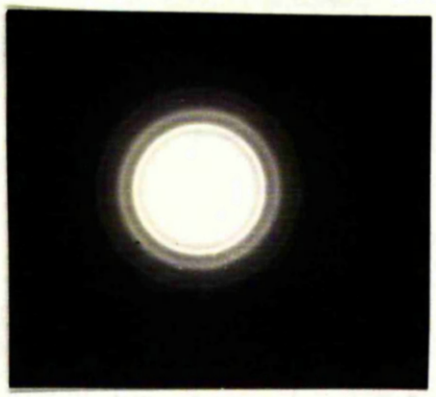

Electron Diffraction
Pattern of 175 A
Manganese Film

Plates 8.4. Electron Micrographs of Manganese Films.

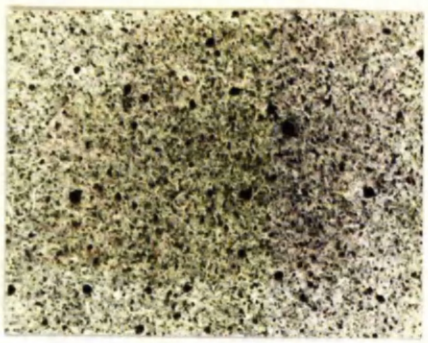

d = 150 A

Magnification 43,200 X

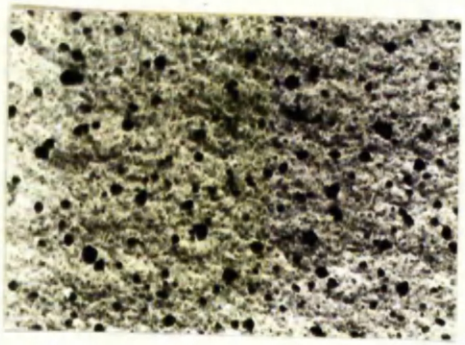

d = 200 A

Magnification 43,200 X

Electron Diffraction
Pattern of 200 A
Nickel Film

Plates 8.5. Electron Micrographs of Nickel Films.

CHAPTER 8 : REFERENCES.

8.1.) Sennett, R.S., and Scott, G.D., Jour. Opt. Soc. Amer., Vol. 40, 1950, p.203.
8.2.) Was, D.A., Physica, Vol. 6, 1939, p.382.

CHAPTER 9 : DISCUSSION.

Early attempts to explain the optical constants of thin metal films and their variation with thickness were based on a theory developed by Maxwell Garnett(9.1.). The theory was originally used by him to explain the colours of the so-called metal glasses wherein finely distributed spherical metal particles are embedded in a glass matrix. Maxwell Garnett extended the work to attempt an account of the optical constants of thin metal films by regarding the thin films as consisting of an assembly of spherical metal particles whose dimensions were small compared to the wavelength of the light employed. Referring to observations on the metal particles in gold ruby glasses made by Siedentopf and Zsigmondy(9.2.), Maxwell Garnett concludes that metal particles in the form of small spheres (i.e. diameter << 1,000 A) will not have the crystalline structure of the bulk material due to the very large value of the surface tension forces compared to the constant "crystallic" forces. Beilby(9.3.) arrived at a similar conclusion when investigating thin metal films deposited from solution. This theory is certainly not denied by electron diffraction observations on very thin films, however the lack of indication of a crystalline structure in electron diffraction could be attributed to the fact that very thin films do not give sufficient intensity for photographic observation except after long exposure to the electron beam, and this can cause recrystallization.

The Maxwell Garnett model gave sufficient agreement with experimental results to warrant its further development. This work was undertaken by David(9.4.) and later by Schopper(9.5.). David regarded the metal aggregates as being ellipsoids of revolution lying with their unique axes perpendicular to the substrate, and he showed that provided the dimensions of the aggregates were small compared to the wavelength of the light the size did not affect the resonance frequency. As shown below the important factor was the shape of the particles.

Consider a distribution of ellipsoidal particles lying in the x, y plane whose unique axes lie in the z direction. If we call ε_b the complex dielectric constant for the interior of one of the particles then by electromagnetic theory

$$\varepsilon_b = n_b^2 - k_b^2 - 2\,i\,n_b\,k_b \qquad \ldots \quad (9.1.),$$

where $\underline{n}_b = n_b - i\,k_b$ represents the complex refractive index of the interior of a particle.

Let the ambient medium surrounding the particles have dielectric constant ε_a, which for simplicity we shall regard as a real number. As the dimensions of a particle are small compared to the wavelength we may regard the instantaneous value of the electric field as uniform throughout a particle. To evaluate the dielectric constant of the assembly of particles we start by considering one particle. A further simplification is given by considering only the case of normal /

normal incidence. A change of co-ordinates assists in the calculation. The co-ordinate system employed in Madelung's ellipsoidal co-ordinates(9.6.) and the transformation to the new co-ordinates u, v, Λ are made using the relations :-

$$\left.\begin{aligned} x &= w\sqrt{u^2+1}\,\sqrt{1-v^2}\,\cos\Lambda \\ y &= w\sqrt{u^2+1}\,\sqrt{1-v^2}\,\sin\Lambda \\ z &= w\,u\,v \end{aligned}\right\} \qquad \ldots \quad (9.2.)$$

For $u = u_o$, a constant, equations (9.2.) define an ellipsoid surface. If a, b, b represent the axes then

$$\left.\begin{aligned} \tfrac{1}{2}a &= w\,u_o \\ \tfrac{1}{2}b &= w\sqrt{u_o^2+1} \end{aligned}\right\} \quad u_o^2 = \frac{1}{\frac{b^2}{a^2}-1} \;;\; w^2 = \tfrac{1}{4}(b^2-a^2) \qquad \ldots \quad (9.3.)$$

Consider the ellipsoid to be placed in a uniform electric field of strength unity in the x direction.

Let $\Delta\phi = 0$ be the Laplacian where ϕ represents the value of the electric potential in the region. Then solving for ϕ inside and outside the boundary of a particle we obtain

$$\left.\begin{aligned} \phi_a &= -x + Cx\left(\frac{\pi}{2} + \text{Arc Tan } u - \frac{u}{u^2+1}\right) \\ \phi_b &= -x + Cx\left(\frac{\pi}{2} - \text{Arc Tan } u_o - \frac{u_o}{u_o^2+1}\right) \end{aligned}\right\} \qquad \ldots \quad (9.4.)$$

where ϕ_a represents the potential just outside the surface of the particle and ϕ_b is the value just inside. The constant C whose value depends on the shape of the particle can be expressed in terms of the parameters by using the condition that the normal component of the electric displacement

$$\varepsilon E = \varepsilon \frac{d\phi}{du}$$

is continuous across the boundary of the particle.

We may therefore write,

$$\varepsilon_a \frac{\partial \phi_a}{\partial u} = \varepsilon_b \frac{\partial \phi_b}{\partial u} \qquad \ldots \quad (9.5.)$$

$$\text{i.e. } \varepsilon_a \left\{ -\frac{\partial x}{\partial u} + C \frac{\partial x}{\partial u} \left[\frac{\pi}{2} - \text{Arc Tan } u - \frac{u}{u^2+1} \right] + Cx \left[-\frac{\partial}{\partial u} \text{Arc Tan } u - \frac{\partial}{\partial u} \left(\frac{u}{u^2+1} \right) \right] \right\}$$

$$= \varepsilon_b \left\{ -\frac{\partial x}{\partial u} + C \frac{\partial x}{\partial u} \left[\frac{\pi}{2} - \text{Arc Tan } u_o - \frac{u_o}{u_o^2+1} \right] \right\} \qquad \ldots \quad (9.6.)$$

Using equations (9.2.) we have $\frac{\partial x}{\partial u} = \frac{x\,u}{u^2+1}$ and putting $u = u_o$ we have

$$\varepsilon_a \left\{ -\frac{xu_o}{u_o^2+1} + C \frac{xu_o}{u_o^2+1} \left[\frac{\pi}{2} - \text{Arc Tan } u_o - \frac{u_o}{u_o^2+1} \right] + Cx \left[-\frac{1}{u_o^2+1} - \frac{1-u_o^2}{(u_o^2+1)^2} \right] \right\}$$

$$= \varepsilon_b \left\{ -\frac{xu_o}{u_o^2+1} + C \frac{xu_o}{u_o^2+1} \left[\frac{\pi}{2} - \text{Arc Tan } u_o - \frac{u_o}{u_o^2+1} \right] \right\} \qquad \ldots \quad (9.7.)$$

Hence,

$$C = \frac{\varepsilon_b - \varepsilon_a}{(\varepsilon_b - \varepsilon_a) f + \varepsilon_a} \quad \frac{u_o (u_o^2 + 1)}{2} \qquad \ldots \quad (9.8.)$$

$$\text{where } f = \tfrac{1}{2} u_o (u_o^2 + 1) \left\{ \frac{\pi}{2} - \text{Arc Tan } u_o - u_o (1 + u_o^2) \right\} \qquad \ldots \quad (9.9.)$$

For the potential ϕ_a at large distances from the ellipsoid compared to its dimensions, i.e. $u \gg u_o$, we write

$$\phi_a = - x + Cx \left(\frac{\pi}{2} - \text{Arc Tan } u - \frac{u}{u^2 + 1}\right)$$

Considering only the contribution to ϕ_a due to the presence of the ellipsoid we have, letting $u \to \infty$

$$Cx \left(\frac{\pi}{2} - \text{Arc Tan } u - \frac{u}{u^2 + 1}\right) \to Cx \left\{ \frac{\pi}{2} - \left(\frac{\pi}{2} - \frac{1}{u} + \frac{1}{3u^3} + \ldots\right) \right.$$

$$\left. - \frac{1}{u} \left(1 - \frac{1}{u^2} + \frac{1}{u^4} - \ldots\right) \right\} \to Cx \frac{2}{3u^2} \to \frac{2}{3} Cw^3 \frac{x}{r^3} \qquad \ldots \quad (9.10.)$$

where $r^2 = x^2 + y^2 + z^2 = w^2 (u^2 - v^2 + 1)$.

Equation (9.10.) however may be regarded as the potential due to a dipole of moment equal to $\frac{2}{3} Cw^3$. Now the electric displacement may be written as

$$\underline{D} = \underline{E} + 4\pi \underline{P}$$

where $\underline{P}$ is the electric polarization due to the field $\underline{E}$. The magnitude of the contribution to the displacement by the particle is therefore

$$4\pi P = 4\pi \varepsilon_a \left(\frac{2}{3} Cw^3\right) = \frac{8\pi}{3} \varepsilon_a Cw^3 \qquad \ldots \quad (9.11.)$$

If there are N particles per unit area of substrate then the contribution per unit area is $\frac{8\pi}{3} \varepsilon_a C w^3 N$ ... (9.12.)

If V_s represents the volume of metal film per unit area of the substrate then the contribution to the displacement may be expressed as $(n^2 - \varepsilon_a) E V_s$ and equating this expression to that of equation (9.12.) we get

$$(n^2 - \varepsilon_a) E V_s = \frac{8\pi}{3} \varepsilon_a C w^3 N \qquad \ldots \quad (9.13.)$$

For unit field strength we then have

$$(n^2 - \varepsilon_a) V_s = \frac{8\pi}{3} \varepsilon_a C w^3 N \qquad \ldots \quad (9.14.)$$

The volume of an ellipsoid

$\Delta V = \frac{\pi}{6} \cdot ab^2 = \frac{4\pi}{3} w^3 u_o (u_o^2 + 1)$, therefore from (9.8.),

$$(n^2 - \varepsilon_a) V_s = \frac{8\pi}{3} \varepsilon_a w^3 \left\{ \frac{\varepsilon_b - \varepsilon_a}{(\varepsilon_b - \varepsilon_a) f + 1} \quad \frac{u_o(u_o^2 + 1)}{2} \right\} . N$$

$$= \left\{ \frac{\varepsilon_b - \varepsilon_a}{(\varepsilon_b - \varepsilon_a) f + 1} \right\} \cdot N \cdot \Delta V \qquad \ldots \quad (9.15.)$$

Now $N \cdot \Delta V$ represents the sum of the volumes of the particles occupying unit area of the substrate and we may thus write $N \cdot \Delta V = V_k$.

David did not take into account the fact that the space occupied by the film per unit area, V_s, could be greater than the sum of the volumes of the number of particles per unit area, V_k.

Schopper(9.5.) has modified David's theory to take this into account. Hence for thin films $V_k < V_s$. Using $q = \frac{V_k}{V_s} = \frac{dy}{dm}$ as defined in Chapter 6 we may then write equation (9.15.) thus

$$\frac{1}{q} \cdot (\underline{n}^2 - \varepsilon_a) = \frac{\varepsilon_b - \varepsilon_a}{\left(\frac{\varepsilon_b - \varepsilon_a}{\varepsilon_a}\right) f + 1} \qquad \ldots \quad (9.16.)$$

The experimental values of q found for Cr and Cu are shown in figs. 6.5. and 6.9. respectively.

To obtain a satisfactory interpretation of the experimental results given by $\underline{n}$ and q we must assign values to ε_a, ε_b and f. The value of ε_a should be that of the medium surrounding the particles. When this is air, $\varepsilon_a = 1$. However some workers, e.g. David(9.4.), Trompette(9.7.), Richard and Roux(9.8.), prefer to assign to ε_a a mean value between air and substrate, i.e. $\varepsilon_a = \frac{1}{2}(n^2 + 1)$, where n represents the refractive index of the substrate. In this work ε_a is taken as being equal to 1 as the arguments for the other case do not appear sufficiently conclusive to warrant its adoption.

The value adopted for ε_b, the complex dielectric constant of a particle depends upon whether or not it is believed that the bulk optical properties pertain within the particle. This is a matter which has not yet been resolved. It is generally agreed that the anomalous optical constants of thin metal films may be attributed to two main effects. These are (i) the effect of the structure of the films and (ii) the effective diminution of the mean free path of the /

the free electrons within aggregates. Fragstein and Romer(9.9.) have concluded that both effects are present but that the effect of the film structure is the more important. In this work it was found necessary to attribute to ε_b values different from the corresponding bulk values in order to obtain agreement between theory and experiment.

Finally the value of f may be determined using equations (9.3.) and (9.9.) if the shape of the ellipsoids is known, i.e. the axial ratio b/a. The value of f varies from 0.5 for $b \ll a$ to 0 for $b \gg a$. These conditions apply when the unique axis is perpendicular to the substrate. Figure 9.1. shows the variation of f with axial ratio. David suggested that a film would be composed of particles whose f values varied according to some distribution function $g(f)$. To determine the effect of all the various particles it would then be necessary to add the contributions of the separate groups with different f values. If we regard the distribution as continuous we may use an integral form thus,

$$\frac{1}{q}\left(n^2 - \varepsilon_a\right) = \int_0^{0.5} \frac{\varepsilon_b - \varepsilon_a}{\left\{\frac{\varepsilon_b - \varepsilon_a}{\varepsilon_a}\right\} f + 1} \; g(f) \; df \qquad \ldots \quad (9.17.)$$

The limits of integration used here, viz. 0 and 0.5 are different from those of David which were 0 and 1. The upper limit of 0.5 was selected because f cannot attain a value greater than 0.5. As will be seen this makes little difference to the final result.

Fig. 9.1. The relationship between f and the axial ratio b/a of the ellipsoid of rotation for the case where the unique axis a is normal to the substrate plane (after David).

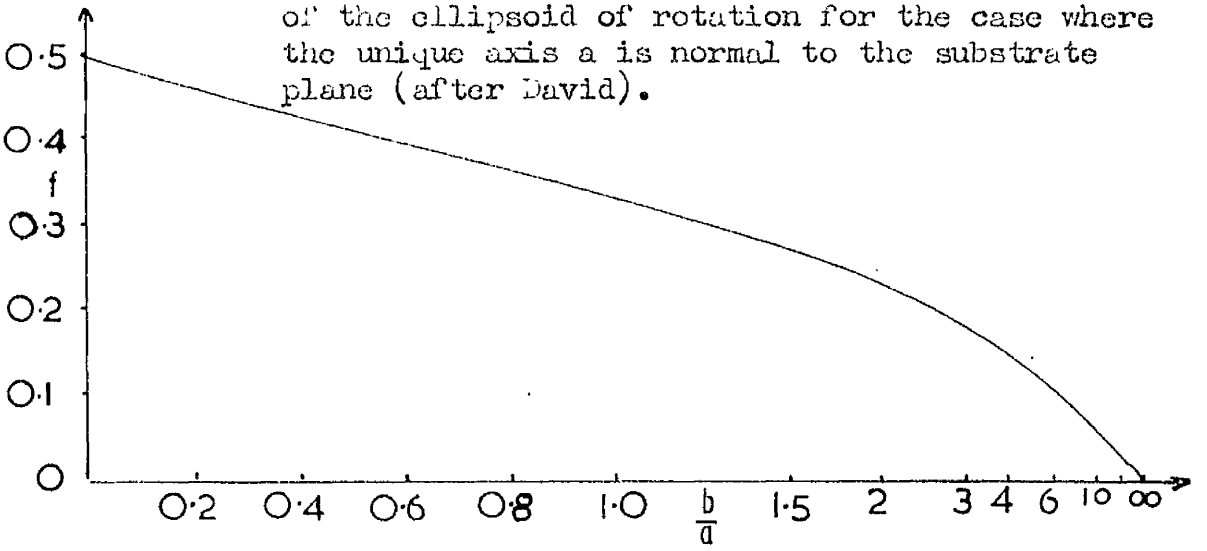

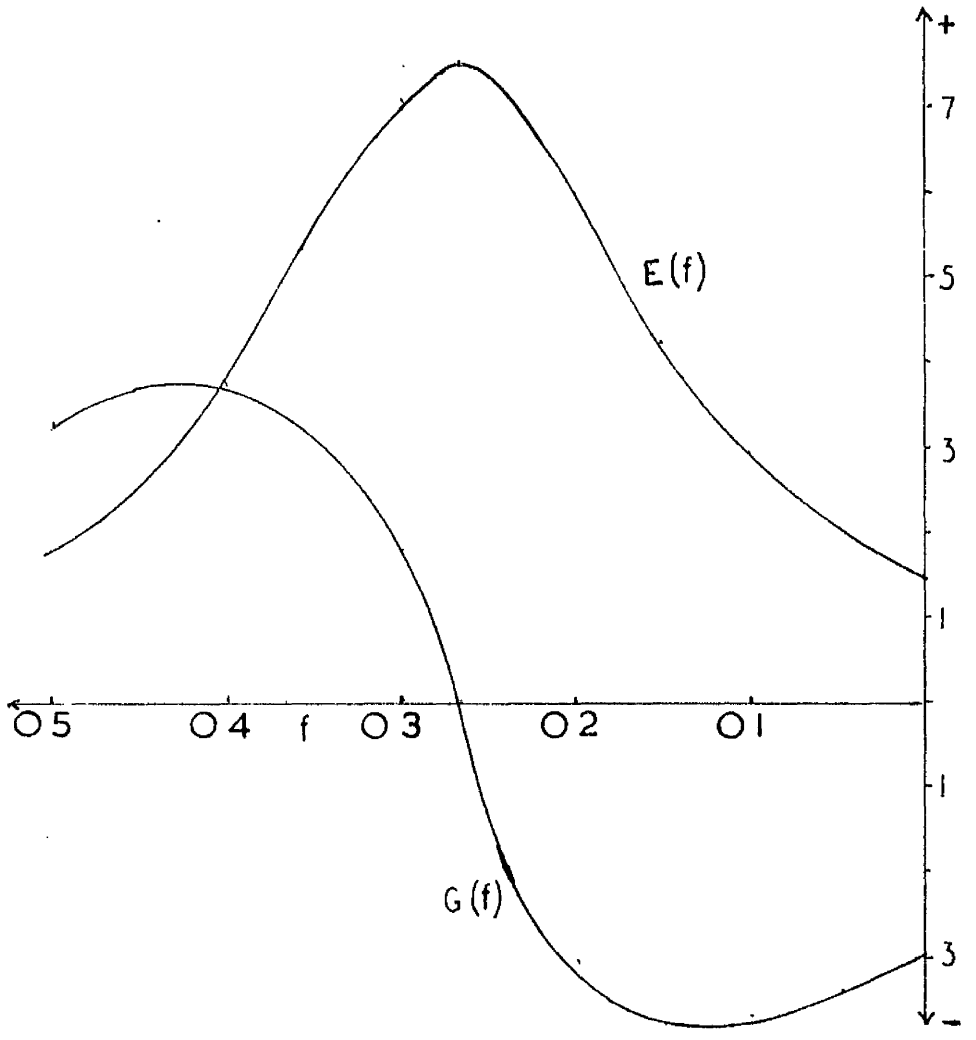

Fig. 9.2. Graph of the variation of the functions

$$E(f) = \varepsilon_a^2 B \Big/ f^2(A^2 + B^2) + 2f\,A\,\varepsilon_a + \varepsilon_a^2 \text{ and}$$

$$G(f) = \frac{A\,\varepsilon_a^2 + \varepsilon_a\,f\,(A^2 + B^2)}{f^2\,(A^2 + B^2) + 2\,f\,A\,\varepsilon_a + \varepsilon_a^2},$$

with f for $n_b = 0.5$, $k_b = 1.5$, $\varepsilon_a = 1$.

Equation (9.17.) may be separated into real and imaginary parts; writing $(n_b - ik_b)^2$ for $\mathcal{E}_b$ we get

$$\frac{1}{q}(n^2 - k^2 - \mathcal{E}_a) = \mathcal{E}_a \int_0^{0.5} \frac{A\,\mathcal{E}_a + f(A^2 + B^2)}{f^2\,(A^2 + B^2) + 2\,f\,A\,\mathcal{E}_a + \mathcal{E}_a^{\,2}}\; g(f)\; df \quad \ldots(9.18.)$$

and

$$\frac{1}{q}\,2nk = \mathcal{E}_a^{\,2} \int_0^{0.5} \frac{B}{f^2\,(A^2 + B^2) + 2\,f\,A\,\mathcal{E}_a + \mathcal{E}_a^{\,2}}\; g(f)\; df \quad \ldots(9.19.)$$

where $A = n_b^{\,2} - k_b^{\,2} - \mathcal{E}_a$ and $B = 2n_b k_b$.

In equation (9.19.) if we graph the expression

$$E\,(f) = \frac{\mathcal{E}_a^{\,2}\,B}{f^2\,(A^2 + B^2) + 2\,f\,A\,\mathcal{E}_a + \mathcal{E}_a^{\,2}}$$

using typical values for n and k we see that the curve drops from a maximum value at $f_1 = \dfrac{-A\,\mathcal{E}_a}{A^2 + B^2}$ to a low value at $f = 0$ and $f = 0.5$.

Figure 9.2. shows this curve for $n_b = 0.5$, $k_b = 1.5$, $\mathcal{E}_a = 1$.

From the manner of formation of the film it would not be expected that the distribution of particle shapes would show a rapid variation with changing thickness, i.e. changing f. Hence to a first approximation we might regard g(f) as constant near to f_1 while E(f) varies. Hence we can take g(f) outside the integral sign and rewrite (9.19.) as

$$\frac{1}{q}\,2nk = \mathcal{E}_a^{\,2}\, g(f) \int_0^{0.5} \frac{B}{f^2 (A^2 + B^2) + 2 f A \mathcal{E}_a + \mathcal{E}_a^{\,2}}\, df \qquad \ldots \quad (9.20.)$$

In figure 9.2. there is also shown the variation of

$$G(f) = \frac{A\,\mathcal{E}_a^{\,2} + \mathcal{E}_a\, f\,(A^2 + B^2)}{f^2 (A^2 + B^2) + 2 f A \mathcal{E}_a + \mathcal{E}_a^{\,2}}$$

with f. The two curves of fig. 9.2. are similar to those for a damped oscillator in the region of its resonance frequency. In particular it may be seen that when E (f) attains its maximum value G (f) passes through zero. We may integrate equation (9.17.) analytically regarding g (f) as constant, thus considering only the part under the integral sign :-

$$\int \frac{\mathcal{E}_b - \mathcal{E}_a}{\frac{\mathcal{E}_b - \mathcal{E}_a}{\mathcal{E}_a} f + 1}\, df = \mathcal{E}_a \int \frac{\frac{\mathcal{E}_b - \mathcal{E}_a}{\mathcal{E}_a}}{\frac{\mathcal{E}_b - \mathcal{E}_a}{\mathcal{E}_a} f + 1}\, df$$

$$= \mathcal{E}_a \ln\left(1 + \frac{\mathcal{E}_b - \mathcal{E}_a}{\mathcal{E}_a} f\right) + C,$$

where C is a constant which may be evaluated by inserting the limits of integration.

Using the limits of f as 0 and 1 as David did, we obtain

$$\int = \mathcal{E}_a \ln \frac{\mathcal{E}_b}{\mathcal{E}_a} = \mathcal{E}_a \ln \frac{1}{\mathcal{E}_a}\,(n^2 - k^2 - 2\,i\,n\,k).$$

Changing to polar form this becomes

$\mathcal{E}_a \ln A \operatorname{Exp} i\,\theta$

where $A^2 = \frac{1}{\mathcal{E}_a^2}\,(n^2 - k^2)^2 + 4\,n^2\,k^2$

and $\theta = \operatorname{Arc\,Tan}\left(\frac{-2\,n\,k}{n^2 - k^2}\right)$

The imaginary part of the above expression is

$I = \mathcal{E}_a \cdot \theta$, i.e.

$$I = \mathcal{E}_a \operatorname{Arc\,Tan}\frac{(-2\,n\,k)}{(n^2 - k^2)}$$

Using limits of integration of 0 and 0.5 the imaginary part becomes

$$I' = \mathcal{E}_a \operatorname{Arc\,Tan}\frac{-2\,n\,k}{n^2 - k^2 + \mathcal{E}_a}$$

Whether I or I' is used it can be seen that at $f = f_1$, θ is very nearly equal to π and hence we may write equation (9.19.) thus

$$\frac{1}{q} \cdot 2\,n\,k = \mathcal{E}_a \cdot \pi \cdot g\,(f) \qquad \ldots \quad (9.21.)$$

Equation (9.21.) may therefore be used to determine $g\,(f)$.

Schopper(9.5.) attempted to obtain a fit with results obtained from gold films by assuming that $g\,(f)$ of equation (9.17.) was a distribution function of Gaussian type, viz.
$g\,(f) = \text{Const.}\ f\ \exp - (f/\bar{f})^2$, where $\bar{f}$ is the most probable value of f for the particles composing a particular film.

This function however does not fulfill all the required conditions of the distribution function, namely that the function should have a value of zero at $f = 0$ and $f = 0.5$ and should have its maximum value at $f = \bar{f}$, the most probable value of f. Schopper's function has a maximum at $f = \frac{1}{2}\bar{f}$. A more suitable function is $g(f) = \text{Const.}\ f^2 \exp - (f/\bar{f})^2$ which satisfies the above named requirements. Attempts to obtain fits with the experimental results for chromium and copper were made using the latter and other distribution functions without obtaining any great improvement on a similar approach in which it is assumed that all the particles have a certain mean axial ratio which varies with thickness. Thus by selecting values for n_b and k_b and then graphing the real and imaginary parts of the right hand side of equation (9.16.) for values of from 0 to 0.5 it is possible to construct a theoretical curve. If now the real and imaginary parts of the left hand side of equation (9.16.) obtained by experiment are evaluated a curve fitting method may be employed to determine the agreement between theory and experiment. This is done by fitting the imaginary part against the theoretical curve and seeing if the real part lies on or near its corresponding curve. This process is repeated throughout the thickness range studied remembering that as d increases, f decreases, since the particles will become more and more plate-like as the film thickness increases.

Figure 9.3. shows examples of the curves

$$R = \frac{(A^2 + B^2)\, f + A}{(A\, f + 1)^2 + B^2\, f^2} \quad , \quad (\varepsilon_a = 1)$$

and

$$I = \frac{B}{(A f + 1)^2 f + B^2 f^2}$$, expressed as functions of f,

where $A = n_b^2 - k_b^2 - 1$ and $B = 2 n_b k_b$, for selected pairs of values n_b, k_b.

A large number of R and I curves was calculated by computer using a wide range of $n_b k_b$ pairs and these were tested against the experimental results obtained for the chromium and copper films measured.

In the case of chromium a fit was obtained using values of $A = -6.4$ and $B = 3.3$. This gives values of $n_b = 0.68$ and $k_b = 2.42$. Hence for the chromium films studied here an explanation of the optical properties for a thickness range from about 200 A up to 1,100 A may be found using the David model with the values of n_b and k_b obtained. Figure 9.4. shows the correspondence obtained between the theoretical curve and the experimental points for chromium.

It may be noted that it was not necessary to use the model of Hill and Weaver, viz. that of a film composed of oxide-coated particles, to obtain a reasonable fit over a wide thickness range. This fact could possibly be explained by the difference already referred to in the nature of the thicker chromium films obtained in this work and those of Hill and Weaver.

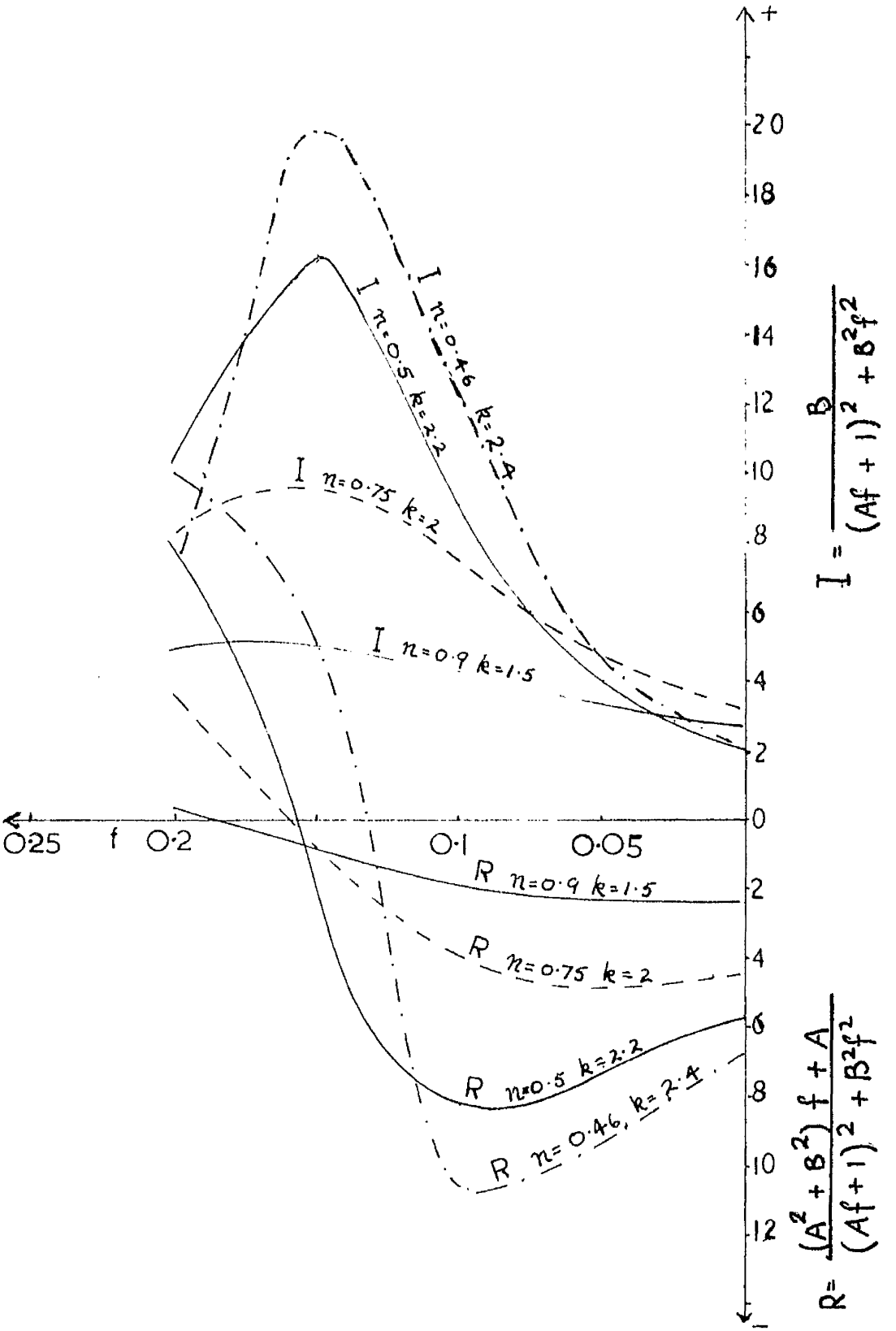

Fig. 9.3. Typical Examples of theoretical curves of

$$R = \frac{(A^2 + B^2)\ f + A}{(Af + 1)^2 + B^2f^2} \text{ and } I = \frac{B}{(Af + 1)^2 + B^2f^2}$$

expressed as a function of f for different n_b, k_b pairs.

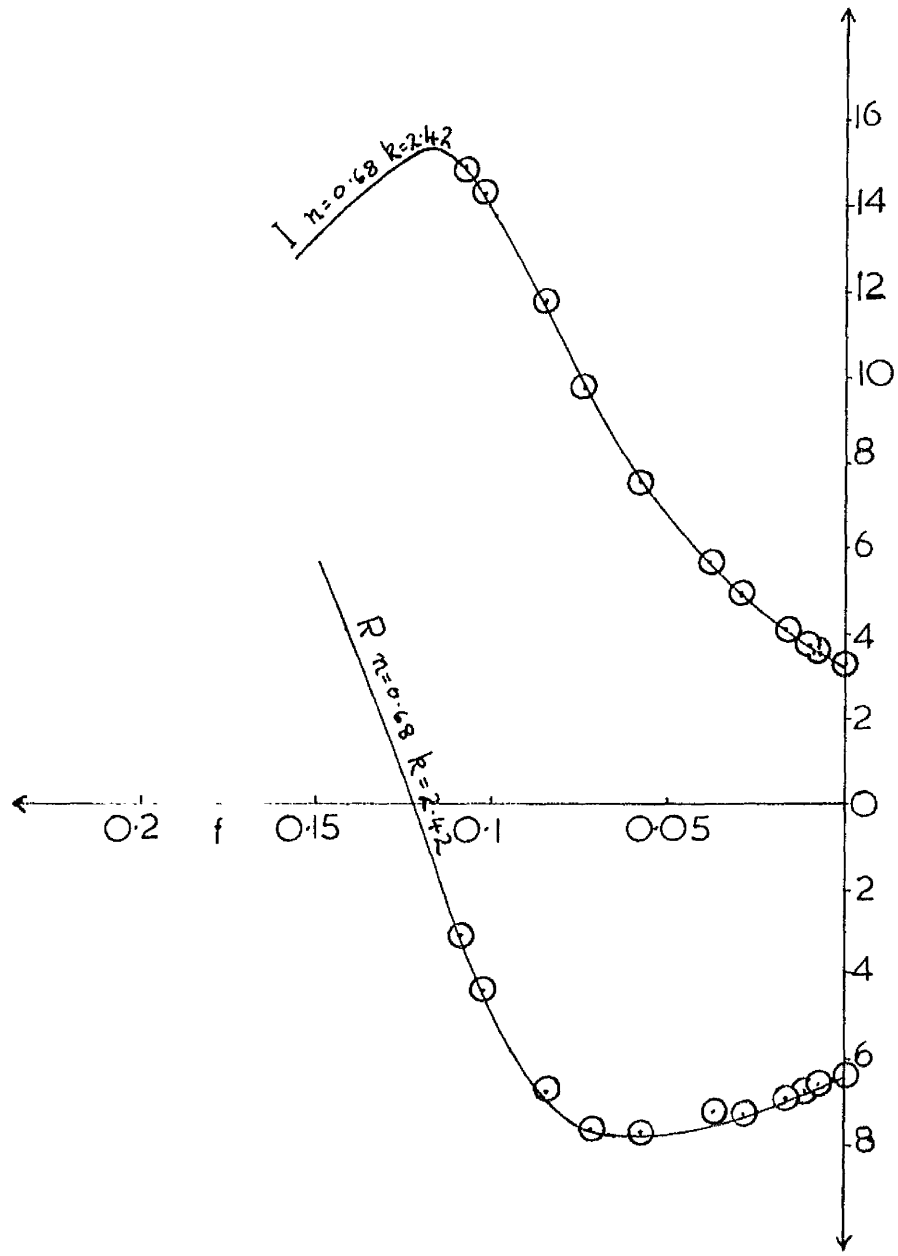

Fig. 9.4. Best fit of theoretical curve with experimental points for chromium. $n_b = 0.68$, $k_b = 2.42$.

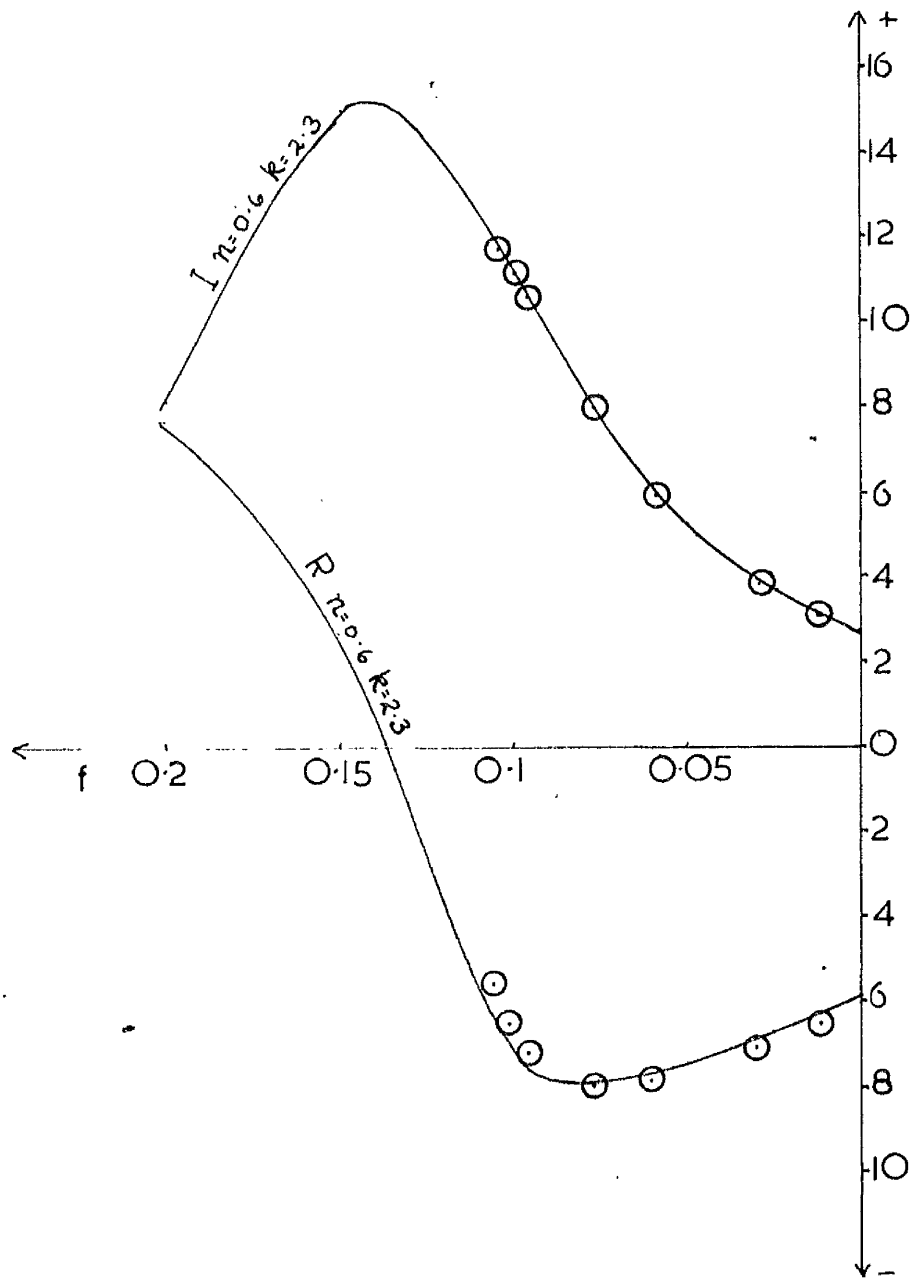

Fig. 9.5. Best fit of theoretical curve with experimental points for copper. $n_b = 0.6$, $k_b = 2.3$.

In the case of copper the curve for best fit of the experimental points is shown in fig. 9.5. This curve is obtained using values of $n_b = 0.6$ and $k_b = 2.3$.

The implication of the results and interpretation of the chromium and copper films is that the films are composed of metal particles and show a variation of refractive index with thickness which tends to a constant value as the films get thicker. The final steady value is not the same as that of the bulk material. This fact may be accounted for by the effect of the structure of the film and/or a diminution in the mean free path of the electrons in the metal particles composing the film. If the results of the David theory had given an n_b and a k_b, the effective optical constants within the particles, which were near to the n and k for the bulk material then one might conclude that the anomalous optical constants of the thin films were due entirely to a structure effect. It appears however that best agreement can only be obtained if we attribute optical constants to the component metal particles which are different from those of the bulk material. The conclusion therefore is that both effects contribute to the optical constants of the films.

The results obtained by the Malé method for chromium and copper films are consistent within themselves. All having been obtained at normal incidence. The validity of the Malé results is confirmed by the calculation and experimental verification of the absolute phase change on reflection at normal incidence. The results /

results obtained for these chromium and copper films by this author and other workers using oblique incidence methods show consistently higher n values and generally higher k values. In the present work the same films were used for both the Malé method and the polarimetric method thus removing the possibility of a different structure applying to the specimens used. In the polarimetric method even allowing for oxide film effects on the metal surface no better correlation with the Malé method was obtained although within the method itself a better consistency was achieved.

It appears therefore that for the specimens used here the method of measuring refractive index at oblique incidence gives radically different results from those obtained using normal incidence. The reason for this is not easy to establish but it might possibly be that the metal films are not plane surfaced, isotropic, or homogeneous as the theory requires when using polatimetric methods at oblique incidence. This doubt with regard to non-normal methods of investigation has been mentioned before with reference to a paper by Bousquet and Rouard(1.19.).

CHAPTER 9 : REFERENCES.

9.1.) Maxwell Garnett, J.C., Trans. Roy. Soc. (London), Vol. 203 A, 1904, 385.

9.2.) Siedentopf, H., and Zsigmondy, R., Ann. der Physik, Jan. 1903.

9.3.) Beilby, G.T., Proc. Roy. Soc., Vol. 72, 1903, p.223.

9.4.) David, E., Zeit. Physik., Vol. 114, 1939, p.389.

9.5.) Schopper, Zeit, Physik., Vol. 130, 1951, p.565., and Fortschritte der Physik., Vol. 2, 1954, p.275.

9.6.) Madelung, E., Die Mathematischen Hilfsmittel des Physikers, 2nd edition, p.150.

9.7.) Trompette, J., Thesis, University of Marseilles, Masson et Cie, Paris, 1960.

9.8.) Richard, J., and Roux, D., Rev. d'Optique, Vol. 41, No. 9, p.469, Sept. 1962.

9.9.) Fregstein, C.V., and Romer, H., Z. Physik, Vol. 151, 1958, p.p. 54 - 71.

CHAPTER 10 : SUMMARY.

The polarimetric studies pursued in the present work gave the refractive index of five metals in the form of opaque films made by thermal evaporation using the theory of Drude. Regarding a film surface as a plane metal/air interface it was found that the calculated value for the refractive index showed a variation with the angle of incidence used in the measurements.

The results for an angle of incidence of 45° differed from those made on the freshly formed film under vacuum at the same angle of incidence. It was assumed that this difference was due to the formation of a surface film, probably oxide, on the metal when it was exposed to the atmosphere. The theoretical treatment of an absorbing film on metal is difficult but oxide films on metals are generally only very slightly absorbing and to an approximation can be treated as if they were completely non-absorbing.

Regarded in this way, a more complicated form of Drude's theory which gave the optical constants of a non-absorbing film on metal and its thickness could be applied. This theory required measurements on a clean metal surface and also on the metal surface with the transparent film present. Since measurements could not be made on a clean metal surface over a range of angles of incidence a different technique was employed.

In this method the optical constants of the metal were assumed and, using the measurements made in air, the refractive index and thickness of the transparent surface film were calculated for a range of angles of incidence. This process was repeated using different values for the refractive index of the metal until reasonably constant results were obtained for the refractive index and thickness of the surface film for all the angles of incidence involved. The metal refractive index giving this constancy was then taken as the true value. The laborious calculations involved in this method were removed to a great extent by using results obtained under vacuum on the freshly formed films for an angle of incidence of 45°. These results acted as a guide in selecting trial refractive index values for the metal in the calculation. Also an electronic computer was used to perform the actual calculations. The final result obtained for the refractive index of each metal was always in good agreement with that given by the vacuum measurement allowing for possible instrumental errors. Moreover the mean value obtained for the refractive index of the surface film was always in very good agreement with that of the oxide of the metal which would be present at room temperature. The thickness obtained for the surface film was in general greater than that which has been reported for oxide films on metals by other workers. The reason for this is not certain but discrepancies in reported film thicknesses have been common. A possible explanation is that of the differing states of the metal surfaces, even when /

when the specimen is an evaporated film. Another possible explanation which has been suggested is that of the great penetration of oxide beneath a metal surface.

Table 10.1. shows the results obtained in this work by the method of polarimetry for the refractive index of several metals. These results may all be regarded as self-consistent within themselves by the confirmation of the results obtained under vacuum and the reasonable values obtained for the oxide films.

Table 10.1.
Refractive Index of Various Metals Using Polarimetry.
λ 5,460 A.

Metal	n (± .05)	k (± .05)
Chromium	3.95	3.00
Copper	1.59	3.22
Tin	1.99	4.32
Manganese	3.05	2.30
Nickel	3.60	3.42

A second method of investigating thin metal films was employed. This was the method of Malé which involved the measurement of the transmittance of a film together with the reflectances from the air and substrate sides. These measurements were carried out at normal incidence over a film thickness range from highly transparent films up to completely opaque films. An electronic computer was used to calculate the curves used in the determination of the refractive index and thickness of the films. For certain metals this method cannot be applied down to low film thickness values. The ability of /

of the relationship of Volter to predict this occurrence was verified for the metals studied here. In the case of those metals for which the Malé method of investigation was valud down to low thickness values (~ 200 A), viz. chromium and copper, the variation of refractive index with film thickness was determined. The chromium films had an n value of 1.5 at 200 A film thickness which fell gradually to a steady value of 0.57 at about 1,100 A film thickness. The k value of the chromium films rose to a maximum of 2.05 at about 350 A film thickness and then fell gradually to attain a steady value of 1.8 at about 1,100 A film thickness. In the case of the copper films the value of n fell gradually from 1.2 at 200 A to a steady value of 0.5 at about 1,000 A film thickness. The k value rose to a constant value of 1.5 at about 500 A without showing a distinct maximum.

The general form of the variation of refractive index with film thickness obtained for chromium and copper films showed good agreement with results obtained by other workers for other metals. The correctness of the results was verified in the case of chromium by checking the calculated absolute phase change on reflection as a function of film thickness with values obtained by experiment. The experimental determination of absolute phase change on reflection was performed in two separate ways. The first method was that devised by Rouard, the interpretation of which has been well established but which required delicate adjustments when performing /

performing measurements. The second method was a recently reported one by Weaver, Hill and MacLeod which was easier to perform experimentally but which required verification in interpretation. The two methods gave results in agreement with each other, and within the experimental error also agreed with the calculated values.

Electron microscopy was employed to determine the structure of the thinner metal films. It was found that chromium and copper films maintained a continuous fine microcrystalline structure throughout the range of thickness investigated. This continuous microstructure was not observed with the other metals investigated by electron microscopy. For all the metals examined the thicker films showed increasing aggregation. With increasing thickness these aggregates eventually joined up giving the film surface a resemblance to a relief map of very mountainous terrain possessing high rounded peaks and ridges separated by deep fissures. Even for the thickest films which it was possible to examine using transmission electron microscopy there was no indication of any levelling off process. It is therefore probably a great simplification to regard such films as being plane parallel-sided and uniform.

An interpretation of the results obtained by the Malé method for chromium and copper was attempted. This interpretation was based on a model due to David which regards a thin metal film as composed of metal particles whose mean shape is that of ellipsoids of revolution lying with their unique axes perpendicular to the substrate. The interpretation based on this model was fairly /

fairly successful if it was allowed that the refractive index of the metal composing the aggregates was different from the refractive index of the bulk metal. This assumption is reasonable since the particles were of the same dimensions as the mean free path of the free electrons in the metal and hence it would be expected that there would be a change in the refractive index due to this cause.

A comparison of the results obtained by both the polarimetric method and the Malé method for chromium showed a wide discrepancy. This was also the case when the different sets of results for copper were compared. Both methods of investigation gave results which were entirely consistent within themselves and since the same specimens were used in both sets of measurements the possibility of differing structures could be ruled out. The conclusion is therefore that methods of investigation involving oblique incidence of light, i.e. in this case polarimetry, can give results which differ markedly from those obtained using normal incidence only. Recently certain authors have cast doubt on the validity of refractive index investigations which employed oblique incidence of light. Bousquet and Rouard(1.19.) have concluded that the oxide films present on metal surfaces are not homogeneous, isotropic and plane parallel-sided films and hence that only normal methods of investigation are really valid. This theory is certainly supported by the evidence of electron microscopy where the unevenness of metal films is shown and in some cases by electron diffraction /

diffraction where it is frequently found that there exists a certain degree of fibre orientation in thin metal films.

Suggestions for Further Work.

At the present moment it is of prime importance to resolve the question of the disagreement of results of refractive index as obtained by normal incidence and oblique incidence methods. The polarimetry method cannot be applied at normal incidence since the p and s components lose their identity at normal incidence. Even measurements made at up to 30° angle of incidence by polarimetric methods are of no help due to the gross inaccuracies which can occur. A possible approach could be to develop the Malé method of investigation to the case of oblique incidence. The equations governing the curves of reflectance and transmittance as a function of film thickess are very cumbersome when using oblique incidence but with the aid of computers the drudgery involved in compiling the curves may be removed. Thus one could obtain for an angle of incidence of say 45° curves of R, R' and T for each of the p and s components of an incident light beam. The experimental measurements would also be relatively simple since one could adapt an existing instrument used for normal incidence measurements by inserting a polarizer between the light source and the film.